

Dear Editor,
Dear Reviewer,

We would like to thank you for the very constructive reviews, which we have received with much appreciation. The comments and suggestions by the referees contributed to greatly improve the organization and the science of our paper.

The major changes include

- A better focus of the introduction, thereby addressing the aim of the manuscript in a clearer way.
- An expansion of the state of knowledge, explaining the architecture and evolution of the Alps and the Molasse basin, and an overview of published work on the Upper Marine Molasse
- A clear, but concise, focus on the sedimentology of the Upper Marine Molasse, which is our major contribution
- A separation between methods, results and interpretation of the sedimentological data
- A presentation of references to published sedimentological work within an overview table
- A plate with photos from the field in the supplement
- A re-organization of the discussion. We have reframed the re-assessment of the chronological framework as a first chapter of the discussion, followed by a discussion of the evolution of the Molasse basin within a geodynamic framework.
- We linked subduction tectonics with (i) the formation of accommodation space in the Molasse basin and with (ii) changes of the drainage network on the surface of the Alps, which could explain the reduction of sediment flux.

We have addressed all other questions and suggestions made by the reviewer. Below, we present a point-by-point response of how we have modified the manuscript.

Referee #1: Kei Ogata

Dear Editor,

The paper represent a broadband reappraisal of the Alpine Molasse basin through the implementation of different stratigraphic techniques in order to illustrate different scenarios from the lithospheric to the basin scale. Although the large amount of processed material, bibliographic review and some interesting considerations, the overall manuscript reads quite poorly and the overall message struggle to pass through. The main issues are: 1) unclear subdivision between original data and literature, 2) mixed results-interpretations, 3) poor logic organisation and structure, 4) too long and complicated sentencing and paragraphing, 5) poor graphical support, 6) unclear link between presented data and interpretations, and 7) unbalanced manuscript-supplementary material. These and several other points are detailed in annotated pdf attached.

Sincerely, Kei Ogata

Our response:

We have fully restructured the article to comply with these requests:

- 1) Original and literature data has been separated into distinct chapters following the recommendations of reviewer 3. We also have largely expanded the setting chapter where we outline the state of current knowledge about the Alps, the Molasse and the related evolutionary processes. These built the basis for the discussion presented in chapter 6.
- 2) Results and Interpretations are now presented in two different chapters. Please note that all references in this context are presented in tables 1 to 5, which are now fully integrated in this text. We decided to proceed in this way because the text is easier to read.
- 3) We have fully reconsidered the organization and structure of the paper according to the current state of the art. Introduction is now followed by an extended local setting chapter, an extended method section, followed by results, interpretation, discussion and conclusion. Here we mainly followed the recommendations by reviewer 3.
- 4) We have corrected and shortened the text particularly in the middle part where we present the sedimentological observations. Nevertheless, we decided not to cut the level of information and thus shifted more details into tables 1 to 5, which are now fully integrated into the text. This was also recommended by reviewer Ogata. Reviewer Eriksson provided useful comments in this regards, which we fully acknowledged and took into account.
- 5) We included two more figures in order to provide more information to follow the text. In addition, based on the detailed comments in the annotated documents, reviewer Ogata required that the figures should be better integrated into the text. We have seriously considered this point and updated the text accordingly. In this context, we greatly appreciate the suggestions by reviewer 3 in his annotated text.
- 6) Please see our response above. In addition, we have made distinct links between our sedimentological observations and interpretations, and the discussion. This was also required by reviewer 3, who made clear suggestions of how to proceed. We adapted all recommendations by reviewer 3 and updated the text accordingly. This resulted in re-structuration of the discussion.
- 7) We shifted the tables with sedimentological details to the main text as required by reviewer Ogata. We have improved the referencing between the main text and additional information presented in the supplementary file.

In addition, we followed all recommendations presented in the annotated file. These mainly concern editorial requests.

Referee #2 – Kenneth Eriksson

General comments:

The authors have integrated a large data base consisting of previous studies and new observations to discriminate the effects of tectonics, eustatic sea level changes and variations in sediment flux in explaining the Upper Marine Molasse in the Swiss Alps. Discriminating between these controls in understanding the stratigraphic record has long been a subject of discussion amongst stratigraphers and sedimentologists and the authors are to be complimented on their contribution to this to this ongoing debate.

The paper consists of 3 main sections, Chronology, Sedimentology and Controls. The first and third sections are well argued but the sedimentology sections requires major revision including drastic shortening and reference to modern and ancient analogs in support of the conclusions of depositional environments. Such references are surprisingly lacking but are essential to presenting convincing interpretations. Also, the sedimentology section contains numerous examples of interpretations within the descriptive sections and vice versa.

In its present form, the paper contains too much sedimentological detail that detracts from the overall message of the paper. I suggest reducing the sedimentological descriptions and interpretations by at least 50% in this paper and to prepare a separate paper that focusses on the sedimentology. The parts of the sedimentological analysis that are germane to this paper the recognition of shoreline and offshore subtidal sand shoals whereas the other details are not necessary for this paper.

Our response:

Thank you for your detailed review and the constructive comments. The sedimentological descriptions and interpretations have been split into two chapters (4. Results and 5. Sedimentological interpretation) and have been substantially shortened. We now present key information only, which will be crucial for following the discussion about tectonics, sediment flux and eustasy as possible controls on the Burdigalian transgression. For the sake of completeness, however, we list all sedimentological details in a table together with the references to previously published work on this topic.

We also include a plate with photos from the field as required by reviewer Ogata.

Referee:

Specific comments:

1. Use of the term “surface controls” in the title and throughout the paper is vague and confusing. Both eustasy and sediment flux are surface controls as noted by the authors so why not just specify eustasy and sediment flux and do away with “surface”?

Our response:

This has been improved. We specified the term surface controls, which include changes in sediment flux and shifts in the eustatic sea level. These processes have been placed in a geodynamic framework together with deep crustal processes. These mechanisms encompass tectonic changes at the slab scale in the mantle lithosphere, and related to these mechanisms crustal-scale processes at a more regional scale.

Referee:

2. I was not able to access the Table or Appendix but it seems to me that the 2 seismic sections should be included as a figure in the paper because they are referred to in many parts of the text.

Our response:

We apologize for this inconvenience. In the supplement file the reader finds a detailed description on how we calculated the palaeo-bathymetrical conditions from wave ripple marks and from the set-thickness of sedimentary bedforms. Furthermore, also in the supplement file, we marked the relevant part of the seismic line BEAGBE.N780025 in Fig. S4. The seismic line 8307 has been fully published in Schlunegger et al., 1997a (see revised manuscript), so we have not reproduced this section.

The original table S2 of the supplement file has now been included in the main text and split into 5 individual tables where each contains the abbreviations of the facies assemblages, the description of the bedforms and the resulting depositional setting together with a list of references.

Referee:

Technical suggestions:

1. The attached document contains numerous grammatical and editorial suggestions and comments on both the text and figures for the authors to consider in their revision.

Our response:

We have considered all suggestions upon revising our paper.

Referee:

2. As part of my review, I have prepared a document of revised figure captions, which is attached for the authors' consideration.

Our response:

We greatly acknowledge the careful and detailed work and have considered all points upon revising our paper. Please note, however, that we have rephrased most of the sections to comply with the comments of reviewer 1 and 3.

Anonymous Referee #3

General comments:

In this manuscript authors used new sedimentological and existing geological and geophysical data to assess tectonic, eustatic and surface controls on the Burdigalian transgression in the Molasse Basin. Even through most of the data and ideas appear interesting and important; there are some fairly significant items that need modification prior to publication. The comments provided below will require major revision of the manuscript. Manuscript structure needs reorganization.

1) There is no clear separation between existing data and author's own original data. Result and Discussion section include background information that should be presented earlier in Geological setting (section 2).

Our response:

This has been corrected. We improved the manuscript accordingly and provided more information on previously published geologic, chronologic and geodynamic data at the beginning of the paper. This concerns both the Alps and the Molasse basin. In this context, we have added new chapters and thus expanded the local setting significantly. We also restructured the paper such as that description of data and interpretation is clearly separated. The re-assessment of the Molasse chronology is shifted to the discussion section as a first chapter, as this could be considered as a discussion.

Referee:

2) a clear separation of observations and interpretations is missing in Result section;

Our response:

This has been done. Methods, Results and Interpretation are presented in separate chapters. We have also significantly expanded the Methods section to provide more information about how we have proceeded in the field, how we have measured paleo-flow directions and how we have collected information on the facies patterns.

Referee:

3) Scientific methods and workflow are not clearly presented;

Our response:

This has been improved. The various sedimentological methods include logging, paleo-flow measurements, estimates of paleo-water depths and mapping, and taking field notes. We have provided more details on these aspects. The results are organized according to (i) analyzed sections (e.g., Entlen section, Sense section etc), and (ii) the methods applied in the field. Such a re-organization was also requested by reviewer 1. The interpretation follows the same structure. The discussion starts with a re-appraisal of the chronological framework (same as requested by reviewer 1), followed by a discussion of the basin evolution and a possible relationship to tectonic and eustacy controls. In this regard, we combined the erosional flux scenario with tectonic processes (i.e. tectonic processes that control significant shifts in the drainage network with a negative feedback on sediment flux). We have discussed these points more clearly as requested, and we have also refined the workflow, which appears now much clearer to us. Thanks for pointing this out!

Referee:

4) Headings are not informative;

Our response:

We have changed nearly all headings such as that they are more informative.

Referee:

5) Remove of unnecessary repetitions would cut text significantly. Manuscript needs clearer explanation of the links between their own data and conclusions. Authors often jump into conclusions without showing clear link to either their own field data or literature. First, key sedimentary features observed during this study, that could be used to decipher tectonic, eustasy and surface controls, should be better described. Most of important observations in that respect are mentioned for the first time in Discussion section.

Our response:

This has been improved. We carefully streamlined the entire text and shifted published information on the architecture and evolution of the Alps and the Molasse basin to the setting section. We paid special attention on making explicit links between interpretation and observations in all sections of the discussion, and we updated and improved the text accordingly. We additionally paid special attention on carefully addressing all comments that in the annotated manuscript.

Referee:

Second, there is a confusing separation of the processes operating at the lithospheric - and crustal - scale like they are not interacting at all. These processes are poorly defined in the paper and their links to author's field data are not clear. This needs to be improved prior to publication. Detailed examples of problem areas in the text are given below and in the attached pdf.

Our response:

This has been solved. We presented the general knowledge about the processes on the surface of the Alps and at the crustal levels in the setting section. We then placed the surface and tectonic processes in one geodynamic framework, and we rephrased the discussion section accordingly such as that the reader gets a view of how lithospheric and surface processes were closely linked, which finally resulted in the transgression of the Upper Marine Molasse. We also considered all individual annotations in the attached PDF (see also response above).

Referee:

Specific comments Introduction. Opening paragraph of the introduction needs to be focused. Motivation to undertake this study is not clear. What is so controversial about Molasse Basin, i.e. Burdigalian transgression to be further studied? It is not clear what is considered by term surface controls?

Our response:

This has been improved. We specify the non-solved problems regarding the Burdigalian transgression and then outlined more clearly the aim of our contribution.

Referee:

Settings. Section on geological background should be extended. I recommend starting

by adding information on formation and geodynamic evolution of the Alps. Special attention should be given to Aar Massif, Simplon detachment and Lepontine dome (i.e. kinematic, geometry, evolution, lithology of the units involved in faulting etc.) that are in the further text marked as important controls on deposition in Molasse Basin.

Our response:

Done. We organized the setting such as that the architecture of the Alps is being presented first, followed by the geodynamic development. We did the same for the Molasse Basin. Please also see response above.

Referee:

Section 2.2 - Molasse Basin - state of the art, particularly studied Upper Miocene Unit, is poorly defined, most of important back- ground information appears in Results and Discussion.

Our response:

We have shifted the relevant information from the discussion to the setting chapter.

Referee:

Methods. I suggest to explain and list all the methods used in your study. Also, list the methods in the same order that they will appear in the results. Avoid general sentences with vague point. Explain C2 which sequence stratigraphic approach was used.

Our response:

Done. Methods, Results and Interpretation are organized such as that the same line is being preserved throughout the paper. We have expanded the related sections and added additional information on our tasks in different sub-chapters. We actually identify parts within the analyzed Entlen and Sense sections that possibly record the maximum flooding conditions of the transgression. These were then used as correlation tools across the basin. This has been clarified in the revised manuscript.

Referee:

Subchapter 3.2. is not needed. It is difficult to distinguish background data and methods. It looks like reinterpretation of the literature data.

Our response:

We have removed this section.

Referee:

Results. I recommend to start with describing your data and avoid mixing it with interpretation in this section. As written - the text is currently hard to follow. Moreover, section 4.1. includes background information that should be part of Geological setting section and Discussion.

Our response:

Done. Results and Interpretation are now separated in different chapters. In addition, the description of the sedimentological data focuses on those aspects only that will be relevant for the discussion. All other detailed data is summarized in a table to give the reader the full sedimentologic information that can be extracted from the stratigraphic sections. Accordingly, the revised text presents the key information

only, which will be used to link the basin stratigraphy to eustacy, sediment flux and tectonics. All additional information on lithofacies is presented in a table together with full references to previously published work.

Referee:

In the subsection 4.2. please systematically lay out your observations. I suggest grouping already defined lithofacies types into facies associations that are typical for particular depositional environment. This should be followed by definition of stratigraphic sequences that can be further link to suggested controls. Furthermore, this should be associated with illustrations such as your own logs or field photos that show characteristic sedimentary packages and/or stratigraphic surfaces. By doing so, you would be able to follow vertical and lateral transitions and interpret them in the light of tectonic and eustatic controls on the basin evolution.

Our response:

This has been done. The logs are presented on Figures 4a and 4b (summary logs); the details are outlined in a table, and additional photos will be included in the paper as supplement. We mark the location of the maximum flooding surfaces on Figures 4a and 4b.

Referee:

Very important in the section 4.2 Interpretation part – references are completely missing!

Our response:

They were all presented in the table, which we originally have placed in the supplement. However, we see the necessity to present all information in the main text. We thus re-organized our table, shift it to the main text and add references there. We see this as compromise between a clear acknowledgment of previously published work, and the readability of the text (which can be complicated if there are too many references).

Referee:

Discussion. Section 5 should be moved to Discussion. I recommend starting this section with the ideas on basin evolution based on your own findings. Some basin features e.g. backstepping of the alluvial mega fans are described for the first time in this section. Furthermore, it is not clear which mechanism controlled it.

Our response:

This has been done. We also paid special attention on the 'backstepping' issue and have presented the argumentation and the underlying observations more clearly. In addition, we have specified the underlying controls on the transgression in the revised manuscript. We see subduction tectonics as the principal driving force, with contributions by the uplift of individual crustal blocks (here the Aar-massif) and tectonic exhumation, all of which are related to the subduction processes. In addition, the reduction of sediment flux was likely to have been controlled by the tectonics as well through reorganizations of the drainage network when the basement blocks became uplifted. Eustatic changes in sea level possibly explain the hiatus. We have carefully modified the manuscript to make these points clearer.

Referee:

Figure comments: Minor comments are included in attached pdf. Figure 5. How did you

construct mean water depth curve? In some instances, you have contradiction between your sedimentological and paleo-depth data. Please revise curve.

Our response:

We considered all figure comments and revised the bathymetry curve as requested.

Deciphering Disentangling between tectonic, eustatic and surface sediment flux controls on the 20 Ma-old Burdigalian transgression recorded in of the Upper Marine Molasse basin in Switzerland

5

Philippos Garefalakis¹, Fritz Schlunegger¹

¹Institute of Geological Sciences, University of Bern, Bern, CH-3012, Switzerland

Correspondence to: Philippos Garefalakis (philippos.garefalakis@geo.unibe.ch)

10 Abstract

The stratigraphic architecture of the Swiss Molasse basin, situated on the northern side of the evolving Alps, reveals crucial information about the basin's geometry, its evolution and the processes leading to the deposition of the elastic material-siliciclastic sediments. Nevertheless, the formation of the Upper Marine Molasse (OMM) and the controls on the related Burdigalian transgression are not fully understood yet, have still been a matter of scientific debate. During these times, the time period from c. 20 to 17 Ma, the Swiss Molasse basin was partly flooded by a peripheral shallow marine sea, striking SW – NE. We proceeded through detailed conducted sedimentological and stratigraphic examinations analyses of several sites across the entire Swiss Molasse basin in order. An attempt is made to deconvolve the extract stratigraphic signals that can be related surface and tectonic controls. Surface related signals include stratigraphic responses to changes in sediment supply rate, variations in the eustatic sea level and sediment fluxes, while the focus on crustal scale processes lies on the uplift of the Aar massif at c. 20 Ma subduction tectonics.

20

Field examinations investigations show, that the transgression and the subsequent evolution of the Burdigalian seaway was characterized by (i) shifts in the depositional settings, (ii) changes in discharged sediment transport directions, (ii) a deepening and widening of the basin, and (iv) iii phases of erosion and non-deposition. We relate use these changes in the stratigraphic records record to a combination of surface disentangle between tectonic and tectonic surface controls at various scales. In particular As the most important mechanism, roll-back subduction of the European mantle lithosphere, delamination of crustal material and the associated rise delamination of the Aar massif crustal material most likely explain the widening of the Molasse basin particular particularly at distal sites. In addition, the delamination of crustal material also caused uplift of the Aar-massif. This process was likely to have shifted the patterns of surface loads. These Such mechanisms could have caused a flexural adjustment of the foreland plate underneath beneath the Molasse basin, which we use as mechanism to explain the establishment of distinct depositional environments and particularly the formation of subtidal-shoals where a lateral bulge is expected. In the Alpine hinterland, these processes roll-back subduction occurred simultaneously with a period of fast rapid tectonic exhumation accomplished through slip along the Simplon detachment fault and a change in the organization of the drainage network, with

30

the consequence that [the](#) sediment flux to the basin decreased. It is possible that this reduction in sediment supply contributed to the establishment of marine conditions in the Swiss Molasse basin and thus amplified the effect related to the tectonically controlled widening of the basin. Because of the formation of shallow marine conditions, subtle changes in ~~the~~ eustatic sea level contributed to the occurrence [of](#) several ~~hiatus~~[hiatuses](#) that chronicle periods of erosion and non-sedimentation.

- 5 ~~While~~[Whereas](#) these mechanisms are capable of explaining the establishment of the Burdigalian seaway and the formation of distinct sedimentological niches in the Swiss Molasse basin, the drainage reversal during OMM-times possibly requires a change in ~~the tectonic processes at the slab scale~~[tectonic processes at the slab scale, possibly including the entire Alpine range between the Eastern and Central Alps. In conclusion, we consider roll-back tectonics as the main driving force controlling the transgression of the OMM in Switzerland, with contributions by uplift of individual crustal blocks \(here the Aar-massif\), all](#)
- 10 [of which are related to the subduction processes. In addition, the reduction of sediment flux was likely to have been controlled by tectonic processes as well when the basement blocks became uplifted and when slip along detachment faults in the core of the Alps changed the catchment geometries. Eustatic changes in sea level possibly explain the various hiatuses.](#)

~~We conclude that sedimentological records can be used to decipher surface controls and lithospheric-scale processes in orogens from the stratigraphic record, provided that a detailed sedimentological and chronological database is available.~~

1 Introduction

Foreland basins and their deposits have often been used for exploring the tectonic evolution of their hinterlands, mainly because these basins are mechanically coupled with the adjacent mountain belts (Beaumont, 1981; Jordan, 1981; DeCelles, 2004). The formation of these foreland basins occurs through the flexural bending-downwarping of the underlying lithosphere in response to loading, which ~~creates accommodation space~~ results in the formation of a wedge-shaped trough where sediment accumulates (DeCelles and Giles, 1996; Allen and Allen, 2005). The shape of the foreland trough depends on the mechanical properties of the foreland plate (Sinclair et al., 1991; Flemings and Jordan, 1990; Jordan and Flemings, 1991), on the volume and thickness ~~load~~ of the sedimentary fill itself (Flemings and Jordan, 1990; Jordan and Flemings, 1991) and particularly predominantly on the tectonic and geodynamic processes leading to changes in ~~the~~ plate loading (Beaumont, 1981; Jordan, 1981; Allen et al., 1991; Sinclair et al., 1991; DeCelles and Gilles, 1996). ~~In this context, the sedimentary fill, which commonly record Flysch and Molasse phases (Sinclair and Allen, 1992), reveal crucial information about the basin's geometry and evolution. Within this context,~~ This is particularly the case for the North Alpine Foreland Basin (NAFB), ~~or the Molasse basin (Fig. 1), is probably one, situated on the northern side of the best studied foreland basins and European Alps (Fig. 1a), which has been examined~~ investigated in detail over the past decades with a focus on relating changes in the basin's evolution to Alpine orogenic events (e.g. ~~Pfiffner, 1986; Matter et al., 1980; Homewood and Allen, 1981; Allen, 1984; Keller, 1989; Schlunegger et al., 1996, 1997; 1997a; Kempf et al., 1999; Kuhlemann and Kempf, 2002).~~ The approximately 700 km long ENE—WSW striking basin stretches from France to Austria, where it broadens to a maximum width of c. 150 km (Pfiffner, 1986; Fig. 1). The NAFB is limited to the south by the Alpine fold and thrust belt, and to the north by the Jura Mountains and the Black Forest and Bohemian massifs (Homewood et al., 1986).

~~Here, we centre our work on the central part of the NAFB, commonly referred to as~~ 2011). In the Swiss Molasse basin (Fig. 1), which stretches from Lake Geneva to Lake Constance overpart, this basin has experienced two periods when sedimentation occurred within a total length of c. 270 km and a maximum width of c. 80 km (Fig. 2). We particularly focus on the c. 20 Ma old sea (Matter et al., 1980). The Burdigalian transgression and pay special attention on establishing the link between the sedimentary processes recorded by the Upper Marine Molasse (OMM) deposits and the contemporaneous geometrical changes of the basin. The extension and dimension-time (early Miocene), c. 20 Ma ago, was such a period when the basin became occupied by a shallow-marine seaway, linking the Paratethys in the NE with the Tethys in the SW (Allen et al., 1985). The marine ingression resulted in the accumulation of marine sediments, which have been referred to as Upper Marine Molasse group (OMM; Matter et al., 1980; Allen, 1984). Although the history and geometry of the Burdigalian seaway and the related sedimentary processes are well known, and several authors through detailed sedimentological and chronological investigations (e.g. Lemcke et al., 1953; Allen, 1984; Allen et al. 1985; Homewood et al. 1986; Matter, 1964; Burbank et al., 1992; Kempf, 1998; Kempf et al., 1997; Doppler, 1989; Keller, 1989; Jin et al., 1995; Salvermoser, 1999; Strunck and Matter, 2002; Schlunegger, 1996, 1997; Kuhlemann and Kempf, 2002) examined paleo-discharge directions, sedimentary thicknesses, and

depositional environments of the OMM. Furthermore, these authors were also discussing possible controls leading to the marine ingression. Despite these efforts; Reichenbacher et al., 2013), the controls on the Burdigalian this transgression in this basin are not fully understood yet have still been a matter of ongoing scientific debate. Previous authors (e.g. Allen et al., 1985; Homewood et al., 1986; Keller, 1989; Strunck and Matter, 2002; Reichenbacher et al., 2013) proposed a combination of a reduced sediment flux and a rise in global sea level as possible mechanisms. However, the Burdigalian was also the time when the external massifs in the thermo-chronometric data from the core of the Alps experienced a period of fast uplift (Leponine dome, Fig. 1; Boston et al., 2017) and structural work in the external Aar-massif (Fig. 1; Herwegh et al., 2017), which could have contributed to the revealed that the Burdigalian was also the time of major thrusting, tectonic exhumation and surface loading in the Alps. These processes were related to the subduction of the European continental plate underneath the African plate (Schmid et al., 1996). Accordingly, it was proposed that tectonic processes were equally important to have caused a flexural downwarping of the foreland plate and thus to the (Piffner et al., 2002; Schlunegger and Kissling, 2015) and, as a consequence, the transgression of the peripheral sea (Sinclair et al., 1991). It appears that The key to disentangle between these diverging views on the driving forces are mainly due to the rather regional focus of the aforementioned studies. In particular, previous authors mainly focused either on the western (e.g. Strunck and Matter, 2001), the central (e.g. Sinclair et al., 1991; Schlunegger et al., 1996; 1997) or the eastern part (e.g. Keller, 1989; Kempf et al., 1999) of the Swiss underlying mechanisms (eustasy, sediment flux, tectonics) is likely to be situated in the Swiss part of the Molasse basin. Here, we analysed outcrops and sections along the entire Swiss basin situated at both proximal and distal positions in relation to the Alpine front (Fig. 2) with a particular focus on the 20 Ma old Burdigalian, where the marine transgression. We aim to explain, through a sedimentological and stratigraphic approach at the basin scale, the influence of possible controls on this transgression including: (i) an eustatic rise in sea level, (ii) a reduction resulted in sediment flux or (iii) an increase the final connection, and thus in tectonically controlled accommodation space, the linkage, of the Tethys in the SW with the Paratethys in the NE (Allen and Homewood, 1984).

The aim of this paper is to disentangle between tectonic processes, a reduction of sediment flux and changes in the eustatic sea level as controls on the transgression of the OMM in Switzerland. We analyzed OMM outcrops and sections along the entire Swiss Molasse basin at both proximal and distal positions relative to the Alpine front (Fig. 1a). To this extent, we investigated palaeo-flow directions, sedimentary facies, and related depositional settings of the OMM, and we calculated palaeo-water depths using hydrological concepts. However, a chronological framework is absolutely required for correlating sections across a basin where facies relationships are strongly heterochronous, as it is the case for the Swiss Molasse basin (Matter et al., 1980). Therefore, we also re-assessed the temporal framework of the analysed sections through a compilation of previously published magnetostratigraphic and biostratigraphic data, and we correlated the individual sections across the basin.

2 Setting

2.1 The ~~Swiss Molasse Basin and the Central~~ European Alps

~~The deposits of and the Swiss Molasse basin record two large scale transgressive regressive mega sequences deposited between c. 32 and 10–5 Ma (e.g. Sinclair, 1997; Kempf et al., 1997, 1998; Kuhlemann and Kempf, 2002; Cederbom et al., 2004, 2011). These two shallowing up mega sequences consist of four lithostratigraphic groups, for which we employ the common German abbreviations in this work (Matter et al., 1980). Prior to the first mega cycle, from approximately 35 Ma to 32 Ma, the North Helvetic Flysch (NHf, early Oligocene) was deposited during the underfilled Flysch basin stage (Sinclair and Allen, 1992). The Flysch period was characterized by a deep marine trench close to the evolving Alps where turbidity currents resulted in the accumulation of mud and sandstone on submarine fans (Allen et al. 1991; Lu et al., 2018). This stage was followed by a regressive sequence, when the initial rise of the Alps c. 32–30 Ma ago (e.g., Garefalakis and Schlunegger, 2018) was associated with fast erosion and large sediment fluxes to the Molasse basin (Sinclair, 1997). This resulted in the deposition of the Lower Marine Molasse Group (UMM, Rupelian), consisting of shallow marine mud and sandstones (Diem, 1986) and marking the end of the underfilled stage. The first mega sequence was finally terminated by the deposition of conglomerates, sandstones and mudstones of the terrestrial (overfilled basin) Lower Freshwater Molasse Group (USM; Platt and Keller, 1992) between the early Oligocene and the early Miocene (Rupelian to Aquitanian). The second transgressive regressive cycle started with the deposition of the shallow marine sand and mudstones of the Upper Marine Molasse Group (OMM) around 20 Ma (Burdigalian). This second mega cycle ended with conglomerates and sandstones of the regressive, terrestrial Upper Freshwater Molasse Group (OSM) during late Burdigalian to late Serravallian times. Sedimentation in the Molasse basin continued up to c. 10–5 Ma, when a phase of uplift resulted in the erosion and the recycling of previously deposited Molasse deposits (Mazurek et al., 2006; Cederbom et al., 2004, 2011).~~

~~The basin is bordered to architecture and evolution of the south by the Alps~~

~~The doubly-vergent Alpine orogen (Fig. 1b) is the consequence of the late Cretaceous to present continent-continent collision between the European and Adriatic plates (Schmid et al., 1996; Handy et al., 2010). It comprises a nappe stack with a crystalline core that is exposed in the Lepontine dome and the external massifs (e.g. Aar-massif; Spicher, 1980). At deeper crustal levels, the Alpine orogen is underlain by a thick crustal root made up of a stack of lower crustal material derived from the European continental plate (Fry et al., 2010). At deeper levels; Fig. 1b). Beneath the core of the orogen, the c. 160 km-long (Lippitsch et al., 2003) lithospheric slab of the European mantle lithosphere continental plate bends the foreland plate towards the south-east, resulting in a downwarping of the European plate (Fig. 1b). The large scale deflection of the plate and the formation of accommodation space in the Molasse basin is thus the consequence of this bending (Schlunegger and Kissling, 2015). In addition, the modern topography has formed in response to the isostatic equilibrium between the buoyancy of the crustal root and the vertically directed slab load forces (Kissling, 1993; Kissling and Schlunegger, 2018). This bending was mainly driven by slab loads due to the relatively large density of the subducted lithospheric mantle in comparison with the~~

surrounding asthenosphere as seismo-tomography data reveals (Lippitsch et al., 2003). On the northern side of the orogen, the highest unit is made up of Austroalpine nappes that structurally overlie the (meta)sedimentary successions of the Penninic and the underlying Helvetic thrust nappes (Fig. 1a). The front of the Helvetic and Penninic units is referred to as the basal Alpine thrust (Fig. 1b). The southern side of the Alps is made up of the Southalpine thrust sheets that consist of crystalline basement rocks and sedimentary units of African origin. This fold-and-thrust belt is bordered to the south by the Po Basin (Fig. 1a). The north-vergent Alpine thrusts are separated from the South Alpine nappes by the north-dipping Periadriatic line that accommodated most of the shortening during the Oligocene and the early Miocene by backthrusting and right-lateral slip (Schmid et al., 1996). The Lepontine dome (Fig. 1), made up of Penninic crystalline rocks, is bordered to the west by the Simplon detachment fault, where normal faulting resulted in rapid tectonic exhumation of the dome between late Oligocene and early Miocene times with a peak recorded by thermo-chronometric data at 20 Ma (Fig. 1b; Hurford, 1986; Mancktelow, 1985; Mancktelow and Grasemann, 1997; Schlunegger and Willett, 1999; Boston et al., 2017). This was also the time, when the Aar-massif, situated on the European continental plate (Fig. 1b), experienced a period of rapid vertical extrusion (Herwegh et al., 2017).

Recently, slab loads have been considered as the major driving force of the subduction history of the European plate and for the exhumation of crystalline rocks (Kissling and Schlunegger, 2018). This also concerns the uplift of the Aar-massif and the rapid exhumation of the Lepontine dome (Fig. 1). Herwegh et al. (2017) and Kissling and Schlunegger (2018) proposed a mechanism referred to as roll-back subduction to explain these observations. According to these authors, delamination of crustal material from the European mantle lithosphere along the Moho resulted in a stacking of buoyant lower crustal rocks beneath the Lepontine dome and the Aar-massif forming the crustal root (Fry et al., 2010; Fig. 1b). These processes are considered to have maintained isostatic equilibrium between the crust and the subducted lithospheric mantle and thus the elevated topography (Schlunegger and Kissling, 2015). Additionally, they most likely balanced, through the stacking of the crustal root (Fry et al., 2010, Fig. 1b), the rapid removal of upper crustal material in the Lepontine dome at c. 20 Ma (Schlunegger and Willett, 1999; Boston et al., 2017). Delamination of crustal material has also been invoked to explain the contemporaneous rapid exhumation and northward thrusting of the Aar-massif along steeply dipping thrusts (Herwegh et al., 2017). These processes occurred at the same time when (i) the drainage network of the Central Alps was reorganized (Kuhlemann et al., 2001a; Schlunegger et al., 1998), (ii) sediment flux to the basin decreased, as revealed by sediment budgets (Kuhlemann, 2000; Kuhlemann et al., 2001a, 2001b), and (iii) when the Burdigalian transgression occurred in the Swiss part of the Molasse basin. We will thus refer to these processes when discussing the controls on the Burdigalian transgression within a geodynamic framework.

The architecture and evolution of the Molasse basin

The approximately 700 km long and ENE – WSW striking basin stretches from France to Austria, where it broadens from <30 km to a maximum width of c. 150 km (Pfiffner, 1986; Fig. 1a). The Molasse basin is limited to the north by the Jura Mountains and the Black-Forest- and Bohemian-massifs, and to the south by the basal Alpine thrust (Homewood et al., 1986).

Reconstructions of the evolution of the Molasse basin (Fig. 2a) have been the focus of many research articles over the past years (e.g. Matter et al., 1980; Homewood and Allen, 1981; Allen, 1984; Keller, 1989; Schlunegger et al., 1996; Sinclair, 1997; Kempf et al., 1999; Kuhlemann and Kempf, 2002; Ortner et al., 2011; Reichenbacher et al., 2013). This has resulted in the general notion that the large-scale subsidence history of the Molasse basin was closely linked with the geodynamic evolution of the Alps (Sinclair et al., 1991; Kuhlemann and Kempf, 2002; Pfiffner et al., 2002; Ortner et al., 2011; Schlunegger and Kissling, 2015). The development of this basin as a foreland through has been considered to commence with the closure of the Alpine Tethys in late Cretaceous times (Lihou and Allen, 1996; Schmid et al., 1996). This was the time when subduction of the European oceanic lithosphere with a large density beneath the Adriatic continental plate started. Large slab load forces resulted in a downwarping of the European foreland plate and the formation of a deep marine trough (Schmid et al., 1996), where sedimentation occurred by turbidites (Sinclair, 1997). This resulted in the accumulation of mud- and sandstones on submarine fans (Allen et al., 1991; Lu et al., 2018). The material sources of these mass movements were situated in a volcanic arc on the African continental plate that represented the upper plate (Lu et al., 2018; Reichenwallner, 2019). This first period of basin evolution has been referred to as the underfilled or the Flysch stage in the literature (Fig. 2b; Sinclair and Allen, 1992), mainly because sedimentation occurred within a deep marine trough. The related deposits have been called the North Helvetic Flysch in the Alpine literature (NHF, early Oligocene; Sinclair and Allen, 1992). The situation changed at 35 – 32 Ma when the buoyant continental lithosphere of the European plate started to enter the subduction channel. Strong tension forces started to operate at the stretched margin of the European continental crust particularly beneath the Central Alps (Schmid et al., 1996), with the result that the subducted oceanic lithosphere of the European plate broke off (Davies and von Blanckenburg, 1995). The consequence was a rebound of the European plate, a rise of the Central Swiss Alps and an increase in sediment flux to the Swiss Molasse basin (Sinclair, 1997; Kuhlemann et al., 2001a, 2001b; Willett, 2010; Garefalakis and Schlunegger, 2018), which became overfilled at c. 30 Ma (Sinclair and Allen, 1992; Sinclair, 1997). The subsequent post 30 Ma-stage of basin evolution has been referred to as the Molasse, or overfilled stage (Sinclair and Allen, 1992) (Sinclair, 1997). Molasse sedimentation occurred from c. 30 Ma onward and was recorded by two large-scale, transgressive-regressive mega-sequences (Fig. 2b; e.g. Sinclair, 1997; Kempf et al., 1997; 1999; Kuhlemann and Kempf, 2002; Cederbom et al., 2004; 2011). These two mega-sequences consist of four lithostratigraphic groups. The first mega-sequence comprises the Lower Marine Molasse (UMM; Diem, 1986) and the Lower Freshwater Molasse (USM; Platt and Keller, 1992), and the second mega-sequence consists of the Upper Marine Molasse (OMM; Homewood et al., 1986) and the Upper Freshwater Molasse (OSM; Matter et al., 1980). Sedimentation in the Molasse basin continued up to c. 10 – 5 Ma, when a phase of uplift during Pliocene times resulted in erosion and recycling of the previously deposited Molasse units (Mazurek et al., 2006; Cederbom et al., 2004; 2011). The Alpine architecture is the consequence of the Late Cretaceous to present continent-continent collision between the European and Adriatic plates, which resulted in the build up of the Alpine edifice (Schmid et al., 1996). At 20 Ma, the phase of nappe stacking was superseded by a period of vertical extrusion of the Lepontine dome (Hurford, 1986) and the Aar massif (Herwegh et al., 2017). This was also the time, when the slip along the Simplon detachment fault occurred at the fastest rates,

resulting in the fast exhumation of deeper crustal levels to the surface (Manektelow, 1985; Manektelow and Grasemann, 1997; Boston et al., 2017).

2.2 The Upper Marine Molasse

5 This erosion reached deeper stratigraphic levels in the western part of the Molasse basin than in the eastern segment (Baran et al., 2014) with the consequence that the OMM deposits are only fragmentarily preserved in the west (Fig. 2a).
Sediment dispersal has changed during the Molasse stage of basin evolution. Prior to 20 Ma, during USM times, measurements of sediment transport directions (Kempf et al., 1999) and sediment provenance tracing (Füchtbauer; 1964) revealed that the sedimentary material was transported to the east by braided to meandering streams. At that time, a coastline was situated near Munich, separating a deep marine trough farther east from a terrestrial environment to the west of Munich (Kuhlemann and
10 Kempf, 2002). During OMM times, heavy mineral assemblages reveal that the Swiss Molasse basin operated as a closed sedimentary trough, where all supplied material was locally stored (Allen et al., 1985). During OSM times, heavy mineral data imply that material with sources in the Hercynian basement north of Munich or the Bohemian-massif was supplied to the Swiss Molasse (“Graupensandrinne”; Allen et al., 1985; Berger et al., 2005), suggesting that material transport occurred towards the west (Kuhlemann and Kempf, 2002). The details of the reversal of the drainage direction have not yet been elaborated, and
15 related scenarios lack a database with palaeo-flow information, particularly for the OMM. The establishment of such a database will be part of the scope of this article, mainly because the reversal of drainage direction in the basin occurred sometime during deposition of the OMM.

2.3 The Upper Marine Molasse

20 *Lithostratigraphic and sedimentologic framework*

The Upper Marine Molasse (OMM) deposits, which are the focus of this paper study, mainly ~~comprise~~ consist of a suite of sandstones and mudstone interbeds. In the central basin, these sediments were deposited in a shallow marine, ~~e.~~ sandstones and mudstones that were deposited between c. 20 – 17 Ma (Fig. 2) in a c. 70 – 80 km-wide seaway during Burdigalian times between c. 20 – 17 Ma (Allen and Homewood, 1984; Allen et al., 1985; Keller, 1989). At; Strunck and Matter, 2002). Close
25 to the proximal basin border Alpine thrust front, the OMM-successions are up to 900 m thick and thin to a few tens of meters towards the distal basin margin. ~~Thick~~ farther northwest.

Large streams with sources in the Central Alps supplied their material to the Molasse basin, thereby forming megafans with diameters >10 km that interfingered with the sea (Schlunegger et al., 1996; Kempf et al., 1999). Consequently, the facies relationships were strongly heterochronous across the basin, and terrestrial deposits grade into marine sediments over a lateral
30 distance of few tens of kilometres. This is also the case in the study area, where thick conglomerate packages situated at the Alpine thrust front c. 50 km to the NE of the Aar-massif (Napf conglomerates) ~~separated;~~ Matter, 1964) separate the basin into an southeastern and northwestern segments with different lithostratigraphic schemes (Fig. 3a). For simplicity purposes, these areas will be referred to as the eastern and western segment (Fig. 3) segments. East of the Napf conglomerates, in the following

text denoted as the Napf-units of the OSM (Matter, 1964), the OMM has been grouped into in two transgressive-regressive packages referred to as the Lucerne- and the St. Gallen-Formations (Keller, 1989), which. Both units are separated by a m-thick palaeo-soil. For simplicity purposes, we sol (Schlunegger et al., 2016). We will refer to these units as the OMM-I (Lucerne-Fm) and the OMM-II (St. Gallen-Fm), respectively. Keller (1989) additionally categorized the OMM-I east of the Napf-units into a lower wave-dominated unit and an upper unit where tidal processes are recorded, which we refer to as the OMM-Ia and OMM-Ib.

West of the Napf and also at the proximal basin border, the OMM has also been categorized in two units (Fig. 3a) but with a different scheme and different names. These are the Sense-Formation at the base (suite of sandstones with mudstone interbeds) and the Kalchstätten-Formation at the top (alternation of sandstones and mudstones). Further up-section, these marine deposits (Strunck and Matter, 2002) grade into the fluvial conglomerates of the Guggershorn-Formation and thus into the OSM (Strunck and Matter, 2002) (Fig. 3a). Magnetostratigraphic dating showed that the accumulation of the Guggershorn-Formation occurred contemporaneously with marine (OMM) sedimentation at more distal sites. These conglomerates thus represent the deposits of a braided stream that shed its material to the OMM sea, similar to the conglomerates in the Napf. As will be put forward in the discussion of this work, the Molasse deposits on the western side of the Napf can be correlated with the OMM-I and OMM-II units on the eastern side (Fig. 3a).

In the central basin near Fribourg, also on the western side of the Napf, sedimentological investigations of sandwaves (Homewood et al. 1980; Homewood and Allen, 1981) disclosed the occurrence of tidal bundles and a bi-directional dispersal of sedimentary material. These deposits have been assigned to a subtidal environment (Homewood and Allen, 1981), where material with sources in the Central Alps were re-distributed in the basin by strong tidal currents (Allen et al., 1985; Kuhlemann and Kempf, 2002). Lithostratigraphic correlations suggest that the deposits at Fribourg most likely correspond to the lower Sense-Fm (Python, 1996) and thus to the OMM-Ia (see discussion, and Fig. 3a).

In the distal basin, also east of the Napf units, the OMM I deposits comprise a suite of sandstone beds at the base, followed by a succession of between the Lake Neuchâtel and the Wohlen areas (Fig. 2a), coarse-grained sandstones with large-scale cross-beds where individual grains are larger than 2 mm have been interpreted as subtidal sandwaves (Allen et al., 1985). These deposits are either calcareous-sandstones with shelly-sandstones (“fragments, referred to as the “Muschelsandstein”; Jost et al., 2016) at the top. The overlying OMM II comprises conglomerates, sandstones and mudstones” (Allen et al., 1985, Fig. 3a). Alternatively, they occur as coarse-grained cross-bedded sandstones with large litho-clasts, also called the “Grobsandstein” (Jost et al., 2016). West of the Napf units, the OMM has been grouped in three units (Fig. 3), which are from the base to the top: the Sense beds (suite of sandstones with mudstone interbeds), the Kalchstätten Formation (alternation of sandstones and mudstones) and the Guggershorn Formation (succession of conglomerates with sandstone interbeds) (Strunck and Matter, 2002). As will be shown later, the Sense beds and Kalchstätten Fm correspond to the OMM I, while the Guggershorn Fm is a time equivalent of the OMM II. Similar to the east, the western distal basin is made up of sandstones at the base, and “Muschelsandstein” deposits at the top. As outlined above, the Pliocene phase of uplift and erosion (Cederbom

et al., 2004; 2011) resulted in the current exposure pattern where OMM deposits are only fragmentary preserved in the west (Fig. 2).

3 Methods

3.1 Sedimentological investigations and study sites

5 We applied state of the art sedimentological techniques to examine different sections through time. The research sites are located at both proximal and distal positions within the basin. We explored these sections for environmental conditions, the relative palaeo bathymetry and palaeo discharge directions. Correlations between the sections have been accomplished by using interpreted seismic data (Line 8307; Schlunegger et al., 1997) and through compilation of ages constrained by magneto-polarity stratigraphies (Strunck and Matter, 2002; Schlunegger, 1996, 1997) and mammal biostratigraphies (Keller, 1989; Engesser, 1990; Jost and Kempf, 2016). Non-dated sections have been correlated with a sequence stratigraphic approach.

10 We proceeded through detailed sedimentological investigations of key sites (Fig. 2), which expose the OMM I succession in proximal (*Entlen section* east of the *Napf units*; *Sense section* west of the *Napf units*), central (*St. Magdalena site*, *Gurten drill core*) and in distal positions (*Mägenwil site*). The key sites have been analysed in the field and on digital photos at the scale of 1:50. We categorized the sediments into lithofacies types (e.g.

15 *Chronostratigraphic* ~~Schaad et al., 1992; Keller, 1989~~) based on the ensemble of sedimentary characteristics including: grain size, thickness, lateral extend if applicable, sedimentary structure, basal contact, colour and fossil content. Additionally, the sediments have been analysed according their palaeo bathymetrical conditions. Please refer to the supplement for the details of the methodological approaches, the summary of the lithofacies description and interpretation, and for the references to the related articles.

20 Finally, depositional systems were defined as an ensemble of distinct lithofacies types including the related palaeo bathymetric conditions. These depositional systems have been mapped at the scale of 1:10'000 at various sites where suitable outcrops were present (see Fig. 2 for visited sites). Published information from deep drillings (*Boswil 1*; *Hünenberg 1*) and seismo-stratigraphic data (Line 8307; Schlunegger et al., 1997, Line BEAGBE.N780025; Fig. S4, supplement) completed the available database. Palaeo current directions were measured from the occurrence of imbricated clasts, solmarks, parting lineations, orientation of cross beds and ripple marks.

3.2 Reconstruction of the chronological framework

The chronological framework of Ages for the OMM deposits ~~in the region has~~ been established by multiple authors through palaeontological analyses of ~~mammal~~mammalian fragments and teeth (Keller, 1989; Schlunegger, 1996; Kempf et al., 1999) and ⁸⁷Sr/⁸⁶Sr chemo-~~stratigraphies~~stratigraphy (Keller, 1989), ~~yielding~~. The latter ~~yield~~ a numerical age between

30 c. 18.5 and 17 Ma, particularly for the OMM-II (*St. Gallen Fm.*) ~~on the eastern side of the Napf~~. Subsequent magneto-polarity chronologies (Schlunegger et al., 1996; Strunck and Matter, 2002) paired with further micro-~~mammal~~mammalian discoveries (Kempf et al., 1997; Kempf, 1998; Kälin and Kempf, 2009; Jost et al., 2016) allowed ~~to~~an update of the chronological framework (Fig. ~~3~~3b) of Keller (1989) through correlations with the Magneto-Polarity-Time-Scale (MPTS) of Cande and

Kent (1992, 1995) and the most recent astronomically tuned Neogene time-scale (ATNTS, Lourens et al., 2004). The original correlations of the magneto-zones with the MPTS, or alternatively the ATNTS, were based on the inference that sedimentation occurred continuously (Schlunegger et al., 1996; Strunck and Matter, 2002). However, based on a reassessment of the magneto-polarity stratigraphy of the *Napf*-section (*Napf*-units, Fig. 3) and further sections in the eastern Swiss Molasse basin, Kálin and Kempf (2009) suggested that sedimentation was possibly interrupted by several hiatus. Finally, through stratigraphic investigations of the seismic line 8307 (Fig. 2), Schlunegger et al. (1997) proposed that an erosional unconformity and thus a hiatus separates the OMM I from the OMM II. Unconformities separating lower and upper OMM sequences have not been considered by those authors who established the original chronological framework for the OMM sequences in the region (Keller, 1989; Schlunegger et al., 1996; Strunck and Matter, 2002). Consequently, we reassessed the temporal framework through a compilation of the original and most recent information in the literature, and through mapping and sedimentological investigations (2004). This yielded in the notion that the transgression of the peripheral sea and the deposition of the OMM started at c. 20 Ma and was synchronous, within uncertainties, across the entire Swiss Molasse basin (Strunck and Matter, 2002). However, a temporal correlation of sections across the *Napf*, i.e. between eastern and western Switzerland (Fig. 3a), and a harmonization of the stratigraphic schemes (Fig. 3b) has not been accomplished yet. This will be accomplished in this paper, and it will build the temporal framework for the discussion of the development of the basin.

3 Methods

3.4 Results and Interpretation

4.1 Revised chronology **Sedimentological investigations**

Location of sections and available database

Following the scope of the paper, we established the facies relationships and sediment transport patterns during the transgressive phase of the OMM and thus mainly focused on the OMM-I. We proceeded through sedimentological investigations of key-sites (Fig. 2a), which expose the related succession in proximal (Entlen section east of the *Napf*-units; Sense section west of the *Napf*-units), central (St. Magdalena site, Gurten drill core) and in distal positions (Lake Neuchâtel and Wohlen areas). The lithofacies in the Entlen and Sense sections was investigated in the field at the scale of 1:50. At each outcrop along these sections, data was collected as notes in the field book and, hand drawings on digital photos (available from the senior author upon request). The results are then presented as logs on Figure 4, and in Tables 1 and 2. The St. Magdalena site and the Lake Neuchâtel and Wohlen areas only display outcrops rather than sections. Therefore, the sediments at these locations have been sketched in the field and on digital photos, thereby paying special attention on collecting information about the orientation and thickness of cross-beds. The sedimentary material of the c. 200 m-deep Gurten drill core is not available. However, the sediments were photographed at high resolution at the University of Bern in 1989 (see supplement Fig. S3). We used these photos to extract information on the lithofacies association encountered in the drilling.

Reconstruction of sedimentary architecture

The lithofacies have been identified (e.g. [Schaad et al., 1992](#); [Keller, 1989](#)) based on the [assemblage of sedimentary characteristics including: grain size, thickness, lateral extent if applicable, sedimentary structures, basal contact, colour and fossil content \(Tables 1 to 5\)](#). The lithofacies types correspond to individual bedforms (see Tables 1 to 5 for references), which bear information on flow strengths, flow directions, sediment supply and water depths (e.g., [Keller, 1989](#)). The combination of these parameters, usually recorded by distinct assemblages of lithofacies types, can be used to identify distinct sedimentary settings. Related concepts of facies analysis have been documented for fluvial deposits ([Miall 1978; 1985; 1996; Platt and Keller, 1992](#)) but are less standardized for shallow marine deposits. Here, we followed [Keller \(1989\) and Schaad et al., \(1992\)](#), who developed a concept for shallow marine deposits where lithofacies types are grouped to facies assemblages in a hierarchic order, based on which distinct shallow marine settings can be interpreted. We followed these authors and assembled the various lithofacies types into 5 depositional settings, which are from land to sea: Terrestrial, backshore, foreshore, nearshore and offshore. We then mapped the depositional settings at the scale of 1:25'000 at various sites across the Swiss Molasse sequences basin where suitable outcrops were present (see Fig. 2a for visited sites).

Determination of sediment transport directions

Sediment transport directions were determined from orientations of clast imbrications, gutter casts, and dip directions of cross-beds. In addition, the orientation of the coastline can be inferred from sediment transport within the surf-and-swash zone at the wet beach where rolling grains carve mm-thin rills in the beach deposits, which are oriented perpendicular to the coast. These rills are recorded by linear grooves, or parting lineations, on the surface of sandstones ([Allen, J., 1982; Hammer, 1984](#)). We thus measured the orientation of these features where visible. We also determined the strike direction of oscillation-ripple marks to infer the orientation of waves and thus of the coastline.

Calculation of palaeo-water depths

We analysed the sediments in the key sections according to their palaeo-water depths. For oscillation-ripple marks, the ripple metrics (spacing between ripple crests and ripple heights) together with the grain size can be used to infer water depths at the time the oscillation-ripples were formed ([Diem, 1985; Allen et al., 1985](#)). We thus measured the ripple metrics with a meter stick together with grain sizes in the field and calculated the water depths following [Allen \(1997\)](#). Likewise, minimum water depths can be inferred from heights of cross-beds as examples from modern streams have shown ([Bridge and Tye; 2000; Leclair and Bridge, 2001](#)). Please refer to the supplement for the deviation of the related equations. Published information from deep-drillings ([Boswil 1; Hünenberg 1; Schlunegger et al., 1997a](#)) and seismo-stratigraphic data ([Line 8307; Schlunegger et al., 1997a, Line BEAGBE.N780025; Fig. S2, supplement](#)) completed the available database.

4 Results

Proximal basin border to the east of the Napf: Entlen section (site 13 on Fig. 2a)

The sedimentary suite of the c. 370 m-thick OMM-Ia at Entlen (Fig. 4a and Fig. S4a in supplement) records a large diversity of lithofacies types (Table 1). Parallel-laminated (Sp), fine- to medium-grained sandstone packages are cm- to dm-thick and normally graded. These deposits alternate with dm-thick low-angle cross-bedded units with tangential lower boundaries (Sc, Sct_a) and layers with a massive structure (Sm). Gravel and pebble layers (Sg) and shell fragments (Shf) are visible where sandstone units have erosive bases. Current- (Scr) and oscillation-ripple marks (Sos), locally with branching crests (Sbr), as well as flame-fabrics or sand-volcanoes (Sv) are present only in some places. Fine-grained lithofacies including mm- to cm-thick parallel-laminated to massive mudstone layers (Mp, Mm). Siltstone climbing-ripples (Mcl) are subordinate in the OMM-Ia suite. Mudstone drapes (Md), a few mm thick, mostly occur on top of current ripple-marks (Scr). In places, root-casts are associated with yellow- to ochreish-mottled colours.

The overlying c. 430 m-thick OMM-Ib (Fig. 4a and Fig. S4a in supplement) comprises fine- to medium-grained sandstone packages with mudstone interbeds (Table 1). Low-angle trough- (Sct_r) or tabular (Sct_a) cross-bedded sandstone beds are several decimeters thick. The Sct_r-sandstones contain current-ripple marks (Scr) at their base, whereas laminae-sets of Sct_a-sandstones are interbedded with current-ripples (Scr) recording opposing sediment transport direction. At one site, dm-thick sandstone beds display a planar base and a wavy top with a wavelength of several meters (Spw; Fig. 4a). Parallel-laminated (Sp) and massive-bedded (Sm) sandstone beds are dm-thick and mainly found at the top of the OMM-Ib unit. Mudstones mostly occur as mudstone drapes (Md) on top of current ripple-marks (Scr). Lenticular- and flaser-interbeds (Mle, Mfl) are dm thick and characterized by current ripple-marks with truncated crests. The OMM-Ib then ends with a m-thick mudstone displaying yellow to reddish mottling, root casts and caliche nodules.

Estimates of palaeo-water depths (see supplement) reveal that the OMM-Ia sedimentary rocks were deposited in shallow conditions <5 m deep (Fig. 4a and Table S2). At the base of the OMM-Ib palaeo-water depths were >15 m and thus deeper than compared to the OMM-Ia unit (see supplement). The OMM-Ib then shallows towards the top.

Measurements of bedform-orientations of the OMM-Ia deposits reveal sediment transport directions between 315° NW and 60° NE, with a dominant NE-directed transport (Fig. 4a). During OMM-Ib times, transport directions were bi-directional, and measurements reveal the full range between 260° W and 70° E (Fig. 4a). Dominant transport directions of the OMM-Ib sediments change towards the N and to the W up-section.

Proximal basin border in the center: Napf-units (site 12 on Fig. 2a)

The Napf-units, which are a terrestrial interval of the OMM and the OSM (Fig. 3; Schlunegger et al., 1996), are c. 1550 m thick and include a succession of conglomerates, sandstones and mudstone interbeds (Matter, 1964), which we categorize into 5 lithofacies types (Table 2, Fig. S4d in supplement). Individual conglomerate beds are up to 10 m thick and display stacks of 2 – 3 m-thick beds with massive (Gm) to cross-bedded (Gc) geometries. The sandstone beds occur as massive-bedded (Sm) and cross-bedded (Sc) units. Interbedded mudstones are horizontally bedded (Mp) and have a yellowish-reddish mottling,

caliche nodules and root cast. Palaeo-flow measurements imply a change from a NE-directed transport during USM-times to a NW-directed sediment transport between OMM-I- and OSM times.

Proximal basin border to the west of the Napf: Sense section (site 7 on Fig. 2a)

5 The OMM at Sense (Fig. 4b and Fig. S4b) starts with a c. 200 m-thick succession of predominantly sandstones with some mudstone interbeds. Medium- to coarse-grained sandstone beds, up to 2 – 3 m thick, are massive-bedded (Sm), parallel-laminated (Sp) and trough cross-bedded (Sct_t) (Table 3). They also occur as m-scale tabular cross-beds (Sct_a) forming several m-thick sigmoidal fore-sets (Sc) with top- and bottom-sets and pebbly lags (Sg). These packages are well exposed along a nearby road-cut (Heitenried, Fig. 2a; 46°49'27" N / 7°18'42" E; Fig. S4c in supplement). Some of these Sct_t-cross-beds contain
10 current-ripple marks (Scr), which are draped with a muddy layer (Md). Ripple marks also build up tabular sandstone bodies. They are either asymmetric (Scr) or symmetric (Sos) and may display branching crests (Sbr). In places, the sandstone bodies are highly bioturbated (Sf). Mudstone interbeds are 10 – 20 cm thick, massive- (Mm) to parallel-laminated (Mp) and strongly bioturbated (Mf).

15 The first-occurrence of 5 – 10 m-thick sandstone beds at 200 m stratigraphic level (Fig. 4b) marks a distinct shift in the stratigraphic record where several m-thick cross-bedded sandstone beds dominate the sedimentary succession. At this level, (i) 5 – 10 m-thick normally graded sandstone beds overlie an erosive base and display epsilon cross-beds (Sce); (ii) cross-bedded sandstones (Sct_a) are several meters thick and tens of meters wide, and individual laminae-sets are superimposed by current ripples (Scr) with an opposite flow direction than the cross-beds themselves; nearly all cross-beds (Sc) are superimposed by mudstone drapes (Md); and (iii) medium-grained sandstones display ridge-and-swale bedform geometries
20 (Spw) with a small amplitude of a few dm and a large wavelength of several m. Some of these Spw-facies are occasionally covered with oscillation-ripple marks (Sos). The Sense section ends with an alternation of dm-thick mudstone beds (Mm) and m-thick massive- to cross-bedded conglomerates (Gm, Gc). These conglomerates then evolve towards an amalgamation of several m-thick, massive- and cross-bedded packages, characterizing the uppermost c. 50 m suite of the Sense section (Fig. 4b).

25 Estimates of palaeo-water depths range between 5 – 10 m (Fig. 4b and supplement Table S3) during deposition of the lowermost 200 meters. Conditions were deepest at the 200 m stratigraphic level, reaching water depths in the range of up to 30 m (see supplement). Measurements of sediment transport directions cover the range between c. 0° N and 90° E (Fig. 4b) at the base of the Sense section, which then changed to an axial, bipolar SW – NE-directed transport and to a W-directed transport towards the end of the section (Fig. 4b).

30 *Basin axis: St. Magdalena site and Gurten drill core (sites 4 and 9 on Fig. 2a)*

The sandstones within a cave-system near Fribourg (St. Magdalena; Fig. 2a and Fig. S4c in supplement) are medium- to coarse-grained and display an amalgamation of up to 1 – 3 m-wide, cross-bedded troughs (Sct_t) with current-ripple marks (Scr) at their base. The cross-bedded troughs and the ripple marks are both covered by mudstone drapes (Md). The amplitude of the

troughs is in the range of several dm, whereas the cross-sectional widths span several decimetres to meters. The sandstones also occur as massive-bedded units (Sm). They are occasionally interbedded with current-ripple marks (Scr) draped with mudstone layers (Md). Basal contacts are erosive. Measurements of morphometric properties (St. Magdalena; Fig. 2a) allow an estimation of water depth in the range between c. 3 and 5 m (Table S1, supplement). Sediment transport directions measured at the St. Magdalena site reveal a WSW – ESE-dominated sediment transport.

In the nearby c. 260 m-deep Gurten (Fig. 2a) drill core (Fig. S3, supplement), OMM-Ia deposits occur as cross-bedded sandstones (Sc) topped with mudstone drapes (Md). These lithofacies associations (Table 4) are most abundant within the drill core and make up c. 200 m of the log. However, because drill cores offer limited information about the dimensions of the encountered sediments, we were not able to determine if cross-beds can be assigned to tabular-beds (Sct_a) or to troughs (Sct_r).

4.1 Eastern Swiss

Distal basin border in the west and the east: Lake Neuchâtel and Wohlen areas (sites 2 and 16 on Fig. 2a)

Calcareous, shelly-sandstones (Scc) occur at distal sites in the western and eastern Molasse basin and are an assemblage of various lithofacies. This Scc-facies association is made up of 5 – 10 m-thick, coarse-grained sandstone beds with low-angle cross-beds (Sc) that contain coquinas and shell-fragments (Shf) and pebbles (Sg) in places. Interbedded fine-grained sandstones contain current-ripple marks (Scr) recording an opposite flow direction relative to the cross-beds (Sc).

In the west (sites at Lake Neuchâtel area; Fig. 2a and Fig. S4c in supplement), mapping shows that Scc-“Muschelsandstein” deposits are c. 5 m thick and record NNE- to NE-directed sediment transport. Foreset thicknesses of these deposits thin to <1 m towards the front of the Napf-megafan, where herringbone cross-beds imply SW and NE-directed, bi-modal sediment transport. At the NE margin of the Napf, these Scc-“Muschelsandstein” deposits grade into Slc-“Grobsandstein” units, which show m-thick tabular cross-beds (Sct_a) or dm-thick trough cross-beds (Sct_r) where individual troughs have m-wide diameters. Measurements of palaeo-flow directions reveal a SW- and SE-directed transport. These deposits are either time-equivalent sediments of the Scc-“Muschelsandstein” and thus contemporaneous with the OMM-Ib succession, or they mark the base of the OMM-II succession (Jost et al., 2016). Farther east near the Wohlen area (Fig. 2a and Fig. S4d in supplement), foresets of “Muschelsandstein” cross-beds are 6 to 8 m thick, and in some locations up to 10 m thick as reported by Allen et al. (1985). Sediment transport directions were oriented towards the SSW covering the range between 230° SSW and 250° WSW and striking parallel to the topographic axis. Estimates of water-depths of the Scc-“Muschelsandstein” reveal palaeo-water depths (Table S1, supplement) between 60 and 100 m.

5 Sedimentological interpretation

Entlen section

The OMM-Ia sedimentary rocks of the Entlen section are assigned to a backshore to upper nearshore realm, within a wave-dominated environment (Fig. 4a, and please see Table 1 for references). Records of waves are inferred from: (i) tabular, parallel-laminated and normally graded (Sp) sandstones, which are interpreted to represent sediments of the surf-and-swash zone near the wet beach where sedimentation occurs in the upper flow regime; (ii) low-angle cross-beds (Sc) with pebbly lags

and shell fragments (Shf), which could reflect sand-reefs (or shoals), rip channel fills or storm layers, and (iii) oscillation- (Sos) as well as branching-ripple marks (Sbr) pointing to wave-activity (Fig. 4a). Gravels and pebbly-lags (Sg) are either evidence for high-energy storm events or for river inflow from the backshore. Finer-grained lithofacies, which are either indicative of rapid sedimentation (Sv, Mcl, Table 1) or incipient pedogenesis (Mp, Mm; Table 1), are consistent with a shallow marine, wave-dominated environment.

The basal part of the OMM-Ib suite is assigned to a foreshore to lower nearshore setting, shaped by the combined effect of wave- and tidal-activity (Fig. 4a). This is inferred by the observation that current ripple-marks (Scr), which are situated on top of lamina sets of tabular- (Sct_a) and trough-cross-beds (Sct_r), point towards an opposite flow direction than the cross-beds themselves (Fig. 4a). Mudstone drapes (Md) on top of ripple marks together with lenticular- and flaser-interbeds (Mle, Mfl), are supportive evidence for a tidal environment (references in Table 1). The occurrence of waves, however, is inferred from parallel-laminated sandstones (Sp) with parting lineations, and ridge-and-swale (Spw) structures at the base of the OMM-Ib-suite. Towards the top of the OMM-Ib, massive sandstones (Sm) and mudstones with mottled colours, root casts and caliche nodules mark the presence of a backshore, possibly terrestrial setting.

The change from a nearshore, wave-dominated environment (OMM-Ia) to an environment with tidal records (OMM-Ib) was additionally associated with a deepening from <5 m to >15 m, particularly at the base of the OMM-Ib. We thus consider the base of this unit as the maximum-flooding surface (MFS), separating the OMM-I into a transgressive OMM-Ia unit and into a regressive OMM-Ib succession (Figs. 4a and 5a).

Napf-units

We interpret the association of massive (Gm) to cross-bedded (Gc) conglomerates, and massive- to cross-bedded sandstones (Sm, Sc) as deposits within a braided river system (Table 2, see references there). In such an environment, conglomerates are common records of active channels. Massive- (Sm) to cross-bedded (Sc) sandstones alternating with mottled mudstones were most likely formed on the floodplains bordering the network of braided channels, when bursts resulted in the accumulation of crevasse-splay deposits (Platt and Keller, 1992). Mudstone interbeds (Mp) with evidence for palaeo-sol genesis formed when channel belts shifted away from the axis of the section (Platt and Keller, 1992). This facies-association was mapped over tens of kilometres, both across and along strike of the basin orientation. It is thus assigned to an alluvial megafan (Schlunegger and Kissling, 2015).

Sense section

We assign the OMM of the Sense section to a tidal-dominated environment where deltaic estuaries dominated the sedimentary facies (Fig. 4b and please see Table 3 for references). This is inferred from: (i) sigmoidal cross-bedded sandstones (Sc) with distinct top-, fore- and bottom-sets and pebbly-lags (Sg) that are indicative of a delta, and (ii) trough cross-bedded (Sct_r) and massive bedded (Sm) sandstones that could represent mouth-bar deposits where estuaries (or tidal inlets) end. In such an environment, current-ripple marks (Scr) with mudstone drapes (Md) at the base of tabular cross-beds (Sct_a) point to rhythmic

changes of tidal-current slack water stages within a subtidal setting, whereas ripple-marks (Sos) with branching crests (Sbr) and parallel-laminated sandstones (Sp) were most likely formed under the influence of waves close to the beach. Massive-bedded (Mm), parallel-laminated (Mp) and strongly bioturbated (Mf) mudstone interbeds are assigned to a tidal flat that established on the landside margin of the delta. Towards the top of the section, the facies successively evolves into a fan delta setting. This is inferred from the observation that the conglomerate beds become more frequent and more continuous and display several m-thick beds, with massive- to cross-bedded geometries (Gm, Gc).

The first-occurrence of 5 – 10 m-thick sandstone beds at 200 m stratigraphic level (Fig. 4b) records a remarkable increase of the water depth, when 5 – 10 m-deep tidal channels (Scc-sandstone beds with epsilon cross-beds) grade into several m-thick subtidal sandwaves (Sct_a) and nearshore tempestites (m-scale Spw-sandstones with ridge-and-swale geometries, see Table 3 for lithofacies and references). These two latter lithofacies (Sct_a, Spw) are interpreted to record the deepest palaeo-water depth in the Sense section, when water depths were in the range of up to 30 m. We consider this stratigraphic level to record the maximum-flooding surface (MFS) within the Sense section (Fig. 4b), and we will use it for correlation purposes with the OMM succession at Entlen (see discussion).

St. Magdalena site and Gurten drill core

The several m-thick outcrops near Fribourg are interpreted as subtidal shoal deposits, which accumulated within a tide-dominated environment (Table 4, see references there). This is inferred from: (i) m-scale cross-bedded troughs (Sct_r) with current-ripple marks (Scr) at their base (see also Homewood et al., 1981; for a similar interpretation). Alternatively, sandstone troughs (Sct_r) could be assigned to a mouth-bar environment, where massive-bedded sandstones (Sm) would represent records of rapid sedimentation. In contrast, mudstone drapes (Md) on top of the ripple-marks (Scr) and cross-beds (Sc) are formed during low-energy tides, or possibly during slack stages. Similar deposits (Sct_r, or possibly Sct_a) within the Gurten drill core could also be interpreted as sediments of subtidal shoals, however, due to limited exposure, interpretations are non-conclusive. Shallow palaeo-water depths are also inferred from estimates of water depths ranging between 3 and 5 m.

Lake Neuchâtel and Wohlen areas

We interpret the Scc-“Muschelsandstein” (Table 5) sediments (containing coquinas and shell-fragments (Shf) and pebbles (Sg)) to have been deposited within the topographic axis of the Burdigalian seaway, (see also Allen et al., 1985, and Jost et al., 2016, for a similar interpretation). Meter-scale cross-beds (Sct_a), locally superimposed by current-ripple marks (Scr), have been interpreted to reveal deposition under strong tidal currents (Allen et al., 1985). These deposits are thus assigned to offshore, tide-dominated sandwaves, where sediment transport was NNE- (Lake Neuchâtel area; Fig. 2a) or SSW-directed (Wohlen area, Fig. 2a). In places, pebbly-lags (Sg) are interpreted as flood-related splays of gravels into the offshore setting, derived from the neighbouring Napf-megafan. In contrast, the coarse-grained sandstones (Slc-“Grobsandstein” sediments; Table 5) reveal similarities to the subtidal-shoal deposits encountered at the St. Magdalena site where trough cross-bedded sandstones (Sct_r) and tabular cross-beds (Sct_a) dominate the facies assemblages. However, the deposits in the Wohlen area are

coarser-grained, and cross-beds (Sc) have larger diameters, but similar thicknesses. We relate the coarse-grained nature of these deposits to the proximity of the Napf-megafan in the SW. The cross-beds with larger wavelengths and similar amplitudes possibly imply stronger currents compared to the subtidal shoal-deposits near St. Magdalena.

5 6 Discussion

~~At the eastern proximal basin border, marine sedimentation started with the OMM I (Lucerne Fm, Fig. 3), which is best presented by the c. 800 m thick Entlen section (Keller, 1989). There, the overlying OMM II (St. Gallen Fm) is only 50 m thick, and sedimentation was superseded by the accumulation of fluvial conglomerates of the Napf megafan (Napf-units), which gradually replaces the marine strata of the OMM I c. 20 km farther to the west (Haldemann et al., 1980) upon approaching the Napf megafan apex (Schlunegger and Kissling, 2015; Figs. 3 and 4). This heterochronicity of facies relationships complicates any temporal reconstructions of the OMM sedimentation in the east. Nevertheless, the basal part of the OMM I follows upon a sharp contact to the underlying USM deposits, as recorded by the Fischenbach-section along a river cut (47°00'14" N / 8°08'26" E; Schlunegger et al., 2016). There, the topmost normal magnetozone of the USM was considered to correlate with C6An1 of the MPTS or the ATNTS, respectively (Schlunegger et al., 1996). For the OMM I, a time interval from MN3a through MN3b (European Neogene mammal units; Mein, 1975; 1979; 1989) has been assigned by Keller (1989) based on micro-mammal records within a section c. 20 km farther to the east (Fig. 3). However, more precise age assignments for the base and the top of this unit are complicated because of a lack of magneto-polarity chronologies. Here, we constrain the age of the basal transgression using two pieces~~
6.1 Re-appraisal of chronostratigraphic framework

20 Entlen section

No magnetostratigraphic data is available for the Entlen section, but a temporal calibration of the deposits can be achieved through indirect lines of evidence. This particularly concerns the reconstruction of an age constraint for the basal transgression, which is accomplished using two lines of evidence: First, the transgression post-dates the deposition of the USM, which terminated at C6An1 at the Fischenbach-section (Fig. 3b; Schlunegger et al., 1996). Second, based on stratigraphic interpretations of palaeo-dischargeflow direction data, Strunck and Matter, (2002) considered that the transgression of the OMM progressed from the east towards the west, where the first marine sediments have been dated with C6r in the Sense-section (Fig. 3 and 4a; Figs. 3b, see next section). An E – W transgression of the OMM is also seen in seismic line BEAGBE.N780025 (supplement, Fig. S2), where OMM deposits onlap onto the USM in a westward direction. Accordingly, the onset of the OMM at ~~the~~ Entlen on the eastern side of the Napf predates the transgression at ~~the~~ Sense- farther west. Based on these arguments, we ~~propose~~ set an age of c. 20 Ma for the base of the OMM-I in the eastern Swiss Molasse basin (Figs. 3 3b and 5), which is consistent with Kálin and 4).

An age for Kempf (2009). For the top of the OMM-I (Lucerne Fm) can be estimated by, we determine an age using the magneto-stratigraphy of the Napf-section (Napf-units, Fig. 3 3b) c. 10 km to the west of the Entlen (Schlunegger et al., 1996). This section includes an alternation of 6 reversed- and 5 normal-polarized magnetozones– (Schlunegger et al., 1996). The

lowermost, very long normally polarized interval (N1, Fig. ~~3 and 4a 3b~~) includes the ~~mammal~~mammalian fossil site Hasenbach I recording an MN3b age (Schlunegger et al., 1996) or even a lower-MN3b age, as a revision of the ~~fossiliferous~~mammalian material has shown (Kälin and Kempf, 2009). This allows a correlation of the normally polarized interval N1 with chron 5En of the MPTS (Cande and Kent, 1992, 1995) or the ATNTS (Lourens et al., 2004), respectively (Fig. ~~3 3b~~). Since the third reversed magnetozone of the Napf ~~units~~section is very short (R2), and since the ATNTS chron 5D ~~includes~~spans several 100 kyr and is thus quite long, it is most likely that a hiatus encloses C5Dr2 to C5Dr1 (Fig. ~~3 3b~~). In addition, because (i) the change from MN3b to MN4a has been calibrated with C5Dr2 (Jost et al., 2016), and since (ii) the base of the overlying OMM-II (*St. Gallen Fm*; Fig. ~~3 Figs. 3b and 4a 5~~) has been dated with MN4 (Keller, 1989), we suggest that the inferred hiatus ~~falls into~~coincides with the boundary between the OMM-I and the OMM-II (Fig. ~~4 Figs. 3b and 5~~).

10 This age assignment is consistent with magneto-polarity ~~stratigraphies~~stratigraphy in the ~~eastern Swiss~~-Molasse basin c. 70 km farther east (Kempf and Matter, 1999). It is also ~~coherent~~consistent with micro-~~mammal~~mammalian investigations in the distal Molasse basin c. 30 farther north where Jost et al., (2016) found that deposits spanning MN3b and MN4a are missing. Based on these constraints, we suggest that the top of the OMM-I correlates with C5Dr of the MPTS or C5Dr2 of the ATNTS, respectively, followed by a c. 0.5 Ma-long hiatus (Fig. ~~3 and 4~~). ~~The overlying magnetozones of the Napf units are correlated with the ATNTS following Sant et al. (2017). Figs. 3b and 5). According to this correlation, the sediments recording the maximum-flooding conditions in the Entlen section are c. 19 Ma old.~~

15 ~~This correlation implies that sedimentation within the OMM I was continuous, which we justify through the deepening and shallowing upward sequence recorded in the Entlen section (see 4.2.1). A maximum flooding surface (MFS, Fig. 4a), which we infer from the sedimentological analyses across the basin (see 4.2), allows to subdivide the OMM I into a lower and an upper unit referred to as OMM Ia and OMM Ib, respectively (Figs. 3 and 4). Note, that it is possible that sedimentation was interrupted between the OMM II and the OSM by short intervals (Kälin and Kempf, 2009). The consequences of our refined correlation are a constant sediment accumulation rate of c. 400 m/Ma from the base to the top of the OMM I, and the occurrence of a c. 0.5 Ma long hiatus between c. 18 and 17.5 Ma separating the OMM I from the OMM II (Figs. 3 and 4).~~

20 ~~In the distal eastern part of the basin, the stratigraphic architecture of the OMM is made of sandstones of the Lucerne Fm at the base, which is overlain by the “Muschelsandstein” unit (Fig. 4b; see 4.2.4) at the top (Jost et al., 2016). Mapping shows that the “Muschelsandstein” near Mägenwil (Fig. 2) is c. 5–10 m thick and thins towards the depocenter of the Napf megafan deposits to less than 1 m.~~

Wohlen area

25 ~~Correlations of these the OMM deposits across the basin have been from the Entlen section to the Wohlen area was accomplished by Schlunegger et al., (1997a) through a seismostratigraphic analysis of the seismic line 8307 (Schlunegger et al., 1997; Fig. 2). There, the sediments of 2a). The seismic data shows that the OMM-I (*Lucerne Fm*) deposits onlap onto USM strata and then overlap this unit (Fig. 4b). The overlapping sequence has been referred to as Unit B in 5b). Schlunegger et al. (1997), which in turn (1997a) correlated the OMM-I sequence with their Unit B in the Entlen section, which corresponds to~~

30

the top of ~~the~~ OMM-Ia in our stratigraphic scheme. In addition, our field investigations and micro-mammal correlations ~~(mammalian data by~~ Jost et al., (2016) ~~reveal~~ revealed that the “Muschelsandstein” follows on top of the OMM-Ia and most likely corresponds ~~in age~~ to the OMM-Ib. Based on these ~~constraints~~ arguments, we ~~suggest that~~ constrain the deposition in the distal basin ~~occurred to the time interval~~ between c. 19 and 18 Ma (Fig. ~~4b~~5b). However, ~~as visible in~~ based on ~~seismostratigraphic investigations of~~ line 8307-~~(, Schlunegger et al., 1997), (1997a) proposed that~~ sedimentation was interrupted at c. 18 Ma by a c. 0.5 Ma-long or possibly longer hiatus. This time span has ~~later~~ been specified through new micro-mammal ~~mammalian~~ discoveries by Jost et al., (2016), who noted that ~~records a record~~ of MN4a is missing ~~in the~~ ~~Wohlen area~~ and that the base of the OMM-II (~~St. Gallen Fm~~) hosts ~~mammal~~ mammalian fragments that correspond to MN4b. The interpretation of an inferred unconformity is additionally supported through observations of vadose cements (Allen et al., 1985) within the “Muschelsandstein”, and through evidence for a thick ~~palaeosol~~ palaeo-sol separating OMM-I from OMM-II (Fig. 4), ~~as own mapping near~~ in the Entlen -section ~~has shown. This information suggests~~(see chapter 4 and 5). We use the ~~occurrence of vadose cements and the palaeo-sol to propose~~ that the uppermost beds of the OMM-Ib (including the “Muschelsandstein”) were exposed to erosion, ~~or non-sedimentation~~, after deposition ~~(Allen et al., 1985; Jost et al., 2016).~~ ~~Because of post depositional erosion of the entire Molasse sequences since the Pliocene (Cederbom et al., 2004; 2011), the~~ ~~continuation of the sedimentary history cannot be constrained.~~ Furthermore, because the “Muschelsandstein” unit records the ~~deepest water depth during OMM times at distal sites, we tentatively suggest that deposition of these mega-sandwaves started at the same time when the deepest conditions (MFS) were recorded within the Entlen section (Fig. 5b).~~

Sense section 4.1.2 Western Swiss Molasse

~~At the proximal basin border in the west,~~
Magnetostatigraphic data for the Sense section was presented by Strunck and Matter (2002). These authors placed the USM/OMM-boundary ~~of the c. 650 m thick Sense section at this site~~ within C6r of the MPTS (Cande and Kent, 1992; 1995), or alternatively of the ATNTS (Fig. ~~3~~3b; Lourens et al., 2004). The subsequent alternation of normal and reverse magnetozones ~~were~~ was correlated by these authors with chrons 6r through 5Dn of Cande and Kent’s MPTS (1992; 1995), the latter of which corresponds to C5Dn1 of the ATNTS (Lourens et al., 2004). Following Strunck and Matter (2002), a possible hiatus prior to c. 17.5 Ma ~~(Figs. 3 and 4)~~ is likely to be ~~registered~~ recorded also within the Sense -section (~~Fig. 5b~~Figs. 3b and 5a). This ~~correlation implies that the lower Sense-Formation corresponds to the OMM-Ia, whereas the upper Sense-Fm and the Kalchsätten-Fm are time equivalent units of the OMM-Ib (Figs. 3a, 3b). The topmost 50 m of the Kalchstätten-Fm, where the base was characterized by the first appearance of conglomerates, follows upon this hiatus and corresponds to the OMM-II in our scheme (Figs. 3 and 5a). This further implies that a hiatus separates the OMM-I from the OMM-II across the entire basin (Fig. 5a), Figs. 3 and 4) and that the~~ ~~In addition,~~ subsequent sedimentation (base of OMM-II) progressed from the west to the east. ~~The consequences of this chronological framework are a constant (Fig. 5a). In the same sense, the sediment-accumulation rate of c. 285 m/Ma during deposition of the western OMM I, however, sedimentation was possibly interrupted by a short~~

hiatus at the top of the OMM-Ib (Fig. 3) packages recording the maximum-flooding conditions (MFS) have most likely the same age across the entire basin (Fig. 5a).

Lake Neuchâtel area

5 No micro-mammal/mammalian sites have been reported so far for the OMM deposits in the distal western Molasse basin. Therefore, we cannot provide further constraints on the history of sedimentation. However, mapping our field inspections in the area of Lake Neuchâtel (Fig. 2) shows a sedimentary succession similar to that in the east, where amalgamated sandstone beds are overlain by the “Muschelsandstein” unit. Mapping Our field inspections also shows that these limestone-calcareous, shelly-sandstones thin from c. 10 m in the Lake Neuchâtel area in the west to a few meters towards the
10 distal margin of the Napf-megafan, consistent with the results by Allen et al., (1985). Because of the architectural similarity between the “Muschelsandstein” deposits in the east and the west, we tentatively consider that the deposition of the “Muschelsandstein” occurred synchronously across the entire Swiss Molasse basin. Similar to the east, the post-depositional erosion during the Pliocene (Cederbom et al., 2004; 2011) prevents us from presenting any further details on the continuation of the sedimentary history.

15 4

6.2 Lithofacies, sedimentary processes and identification Evolution of depositional environments

4.2.1 Eastern proximal the Molasse basin border: Beach sequences

The chronostratigraphic framework together with a tidal influence recorded at the Entlen section

Characterization

20 We group the 800 m thick suite of the OMM-I deposits at the Entlen (Lucerne Fm) into the two subunits OMM-Ia and OMM-Ib based on differences in the lithological architecture (Fig. 5). The lowermost c. 370 m thick OMM-Ia is made up of an amalgamation of c. 5–10 m thick tabular sandstone packages with mm to cm thick mudstone interbeds. The overlying c. 430 m thick OMM-Ib sequence comprises an alternation of 2–3 m thick lenticular sandstone beds and dm thick mudstone layers (Fig. 5a).

25 The sedimentary suite of the OMM-Ia records a total of 14 lithofacies types (Table S1, supplement). Fine to medium grained sandstones occur as packages of cm to dm thick normally graded sequences. These deposits either occur as several m thick tabular, parallel laminated units (Sp) that laterally grade into <1 cm thick cross beds (Sc), or as several dm thick low angular cross bedded units with tangential lower boundaries (Sc). Parallel laminated sandstone beds also display transeurrent laminations (Sp). These lithofacies associations dominate the OMM-Ia sequence with a relative contribution of >50% (Fig.
30 5a). Some sandstone beds contain gravels and pebbles in a few places (Sg), and shell fragments (Shf) are visible where sandstone units have erosive bases. A few packages of cross bedded sandstones (Set_o) contain current ripple marks (Ser) at their base, or they have a massive structure (Sm). Centimetre thick oscillation ripple marks (Sos facies), sometimes with

branching crests (Sbr), are present only in some places. The basal contacts of this class of sandstone beds are both erosive and planar (Fig. 5a). Some fine grained sand and siltstone interbeds display water escape structures such as flame fabrics or sand volcanoes (Sv). Most of the siltstone beds occur as climbing ripples (Mel). The mudstone interbeds are present as mm to cm thick parallel laminated to massive layers (Mp, Mm). Thin muddrapes (Md), a few mm thick, mostly occur on top of current ripple marks (Scr). In places, root casts are associated with yellow to ochreish mottled colours.

Estimates of sedimentological data and palaeo-bathymetric conditions (see supplement) reveal that the OMM Ia sediments were deposited in water depths <5 m (Fig. flow 5a). This is consistent with the inferred near shore environment (see below; Short, 2012). Measurements of bedform orientations reveal discharge directions between 315° NW and 60° NE, which are used to propose a dominant NE directed transport (Fig. 5a).

The overlying OMM Ib comprises a total scenario of 9 lithofacies types (Table S1, supplement). Fine to medium grained sandstone packages occur as m thick lenticular bodies that display several dm thick low angular trough (Set_t) or tabular cross-beds (Set_a). Set_t sandstones contain current ripple marks (Scr) at their base, while laminae sets of Set_a sandstones are interbedded with current ripples (Scr), which record an opposite flow direction. At one site, dm thick sandstones with a planar base and a wavy top and with wavelengths of several meters could be assigned to a ridge and swale (Srs) structure (Fig. 5a).

These lithofacies assemblages contribute to >50% of how the sedimentary sequence of the OMM Ib. Parallel laminated sandstone beds with transcurrent laminations (Sp) are dm thick and mainly found at the top of the OMM Ib unit. In a few places, the sandstones also occur as massive beds (Sm). Mudstone interbeds are dm thick and mostly occur as muddrapes (Md) on top of current ripple marks (Scr). Lens (or lenticular) and flaser interbeds (Mle, Mfl) are dm thick and characterized by current ripple marks with truncated crests. In the *Entlen* section, the OMM Ib ends with m thick palaeo soils, displaying yellow to reddish mottling, root casts and caliche nodules (Fig. 5a).

Palaeo bathymetric conditions of the OMM Ib reveal an increase of water depths to >15 m compared to the OMM Ia unit (supplement). This dataset is corroborated with our inferred near shore to transitional environment (see below). The OMM Ib shallows towards the top and is capped by a thick palaeo soil. Discharge directions measured from bed form orientations reveal the full range between 260° W and 70° E (Fig. 5a), which is consistent with the observed bi axial sediment transport of the associated lithofacies types (see below: Set_a, Set_t and Scr). Interestingly, dominant discharge directions of the OMM Ib sediments change towards the N and finally to the W.

Interpretation

The OMM Ia sediments of the *Entlen* section are assigned to a near shore environment, which comprises the lower and upper shoreface where wave activities shape the coastal morphology of a beach (Fig. 5a). Related processes are inferred from the occurrence of tabular, parallel laminated (Sp) sandstones, which are interpreted to represent sediments of the surf and swash zone near the wet beach. Alternatively, this lithofacies association can be placed in the wave transformation zone where the waves brake. This is particularly the case where these beds laterally grade into <1 cm thick cross bedded ripples (Scr) and where normal grading is clearly visible. Low angular cross beds (Sc) are interpreted to represent sand reefs, where pebbly-

lags (Sg) and shell fragments (Shf) record the occurrence of storm events. Oscillating ripple marks (Sos) are presumably formed in the lower shoreface and are evidence for wave activities (Fig. 5a). Furthermore, these Gp and Cs facies are often visible at the base of rip current channels. Water escape structures, sand volcanoes (Sv) and climbing ripples (Mcl), are distinct recorders of fast sedimentation from sediment saturated water within a wave dominated beach. In places, the presence of backshore channels (Sc) and floodplains with splays (Sc and Sm facies) are inferred where root casts and incipient pedogenesis are observed (Mp, Mm). Accordingly, these deposits are interpreted to have been deposited in backshore ponds. Contrariwise, tidal processes are related to cross bedded sandstones (Set_a) with mud drapes (Md) on top of the current ripple marks (Ser). These Md and Ser facies, if associated to the Set_a sandstones, are distinct features of a slack water stage due to a possible tidal influence. Alternatively, they might register the occurrence of standing water in a wave protected area. Root cast are visible in parallel laminated (Sp) and massive bedded (Sm) sandstones and mudstones (Mp, Mm).

The OMM Ib sediments of the *Entlen section* are assigned to a near shore to transitional environment, shaped by the combined effect of wave and tidal activities (Fig. 5a). We infer the occurrence of tidal processes by the observation that current ripple marks (Ser), which are situated on top of lamina sets of tabular (Set_a) and trough cross beds (Set_t), point towards an opposite flow direction than the cross beds themselves (Fig. 5a). In addition, the size of these facies assemblages forming m scale lenticular shaped sandbodies requires an accommodation space, which is consistent with a lower near shore setting. In such an environment mud drapes (Md) on top of the ripple marks are recorders of slack water phases. Finally, lens (or lenticular) and flaser interbeds (Mlc, Mfl), both dm thick, are assigned to a similar setting. In contrast, sediment transport by waves is recorded by parallel laminated sandstones (Sp) with transcurrent laminations, which mark the presence of a surf and swash zone. In this context, sandstone beds referred to as ridge and swale (Srs) structures could record the occurrence of high energetic waves. Furthermore, massive sandstones (Sm) and palaeo soils with mottled colours, root casts and caliche nodules, mark the presence of a back shore, possibly terrestrial environment.

In summary, the change of the sedimentary environment within the OMM I at the *Entlen*, from a near shore, wave dominated setting to an environment with tidal records, was associated with a shift towards deeper bathymetric conditions (Fig. 5a). In this context, the deepest inferred bathymetry at the base of the OMM Ib is assigned to the maximum flooding surface (MFS) within the OMM I sequence, which separates the transgressive OMM Ia from the regressive OMM Ib (Fig. 6a). This deepening and shallowing upward trend is associated with a $\sim 90^\circ$ westward rotation of the discharge directions, from an originally unidirectional NE to an axial NE-SW directed (MFS) and finally to a transverse N-oriented transport.

4.2.2 Western proximal basin border: Estuarine sequences recording tidal processes at the *Sense section*

Characterization

We group the c. 650 m thick *Sense section* (Figs. 5b and 3), which comprise OMM I and OMM II deposits, into three packages based on distinct facies associations. OMM Ia deposits are c. 200 m thick and comprise the *lower Sense beds*. The superseding

OMM-Ib sediments are encountered in the *upper Sense-beds* (c. 125 m thick) and the *Kalchstätten Fm* (c. 275 m thick). The *Sense-section* ends with the *Guggershorn Fm*, which is c. 50 m thick. Based on our refined chronology (see 5.1 and Fig. 3), we assign this c. 50 m thick uppermost sequence to the OMM II.

5 Within the *Sense-section*, the OMM Ia is present as 13 lithofacies types (Table S1, supplement). Middle to coarse grained sandstone beds are up to 2–3 m thick and massive bedded (Sm). Individual sandstone beds are parallel laminated (Sp). They also occur as m-scale tabular cross beds (Set_a) with well visible top and bottom sets and as sequences of cross bedded troughs (Set_c). Meter scale tabular cross beds (Sc) with sigmoidal geometries contain pebbly lags (Sg) at the bottom sets and are well exposed along a nearby road cut (46°49'27" N / 7°18'42" E). Some of these cross beds contain current ripple marks (Ser) at the base of Set_c sandstones, often draped with a muddy layer (Md). ~~Ripple marks also build up tabular sandstone bodies. In this case the ripples are either asymmetric or symmetric (Sos), and in some cases the crests are branching (Sbr). Mudstone interbeds are 10–20 cm thick, massive (Mm) to parallel laminated (Mp) and strongly bioturbated (Mf).~~

10 Estimates of bathymetric conditions reveal water depths of up to 10 m (Fig. 5b and supplement). This is consistent with the inferred tidal dominated environment within an intertidal bathymetry (see below). Measurements of discharge directions reveal a dominant NE directed sediment transport, which covers the range between c. 0° N and 90° E (Fig. 5b).

15 The basal part of the OMM Ib sequence (*upper Sense-beds*, Fig. 3 and Fig. 5b) displays a similar large scale architecture as the OMM Ia unit. However, it comprises 4 additional lithofacies types and discloses subtle differences: (i) up to 5–10 m thick sandstone beds are normally graded, follow upon an erosive base and display epsilon cross beds (See); (ii) m-scale cross bedded sandstones (Set_a) are several meters high and tens of meters wide. Current ripple marks (Ser), which occur on top of individual laminae, are draped with mud (Md) and have orientations that imply an opposite flow direction; (iii) medium-grained sandstones show ridge and swale structures (Srs) with a small amplitude of a few dm and a large wavelength of several m; they are additionally covered with pebbles (Sg); and (iv) Srs structures are sometimes also covered with oscillating ripple marks. This 125 m thick sequence ends with a c. 20 m thick succession of mudstones and a c. 15 m thick amalgamation of sandstone beds. Mudstones are massive bedded (Mm), contain exichnias (Mf) and are arranged as individual dm thick packages. Sandstones display massive beds (Sm), with current ripple marks (Ser) and bioturbation (Sf) in places.

20 Water depth estimations return values of up to 30 m at the base of the OMM Ib, which shallow to <5 m further upsection (Fig. 5b). This deepening and shallowing trend is consistent with the inferred subtidal environment at the base and higher up in the section (see below). Orientation of discharge directions show an axial, SW-NE directed transport where we reach the deepest bathymetrical conditions. Sediment transport changes towards a transverse N directed discharge at the end of the sequence.

25 The c. 300 m thick upper part of the OMM Ib (*Kalchstätten Fm*) (Figs. 3 and 5b; Strunck and Matter, 2002) displays two major differences (Table S1, supplement): (i) dm thick mudstone interbeds appear more frequently; and (ii) alternations of sandstone and mudstone beds are interfingering with m thick massive to cross bedded conglomerates (Gm, Ge). The sedimentary suite thus starts with 5–10 m thick sandstone beds, which are massive (Sm), tabular cross bedded (Set_a) and

trough cross-bedded (Set_r). Sandstones also display tabular geometries and contain bioturbation in places (Sf). Occasionally, current ripple marks (Scr) are draped with mud (Md). Up to m thick, massive bedded conglomerates (Gm), sometimes only visible as dm thin pebbly lags interbedded in sandstone beds (Sg), appear approximately in the first quarter of this sequence and are embedded in massive bedded mudstones (Mm) and sandstones (Sm). The conglomerates then change towards several m thick, massive (Gm) and cross bedded geometries towards the top of the section (c. 50 m thick OMM II).

No quantitative data are available to define bathymetric conditions. Nevertheless, sandstones at the base of this unit display similarities to the sedimentary architecture of the subtidal shoals at *St. Magdalena*, where water depths of c. 5 m are estimated (see below). We thus suggest subtidal conditions for the base of this unit. A shallower bathymetry is inferred from the occurrence of conglomerates in the OMM II suite, possibly deposited within coarse grained rivers in a backshore environment at the top where conglomerates start to dominate the sedimentary suite. Measurements of palaeo currents from imbricated clasts (Strunck and Matter, 2002) reveal a transverse to W directed sediment discharge, which is consistent with own observation, covering the full range between 230° SW and 330° NW.

Interpretation

We assign the OMM Ia (*lower Sense beds*) to an intertidal environment bordered by deltas, estuaries and tidal flats (Fig. 5b). This is inferred from the occurrence of sigmoidal cross bedded sandstones (Sc) with distinct top, fore and bottom sets, which also contain pebbly lags (Sg) at their base. These facies assemblages are characteristic for deposits of a Gilbert Delta (e.g. Bates, 1953). In this context trough cross bedded sandstones (Set_r) and possibly massive bedded (Sm) units can be assigned to mouth bar deposits where estuaries end, or alternatively to tidal inlets. The presence of current ripple marks (Scr) with mud drapes (Md) at the base of tabular cross beds (Set_a) can be assigned to an intertidal setting, where ripple marks record the activity of tidal currents, while mud drapes form during slack phases. Additionally, ripple marks (Sos) with branching crests (Sbr) and parallel laminated sandstones (Sp) were most likely formed in shallow water conditions, possibly under the influence of waves. The massive bedded (Mm), parallel laminated (Mp) and strongly bioturbated (Mf) mudstone interbeds are assigned to a tidal flat.

The sandstones with cross beds (Sc) encountered at the base of the OMM Ib (*upper Sense beds*) are assigned to tidal channels, where epsilon cross beds (See) are records of slip faces of meanders. In support of the inferred recorders of tides, meters high cross bedded sandstones (Set_a) with draped (Md) current ripple marks (Scr) on top of sandstone laminae are distinct characteristics for tidal sandwaves. In this context, the several tens of m wide sandwaves are possibly formed in a subtidal environment. In contrast, the occurrence of wave activities is inferred from m scale ridge and swale (Srs) structures and oscillating ripple marks (Sos). Likewise, pebbly layers (Sg) among the Srs sandstones are evidence for high energetic storms. These two latter lithofacies (Set_a , Srs) record the deepest bathymetrical point of the *Sense section*. Massive bedded (Mm) mudstones and sandstones (Sm) with bioturbation (Mf , Sf), which are encountered at the end of the lower part of the OMM Ib, are assigned to a tidal mud and sand flat environment.

The upper part of the OMM Ib (*Kalehstätten-Fm*) is assigned to a regressive, shallow marine sequence. Similar to the OMM-Ia unit, we assign the OMM Ib deposits to an environment with estuaries bordered by subtidal shoals and possibly tidal flats. The occurrence of estuaries is inferred from cross-bedded sandstones (Set_c) superimposed with current ripple marks (Ser) and mud drapes (Md). In such an environment, cross-bedded troughs (Set_c) with massive bedded sandstones (Sm) could represent mouth bar deposits at the end of estuaries or tidal inlets, which laterally grade into subtidal shoals (Set_c). Bioturbated sandstones (Sf) could either be assigned to a tidal sand flat environment or are records of organisms within subtidal conditions. Massive and cross-bedded, a few m thick conglomerates (Gm, Ge), which are embedded within massive bedded mudstones and sandstones (Mm, Sm), are assigned to distal recorders of floods, where gravels were supplied by a stream with sources in the Alps. In this context, conglomerates are also only visible as a dm thin layer among sandstones (Sg). Up section, the conglomerate beds become more frequent and more continuous and display several m thick beds, with massive to cross-bedded geometries (Gm, Ge). These deposits are assigned to coarse grained rivers interfingering with the Burdigalian sea (Strunck and Matter, 2002) and finally correspond to the OMM II and its terrestrial equivalent (*Guggershorn-Fm*).

In summary, the *Sense section* (OMM I and OMM II) records a distinct change of the sedimentary environment and the bathymetrical conditions. The deposits of the OMM Ia show a transition from an estuarine towards a subtidal environment. Largest water depths are inferred from deposits at the base of the OMM Ib, which is thus likely to represent the maximum flooding stage (MFS) of the OMM I. The sediments encountered towards the top of the OMM Ib are assigned to water depths within a subtidal to intertidal bathymetry. Measurements of discharge directions in this large scale deepening and shallowing upward cycle reveal a shift from a transverse NE directed sediment transport to an axial SW-NE directed transport (MFS) and finally to a N directed discharge at the top of the OMM I.

The overlying conglomerates, deposited within fluvial streams forming a deltaic environment (OMM II and then OSM), record a shallowing upward sequence, evolving towards a braidplain towards the top. There, measurements of palaeo-currents reveal a W directed discharge direction (Strunck and Matter, 2002), which is associated with a 90° westward rotation in comparison to the OMM Ib.

4.2.3 Central proximal basin border (Napf units): Alluvial megafan deposits

Characterization

The *Napf section*, which is a terrestrial equivalent of the OMM group (Figs. 3 and 4; Schlunegger et al., 1997), is c. 1550 m thick and includes a succession of conglomerates, sandstones and mudstone interbeds (Matter, 1964), which are categorized into 5 lithofacies types (Table S1, supplement). Individual conglomerate sequences are up to 10 m thick and display stacks of 2–3 m thick beds with massive (Gm) to cross-bedded (Ge) geometries. The sandstone beds occur as massive bedded (Sm) and cross-bedded (Sc) units. The interbedded mudstones display a tabular (Mp) fabric and have a yellowish reddish mottling, calciche nodules and root cast. Palaeo flow measurements based on orientations of solmarks imply a NE directed transport

during USM-times (Schlunegger et al., 1997). Own measurements of imbricated clasts reveal a change from a NE- to a NW-direction between OMM I and OSM times.

Interpretation

5 We interpret the association of massive (Gm) to cross-bedded (Gc) conglomerates and massive to cross-bedded sandstones (Sm, Sc) as deposits within a braided river system (Table S1, supplement). In such an environment, conglomerates are common recorders of active channels. Massive (Sm) to cross-bedded (Sc) sandstones alternating with mottled mudstones were most likely formed during bursts of channel belts, thereby forming crevasse splay deposits (Platt and Keller, 1992). Mudstone interbeds (Mp) with evidence for palaeo soil genesis formed when channel belts shifted away from the axis of the section
10 (Platt and Keller, 1992). This facies association was mapped over tens of kilometres, both across and along strike of the basin orientation. It is thus assigned to an alluvial megafan (Schlunegger and Kissling, 2015).

4.2.4 Central basin (St. Magdalena, Gurten): Subtidal shoal deposits

Characterization

15 Outerops within a cave system near *Fribourg* (St. Magdalena, Fig. 2) reveal 3D insights into several m-thick sandstones with cm-thick mudstone interbeds. The sandstones are medium to coarse grained and display an amalgamation of 1–3 m wide, cross-bedded troughs (Set_t) with current ripple marks (Ser) at their base that are covered by mud drapes (Md). The amplitude of the troughs is in the range of several dm, while the cross-sectional widths span several decimetres to meters. The sandstones also occur as massive bedded units (Sm). They are occasionally interbedded with current ripple marks (Ser) draped with mud
20 layers (Md). Basal contacts are mostly erosive. In the nearby c. 260 m-thick *Gurten* (Fig. 2) drill core (Fig. S5, supplement), related deposits occur as cross-bedded sandstones (Sc) topped with mud drapes (Md). These lithofacies associations (Table S1, supplement) are most abundant within the drill core and make up c. 200 m of the log. However, because drill cores offer limited information about the dimensions of the encountered sediments, we were not able to determine if cross-beds can be assigned to tabular beds (Set_t) or to troughs (Set_t).

25 Measurements of morphometric properties (St. ~~evolved~~Magdalena, Fig. 2) allow an estimation of water depth in the range between c. 3 and 5 m (Table S2, supplement), which is consistent with an inferred subtidal shoal environment (see below). Discharge directions measured at *St. Magdalena* reveal a WSW-ESE dominated sediment transport. However, we were not able to carry out quantitative measurements for the *Gurten* (Fig. 2) drill core, neither for bathymetrical conditions, nor for discharge directions for the reasons mentioned above.

30

Interpretation

The several m-thick outerops near Fribourg are interpreted as sediments of subtidal shoals. The m-scale cross-bedded troughs (Set_t) with current ripple marks (Ser) at their base record the occurrence of currents within a subtidal environment and are

interpreted as sand dunes or megaripples. Alternatively, sandstone troughs (Set_r) could be assigned to a mouth-bar environment, where massive bedded sandstones (Sm) would represent recorders of fast sedimentation. Truncated crests of current ripple marks (Ser) record the erosion through strong currents. In contrast, mud drapes (Md) on top of the ripple marks formed during low energy tides, or possibly during slack stages. Similar deposits (Set_r , or possibly Set_a) within the Gurten drill core could also be interpreted as sediments of subtidal shoals, however, due to limited exposure, interpretations are non-conclusive.

Water depth estimations (see supplement) reveal shallow bathymetrical conditions (3–5 m) within a subtidal shoal environment. Discharge directions are assigned to an axial, WSW–ESE directed transport, which is consistent with a tidal-dominated environment where bi-modal sediment transport occurs.

4.2.4 Western and eastern distal basin border (Lake Neuchâtel and Wohlen area): Coarse grained shelly sandstones and coarse grained sandstone sequences

Characterization

Large scale coarse grained sandstones where individual grains might be larger than 2 mm are found along strike in the distal part of the basin between the Lake Neuchâtel and around the Wohlen area (Fig. 2). These deposits are either calcareous sandstones with shelly fragments (Sec) or also called the “Muschelsandstein” of the OMM Ib (Allen et al., 1985: Fig. 4b). Alternatively, they are referred to the coarse grained sandstones with large litho clasts (Sle), also called the “Grobsandstein” (Jost et al., 2016), where coquinas and shell fragments are missing.

Calcareous, shelly sandstones (Sec) occur at distal sites in the western and eastern Molasse basin and are an assemblage of various lithofacies (Table S1, supplement). This Sec facies association is made up of 5–10 m thick, coarse grained sandstone banks with low angular cross beds (Sc). They contain coquinas and shell fragments (Shf) and pebbles (Sg) in places. Interbedded fine grained sandstones contain current ripple marks (Ser) recording an opposite flow direction in relation to the cross beds (Sc). Mapping shows that in the west (near Lake Neuchâtel, Fig. 2), the Sec “Muschelsandstein” deposits are c. 5 m thick and record a NNE to NE directed sediment transport. Foreset heights of these deposits thin to <1 m towards the front of the *Napp* megafan, where herringbone cross beds imply a SW–NE directed, bi-modal sediment transport. Farther to the NE, Sec “Muschelsandstein” deposits grade into Sle “Grobsandstein” units (Jost et al., 2016), which show m high tabular cross beds (Set_a) or dm high trough cross beds (Set_r) with m wide diameters. Measurements of palaeoflow directions reveal a SW and SE directed transport. These deposits are either time equivalents of the Sec “Muschelsandstein” and thus constitute to the OMM Ib sequence, as own observation imply. Alternatively, they also mark the base of the OMM II sequence (Jost et al., 2016).

“Muschelsandstein” deposits are also found in the eastern distal basin near the Wohlen area, where foresets of cross beds are 6 to 8 m, and in some locations up to 10 m high (Allen et al., 1985). In contrast to the deposits near the Lake Neuchâtel, discharge directions are oriented towards the SSW covering the range between 230° and 250° and striking parallel to the

topographic axis. Estimations of water depths of the See “Muschelsandstein” reveal palaeo-bathymetric conditions (Table S2, supplement) between 60 and 100 m, consistent with calculations by Allen et al. (1985).

Interpretation

- 5 The See “Muschelsandstein” sediments are related to tidal deposits along the northern margin of the Burdigalian seaway (Allen et al., 1985, Jost et al., 2016). Cross beds (Set_a) reveal deposition under strong tidal currents (Allen et al., 1985). These deposits are thus assigned to offshore sand waves dominated by strong tides, where sediment transport was NNE (*Lake Neuchâtel*) or SSW directed (*Wohlen* area, Fig. 2). In places, pebbly lags (Sg) are interpreted as flood related splays of gravels into the offshore environment. Contrariwise, the coarse grained sandstones (Sle “Grobsandstein” sediments) reveal similarities to the
- 10 subtidal shoal deposits encountered at *Fribourg* where trough cross bedded sandstones (Set_c) and tabular cross beds (Set_a) dominate the facies assemblages. However, the deposits in the *Wohlen* area are coarser grained, and cross beds have larger diameters, but similar thicknesses. We relate the coarse grained nature of the deposits to the proximity of the Napf megafan in the SW. The cross beds with larger wavelengths and similar amplitudes possibly imply stronger currents compared to the subtidal shoal deposits near St. Magdalena.

15 **5 Evolution of depositional environments**

- As outlined in the previous sections, the lithofacies types encountered in the key sections can be assembled, and thus grouped, into 7 depositional environments including: terrestrial environments and megafans, beaches and estuaries, nearshore to shoreface environments, offshore conditions and subtidal shoals. These depositional environments were mapped within the central Swiss Molasse (see Fig. 2 for sites) according to the criteria outlined above. This section presents the result in the form
- 20 of four paleogeographic maps (Figs. 6a to d).

5.1 USM

- During USM-times, (Fig. 6a), prior to the Burdigalian transgression, the basin was occupied by alluvial megafans at the proximal basin border, which gave way to an axially-directed meanderchannel-belt environment system in the distal basin (Fig. 6a). Palaeo-discharge measurements of sol marks (Schlunegger et al., 1996; this work); Kuhlemann and analysis Kempf;
- 25 2002). Analysis of heavy-mineral assemblages (by Füchtbauer, 1964 (1964) and measurements of palaeo-flow directions in our study area (sole casts, and cross-beds, this paper) and in eastern Switzerland (Kempf et al., 1999) revealed a NE-directed material transport (Fig. 3) towards the Munich region (Fig. 1). There6a). In this area, the Molasse streams ended in a peripheral sea where neritic- to open-marine environment conditions prevailed (Kuhlemann and Kempf, 2002). AWithin the basin, a possible drainage divide for sediment transport was situated somewhere SW of Geneva. We infer such a separation of sediment
- 30 dispersal because orientation of tidal cross-beds to the South of Geneva (Allen et al., 1991; StrunekAllen and Matter, 2002), which may have separated Baas, 1993) imply a southward-oriented discharge to sediment dispersal towards the Tethys in the

S, from a northward, whereas our own and published data from the Swiss part of the Molasse basin reveal a northeast-directed transport to the Paratethys in the NE (Allen et al., 1985). However, the details on the drainage system at that time are not clear, particularly for the region SW of Geneva (Fig. 6a).

5.2 OMM Ia

- 5 The palaeogeographic situation at c. 20 – 19 Ma is shown in Fig. 6b. It illustrates that the central part of the Molasse basin changed to a peripheral shallow-marine sea, which was c. 40 km wide. Palaeo-bathymetric estimates of palaeo-bathymetric conditions revealed and sedimentological data (Figs. 4a and 4b) reveal that the water depths that corresponded to a subtidal and nearshore environment (see supplement). Nearshore to possibly offshore bathymetric conditions (30 – 50 m) are recorded by subtidal mega-sandwaves (Allen and Bass, 1993) south of Lake Geneva and by the predominant occurrence of sandstone-mudstone alternations within the *Wohlen area* Boswil and Hünenberg drill cores in the NE (*Wohlen area*, Fig. 2), where OMM Ia deposits were encountered through drilling (2a; Schlunegger et al., 1997; Farther 1997a). Subtidal shoals, in up to the NE, palaeogeographic reconstructions by Kuhlemann and Kempf (2002) imply that the nearshore to possibly offshore conditions at the *Wohlen area* changed to an open, possibly 5 m-deep marine environment near *Munich*. Subtidal shoals, up to 5 m deep water, occupied the western part of the central Swiss Molasse (Fig. 6b). These deposits separated the deeper nearshore environments on both sides. This was already proposed by Homewood and thus acted as a divide within this peripheral sea. The inferred divide is also corroborated by data about drainage directions (Allen (1981), and Bass, 1993; this work; Fig. 6b); it is here confirmed by our sedimentological data and estimates of palaeo-water depths (supplement). Measurements of sediment transport directions from the shoal deposits themselves (cross-beds) reveal a bi-modal, SW-NE-directed transport, with a dominant NE-orientation. This is particularly the case at the proximal basin border near the Sense section (Fig. 2a) where deltaic foresets accumulated within an estuarine environment (Fig. 4b). Mapping of depositional settings allowed us to trace the shoal deposits towards the northern tip of the Napf-megafan, from where the shoals narrow from c. 20 km to c. 10 km over a 70 km-long distance along strike. It thus appears that the shoals were deflected to the proximal southern basin border and thus towards the topographic axis through a dominant NE-directed material transport (Fig. 6b). This statement interpretation is additionally supported by measurements of the transport directions of the Napf-megafan (i.e. clast imbrications) and the coastal deposits at the Entlen section (i.e. parting-lineation, cross-beds) pointing a material transport towards the NE (Figs. 34a and 6b5a). At the distal margin of the basin, field inspections show that beach sandstones gave way to subtidal-shoal deposits up-section. South of Lake Geneva, sediment discharge transport was oriented towards to the SW (i.e. foresets from subtidal sandwaves and trough. This is indicated by the orientations of cross-beds; (Allen and Bass, 1993; Fig. 6b). It thus appears, that the central Swiss Molasse was a region of sediment export, which was to the northeast and to the southwest. Material transport was most likely accomplished through strong tidal currents (Bieg et al., 2008).

5.3 OMM-Ib

The situation during c. 19—18 Ma ~~includes~~(Fig. 6c) started with the time when the maximum-flooding period (MFS). This surface was formed in the depositional record (MFS; Figs. 5a and 5b). The sedimentological data reveals that this time was characterized by a ~~deepening and~~ widening of the basin to ~~depths > 50 m and~~ widths up to 80 km (Fig. 6e). In comparison to the OMM Ia prior to the maximum flooding conditions, the alluvial megafans at the proximal basin margin experienced a backstepping. This is inferred from the bi-modal E-W orientation of material transport measured from the nearshore sand-waves at the *Entlen* section, which imply a free passage for tidal currents along the basin margin (Fig. 5a) and it was dominated by ~~(6e)~~. Additionally, a deepening of the basin is inferred from the absence of subtidal shoal deposits, or at least from the shifting of this depositional system to the close proximity of the *Napf* megafan. Also in contrast to the OMM Ia, the topographic axis shifted towards the distal basin margin where offshore conditions in the topographic axis with water depths >50 m, as the “Muschelsandstein” deposits imply (Fig. 6c), prevailed (Fig. 6e). There, cross-bed orientations (our measurements of sediment discharge in the distal east (*Wohlen* area) reveal a SW directed transport, while and data by Allen et al., 1985) and heavy mineral assemblages (Allen et al., 1985) reveal that sediment transport in the distal east (*Wohlen* area) occurred towards the SW, whereas sediment dispersal in the distal west (*Lake Neuchâtel* area) was directed towards the NE. Both point towards a possible We use this information to propose that a sedimentary depocenter established at the northern tip of the *Napf*-megafan. In addition, this megafan is interpreted to have experienced a backstepping. We infer such a scenario from the first appearance of a bi-modal E-W-orientation of material transport in the *Entlen* section (Fig. 5a), (see also Allen et al., 1985). Farther Because an E-W-oriented sediment transport requires a free-passage for tidal currents along the southern basin margin, the sea-side margin of the *Napf* megafan had to step back to allow such a passage to the east in the *Munich* area, the offshore marine environment changed to shallow marine conditions (Kuhlemann and Kempf, 2002), form (Figs. 6b and 6c).

5.4 OMM-II to OSM

The palaeogeographic/palaeo-geographic situation shown in Fig. 6d comprises the time span/timespan between c. 18 and c. 14 Ma and displays the evolution from the OMM-II to the OSM. The OMM-II period followed upon a period of erosion and non-sedimentation across the entire *Swiss Molasse* basin (see also, as our re-assessment of the chronological framework of the OMM reveals (Figs. 35a and 45b). This is ~~inferred~~ additionally supported by data from a hiatus encountered within the *Napf* units (this work, Kuhlemann and Kempf, 2009), the seismic ~~lines~~line in the *Wohlen* area (Schlunegger et al., 1997), 1997a), and vadose cements found in the “Muschelsandstein” (Allen et al., 1985) and the best fit correlation of the magnetopolarity stratigraphy in the proximal west (Figs. 3 and 4), 1985). In addition, measurements of discharge ~~direction~~sediment transport directions reveal a SW-oriented sediment transport at proximal positions. (Fig. 5a). This also implies that a possible drainage divided had to shift E-W divide for sediment transport shifted towards the NE and could have been situated somewhere/region near *Munich*, or possibly even farther east. We infer this such a scenario from the supply of

material with sources in the Hercynian basement north of Munich (Fig. 4a) or the Bohemian massif (“Graupensandrinne”; Fig. 6d; Allen et al., 1985; Berger, 1996; Berger et al., 2005; see also setting), which implies a westward orientation of the basin axis. This is consistent with the orientation of the (palaeo-) “Glimmersandrinne” (Berger, 1996) pointing towards the SW (Fig. 6d); tilt of the basin axis. This period ended with the progradation of the alluvial megafans during the time of the OSM, where measurements of discharge directions reveal a NW-oriented transport (Schlunegger et al., 1997; Kuhlemann and Kempf, 2002; Strunck and Matter, 2002; this work).

5.5 Evolution from USM to OSM

In summary conclusion, the establishment of the Burdigalian seaway was accompanied by a change in discharge directions, from an originally NE (USM and OMM Ia times; Figs. 6a and b) to a N to NW directed transport with a strong bi-axial (SW-NE) tidal contribution (OMM Ib and OMM II times (Fig. 6e), and finally to a NW-oriented discharge (OSM times; Fig. 6d). Additionally, the Burdigalian transgression is related to: (i) a deepening and widening of the basin, including a northward shift of the topographic axis to the distal basin margin, where offshore and thus deepest marine conditions established. This shift towards marine conditions was also associated with a change from an overfilled (USM) to an underfilled (OMM) basin. Furthermore, during OMM I times, the central Swiss Molasse acted as a final sedimentary sink situated in front of the Napf megafan. This situation changed during the subsequent OMM II and particularly during OSM times, when the basin became overfilled. At that time, a large fraction of the supplied material became exported towards the SW. These observations point to an incipient tilt of the orientation of the basin axis from the NE to the SW between the OMM I and the OMM II. In support of this interpretation, OMM I sedimentation started slightly earlier in the east than in the west, implying a westward transgression at 20 Ma (see also seismic line BEAGBE.N780025 in the supplement, Fig. S4), while the opposite occurred after e. 18 Ma during 19 Ma, (ii) a reversal of the sediment transport direction from an originally NE-oriented sediment dispersal during OMM-I times, to a SW-oriented sediment transport during deposition of the OMM-II, and (iii) the establishment of a wave-dominated coastline (with some tidal records) on the eastern side of the Napf (Fig. 4a), whereas a tide-dominated estuarine environment characterized the proximal coastal margin on the western side of the Napf (Fig. 4b).

6.3 Controls on the transgression of the OMM II when the sea progressed from the west to the east.

6 Discussion

The Burdigalian transgression of the OMM could be explained by a surface control, where a reduction of supplied sediment volumes (Schlunegger, 1999; Kuhlemann et al., 2001, 2002; Willet, 2010) in combination with an eustatic rise of the sea level (Keller, 2012; Reichenbacher et al., 2013; Pippèr and Reichenbacher, 2017; Müller et al., 1998; Zachos, 2001) have been proposed as plausible mechanisms for an ingression of the peripheral sea to the Swiss part of the Molasse basin (Allen et al., 1985). As will be discussed below, we consider that a reduction of sediment supply rates paired with eustatic variations of the sea level could have contributed to the shift towards an underfilled stage of the basin and the formation of several hiatus. In addition, we will argue that the uplift of the *Aar massif* and the related subduction processes of the European slab (Herwegh

et al., 2017) have most likely been linked with the changes in the basin geometry at the scale of the Swiss Molasse basin. However, these controls are not capable of explaining reversals of discharge directions from the NE to the SW at the scale of the entire basin at least between *Munich* and *Geneva* and beyond (Kuhlemann and Kempf, 2002), which ask for a tectonic control situated at deeper crustal levels. Pfiffner et al. (2002) explored these mechanisms and proposed that the drainage direction reversals occurred in response to a tilt orientation of European foreland plate caused by shifts in the tectonic loading at the crustal scale, which is presented in the next section.

6.2 Stratigraphic signals related to lithospheric scale processes: The reversal of the drainage direction

An interpretation of the drainage reversal requires an overview of the history of the NAFB at a larger spatial and temporal scale. This is presented in this section, but we acknowledge that further research is needed to fully support the interpretation of a possible lithospheric control.

Possible controls on the reversal of the drainage direction and the widening of the basin

We relate the reversal of the drainage direction between the OMM-I and the OMM-II at c. 18 Ma to tectonic processes operating at deeper crustal levels beneath the Alps. This interpretation is guided by a publication of Pfiffner et al. (2002), who related changes in sediment dispersal within the basin to a possible tilt of the foreland plate, caused by the westward shift of the Ivrea body. This tectonic unit comprises mantle rocks with a high density (Fig. 1a) and could thus have influenced the deflection of the foreland plate (Pfiffner et al., 2002). We present a possible geodynamic scenario to explain the change in the drainage direction in the next section, but we also acknowledge that this interpretation is speculative at this stage and warrants further investigations. Such an exploration, however, requires that the geodynamic processes prior to 20 Ma are also considered.

Between 33 and 30 Ma, beneath the Central Alps of Switzerland, the continental lithosphere of the European plate entered started to enter the subduction channel underneath the Adriatic continental plate (Schmid et al., 1996; Kissling and Schlunegger, 2018), while subduction of the European oceanic lithosphere continued beneath the eastern Alps, as palinspastic restorations revealed (Handy et al., 2015). Strong tension forces started to operate at the stretched margin Beneath the Swiss Alps, incipient subduction of the European buoyant continental crust particularly beneath material was considered to have triggered the Central Alps (Schlunegger and Kissling, 2015) with the result that the break-off of the subducted oceanic lithosphere of the European plate broke off (Davies and von Blanckenburg, 1995) (Schmid et al., 1996). The consequence was a rebound of the European plate, a the rise of the Swiss Alps Alpine topography and an increase in a large sediment fluxes flux to the Swiss Molasse basin (Sinclair, 1997; Kuhlemann et al., 2001a; 2001b; Willett, 2010; Garefalakis and Schlunegger, 2018), which finally became overfilled at c. 30 Ma (Sinclair and Allen, 1992; Sinclair, 1997; see also 2.1). East of Munich, however, the basin was still remained underfilled until c. 20 Ma as testified evidenced by deep marine sedimentation, where debris flows and proximal turbidites accumulated within the basin axis (Fertig et al., 1991; Malzer et al., 1993; Lu et al., 2018). We use these observations to propose that vertical vertically-directed slab-load forces were still downwarping the foreland plate beneath the eastern margin of the Eastern Alps- to allow such a deep trough to form, while slab break-off beneath the Central

Alps caused a rebound of the foreland plate in Switzerland (Schmid et al., 1996; Schlunegger and Castellort, 2016). This most likely resulted in a stronger deflection of the European foreland plate beneath the Eastern Alps compared to the Central Alps, which could explain the east-directed sediment transport prior to c. 20 Ma (Fig. 6a).

Between c. 20 – 17 Ma, i.e. during OMM-times, a remarkable change was recorded in the Molasse basin. The eastern Molasse basin experienced a change from deep to shallow marine conditions (Kuhlemann and Kempf, 2002), while the Swiss Molasse basin recorded a reversal of the drainage direction from the E to the W, and material sediment with an eastern provenance signal was supplied to the Swiss Molasse basin through the “Graupensandrinne” (Kuhlemann and Kempf, 2002; see also 2.1).

We relate these observations to changes this reversal in the dispersal of sedimentary material to a SW-directed tilt of the foreland plate, possibly caused by a change in the pattern of slab-load forces along-strike underneath the Alps. Particularly, in the eastern Molasse basin, the change from deep to shallow marine conditions could reflect the occurrence of slab unloading through delamination, or break-off, of the subducted European lithosphere (Ustaszewski et al., 2008), while slab downwarping roll-back subduction of the European plate beneath the Central Alps of Switzerland continued (Kissling and Schlunegger, 2018), and was possibly accelerated, as will be outlined in the next section. We suggest that the inferred Kissling and Schlunegger (2018) proposed. The causes for the along-strike differences in the slab geometry resulted in a tilt of the basin axis towards the west, which is seen in the reversal of the drainage direction between 20 and 18 Ma.

6.3 Stratigraphic signals subduction mechanisms are not clear at this stage and could either be related to crustal-scale processes: The uplift of the Aar massif and the widening of the Swiss Molasse basin

During the Burdigalian, a short phase of fast exhumation ((i) inheritance related to the Mesozoic phase of rifting (Schmid et al., 2004; Handy et al., 2010), (ii) differences in the mechanical strengths of the foreland plate between the Swiss and the German/Austrian Molasse basins (Tesauro et al., 2009; 2013), (iii) and possible differences in rheological conditions as discussed by Mey et al. (2016). In addition, also at 20 Ma, we propose that the velocity of roll-back subduction beneath the Central Alps of Switzerland was likely to have accelerated. We justify this interpretation through the observation that (i) tectonic exhumation of the Lepontine dome (Fig. 1), accomplished through slip along the Simplon detachment fault (Mancktelow and Grasemann, 1997) occurred at the highest rates at that time (Boston et al., 2017; Schlunegger and Willet, 1999), which occurred in the Lepontine area situated in the central Alps of Switzerland (Spicher, 1980), was associated with an uplift pulse of the Aar massif situated farther north (Herwegh et al., 2017; Fig. 2). Kissling and Schlunegger (2018) proposed a mechanism referred to as roll back subduction as an explanation for these observations. According to these authors, delamination of crustal material from the European mantle lithosphere along the Moho resulted in a stacking of buoyant lower crustal rocks beneath the Lepontine dome and the Aar massif forming the crustal root (Fry et al., 2010; Fig. 1b). These processes are considered to have maintained the isostatic equilibrium between the crust and the subducted lithospheric mantle and thus the elevation of the topography (Schlunegger and Kissling, 2015), and and that (ii) they most likely balanced, through the stacking of the crustal root (Fry et al., 2010, Fig. 1b), the fast removal of upper crust material in the Lepontine area at that time (Schlunegger and Willet, 1999; Boston et al., 2017). Delamination of crustal material was also invoked to explain the

rapid ~~exhumation and northward thrusting~~ rise of the Aar-massif ~~along steeply dipping thrusts~~ (Fig. 1) also commenced at ~~e-~~ 20 Ma (Herwegh et al., 2017). This process was most likely accompanied by a short period of fast roll back subduction of the European mantle lithosphere, which was recorded in the Swiss Molasse basin by a 20–40 ~~2017~~. Following Kissling and Schlunegger (2018), these processes require a mechanism where several tens of km ~~northward shift of the distal basin border~~ (Schlunegger and Kissling, 2015; Fig. 1b). ~~thick buoyant crustal material was delaminated from the subducting European continental plate and accumulated within the crustal root (Fig. 7) within a short time period. Such a rapid phase of roll-back subduction would also shift the basin axis to more distal sites, as proposed by Kissling and Schlunegger, (2018; see their Fig. 7).~~ We use these mechanisms to explain the ~~cross-sectional widening of the Molasse Basin at 19 Ma and a deepening the northward shift~~ of the basin ~~in the central Swiss Molasse axis (Fig. 7), thereby~~ giving way to the deposition of the offshore “Muschelsandstein” (Figs. 6b and 6c) ~~particularly during OMM Ib times. Interestingly, this).~~ This lithofacies association has been mapped along the distal basin border adjacent to the external massifs only.

~~In the Aar massif, structural mapping (Wehrens et al., 2015; 2017) revealed that this crustal block was Controls on the establishment of a wave-dominated coast in the east and tidal records in the west~~
Roll-back subduction and the related delamination of crustal material from the subducting European foreland plate was also considered to have resulted in the rise of the Aar-massif (Herwegh et al., 2017), which in turn was likely to have increased the topography surrounding this massif, thereby forming a positive anomaly in the topographic load in the region (Fig. 7). We elaborate the details of these relationships in the following section and then relate the along-strike differences in the depositional environments (wave-dominated coast to the east of the Napf, and estuaries on the western side) to these processes. Structural mapping in the Aar-massif (Wehrens, 2015; Wehrens et al., 2017) has revealed that crustal blocks were rising along steeply SE-dipping thrust faults (Fig. 1b). Accordingly, roll-back subduction, the related delamination of crustal material and the rise of the Aar-massif (Herwegh et al., 2017; Fig. 1b) also resulted in ~~lifted~~ the build-up of topographic loads and topography above the ~~subsequent~~ Aar-massif to higher elevations (Fig. 7). We base this interpretation on the re-routing of the drainage systems (Kühni and Pfiffner, 2001) ~~within the Central Alps. We suggest that the effects related to the rise of the Aar massif are also registered in the basin sedimentology at a smaller scale through subtle details around the region of this external massif, which possibly commenced at that time. As a result, the topographic loads on the foreland plate were likely to have increased in this area.~~ Sinclair et al. (1991) ~~and Sinclair (1996; 1997)~~ explored ~~these a possible~~ stratigraphic ~~responses~~ response to topographic loading, associated with uplift of the Aar-massif (Sinclair et al., 1991), through the application of a linear elastic plate model where thrusting and erosion are dynamically coupled. In their model, the distance between the location of thrusting (Aar-massif) and the site in the basin where a signal is expected depends primarily on the ~~mechanical strength~~ flexural rigidity (or alternatively the elastic thickness or the T_e -value) of the crustal rocks underlying the foreland ~~plate~~ basin (Sinclair, 1996). The flexural rigidity of the ~~plate underlying rocks beneath~~ the Swiss Molasse basin has been quantified with an elastic thickness ranging between of c. 10–30 ~~km~~ km using stratigraphic constraints (Sinclair et al., 1991). This estimate is particularly based on thickness gradients of accumulated Molasse deposits across a section from the distal basin border to the Alpine thrust front. This pattern, however, could have been influenced by upper crustal in-homogeneities (Waschbush and Royden, 1992) such as

e.g. pre-existing faults (Pfiffner, 1986). This could explain why estimates of T_e -values that are based on stratigraphic data are lower (Sinclair et al., 1991; Schlunegger et al., 1997b) than estimates that are based on the curvature of the entire European foreland plate beneath from the Swiss distal Molasse basin (Sinclair et al., 1991; border to the core of the Alps and even deeper (Pfiffner et al., 2002). For a foreland plate with these properties,; Schlunegger and Kissling, 2015). If we consider a local, and thus upper crustal response to loading, characterized by a T_e -value of c. 10 km (Sinclair et al., 1991; Schlunegger et al., 1997b), then shifts in surface loads through the km-thick stacking of additional material (in the Aar-massif) is likely to result have resulted in the formation of several tens of meters of supplementary accommodation space at the proximal basin border, as the models of Sinclair et al. (1991) predict. As a result, depocenters in the Molasse basin are predicted to backstep back to proximal positions, (Sinclair et al., 1991), which is consistent with our observations-interpretation of the flow directions and the related implications for the deposition of the Napf conglomerates (see chapter 6.1, and Fig. 6). In addition, according to Sinclair (1996), upward-directed bulging of a few tens of meters is expected at the distal (forebulge) and at the lateral margins of the load (lateral bulge). The spacing between an expected lateral bulge and the location of the surface forcing ranges between 50 – 100 km, km (using a T_e -value of 10 km), which is consistent with the distance between the Aar-massif and the inferred subtidal-shoals in the western Swiss Molasse basin (near Fribourg; Figs. 22a and 6b). Because the plate had an eastward tilt at that time, as inferred from palaeo-flow directions, such a flexural signal could possibly not be recorded on the east-eastern side of the Aar-massif as where the marine conditions were too deep (Figs. 6b and 6c). We also additionally use these mechanisms to explain the establishment/development of different depositional environments at the proximal basin border of the Swiss Molasse Basin. East of the Napf-megafan, a relatively large/high subsidence (rate of c. 400/340 m/Ma for OMM-Ia and c. 430 m/Ma for OMM-Ib, based on data in Fig. 4a) most likely resulted in a steeper submarine gradient compared to the west, where the inferred bulging possibly lowered and subdued the submarine slopes (subsidence rate of c. 285 m/Ma). for both OMM-Ia and OMM-Ib, based on data in Fig. 4b). This could explain why the operation of waves/evidence for wave action is predominantly recorded along the eastern proximal steeper basin margin. Indeed, investigates/investigations on modern coasts have shown that steeper coasts tend to promote the formation of larger waves (Flemming, 2011). In contrast, in the western Swiss Molasse, estuaries and tidal-channels could establish/develop as the wave energy decreased in the subdued coastal landscape. Note, we cannot fully exclude that uplift along basement uplift, which causes modern irregularities in the contour lines/off-faults beneath the Molasse base/basin in western Switzerland (Spicher, 1980), was shifting) shifted the peripheral sea to shallower bathymetries-also during OMM-times. If such a mechanism did occur, then it could have amplified the effects related to flexural bulging- (Waschbusch and Royden, 1992).

In summary, we suggest that the delamination of the Aar massif and the associated roll back subduction of the European mantle lithosphere had two superimposed effects: It resulted in a widening and deepening of the basin particularly at distal sites, giving way to an offshore seaway where the “Muschelsandstein” accumulated and resulting in the establishment of a depositional sink situated to the north of the Aar massif (Fig. 6c). However, it also resulted in a buckling of the foreland plate through shifts in the surface loading, thereby amplifying the subsidence at the proximal basin border, but subduing the submarine topography through the formation of a lateral bulge where subtidal shoals could establish.

6.4 Stratigraphic signals related to surface controls: Eustatic and sediment flux changes recorded by several hiatus and changes to marine conditions

While tectonic processes are registered in the arrangements

Controls related to changes in sediment supply

- 5 The time around 20 Ma was also characterized by a continuous reduction in sediment flux from originally 25'000 km³/Ma prior to c. 20 Ma to c. 15'000 km³/Ma thereafter (Kuhlemann, 2000; Kuhlemann et al., 2001a, 2001b), which could have contributed, together with the tectonic widening of the basin, to the transgression of the peripheral sea in Switzerland (Fig. 8). The mechanisms leading to this reduction in surface mass flux are not fully understood (Kuhlemann et al., 2002), and multiple hypotheses have been proposed including: (i) shifts towards a dryer palaeo-climate paired with a widespread exhumation of
- 10 crystalline rocks with low bedrock erodibilities (Schlunegger et al., 2001); (ii) tectonic exhumation of the Lepontine through slip along the Simplon detachment fault, which occurred in response to rapid roll-back subduction (see above and Kissling and Schlunegger, 2018). Tectonic exhumation was considered to have shifted the drainage divide farther to the north, thereby substantially decreasing the source area of the Molasse basin (Kuhlemann et al., 2001a); and (iii) uplift of the Aar-massif, which was considered to have resulted in a reorganization of the Alpine streams and which was also associated with a reduction
- 15 of the source area of the Molasse basin (Kühni and Pfiffner, 2001). Except for the palaeo-climate hypothesis, all other mechanisms are ultimately linked to the tectonic processes we have outlined in the sections above.

Controls related to changes in eustatic sea levels

- 20 Whereas tectonic processes are recorded in the arrangement of depositional systems in the entire Swiss Molasse basin, signals related to the eustatic changes of ~~the~~ sea level are possibly recorded ~~mainly~~ by several ~~hiatus~~hiatuses. This particularly concerns the times of non-sedimentation between OMM-I and OMM-II, and between the OMM- and the OSM-phase, which we have elaborated in chapter 5.1 (Figs. 4a5a and 78). In this context, $\delta^{18}\text{O}$ -values measured on benthic foraminifera have been used as proxy for establishing patterns of sea level changes (Miller, et al., 1998). In particular, a shift to more positive values of the stable oxygen isotope $\delta^{18}\text{O}$ implies a growth of polar ice sheets, where lighter oxygen isotopes ($\delta^{16}\text{O}$) are preferentially stored
- 25 (Zachos, 2001). As a consequence, ~~the~~ global sea level most likely decreased (amplitude of drop is not really known) during shifts towards heavier (and thus more positive) isotopic records in planktonic organisms (Miller et al., 1998). These patterns have been reconstructed by Miller et al. (1996; 1998) at a high resolution. Interestingly, shifts towards larger $\delta^{18}\text{O}$ values generally coincide with times when hiatus are registered in the Molasse basin (Fig. 7; see also Pippèr and Reichenbacher, 2017; Sant et al., 2017). We thus suggest, that even small drops in global sea level initiated a phase of erosion and recycling
- 30 of previously deposited sediments because of the proximity of the Swiss Molasse to the peripheral seas. As a more prominent signal, it is possible that a reduction in the supply rates of sediment to the Swiss Molasse basin contributed to the shift towards marine conditions (Fig. 7). Kuhlemann et al. (2002) quantified volumes of sediments preserved in the circum Alpine basin (with subsequent modifications by Willett, 2010) and identified the fluxes of material with sources in the Alps. According to the sediment budgets of these authors, the Burdigalian transgression at c. 20 Ma was associated with a c. 30—40 % reduction

of the supply rates of sediment from the Central Alps to the Swiss Molasse basin, from 25'000 km³/Ma prior to c. 20 Ma to c. 15'000 km³/Ma thereafter (Fig. 7). The mechanisms leading to this reduction in surface mass fluxes are not fully understood (Kuhlemann et al., 2002), and multiple hypotheses have been proposed including: (i) shifts towards a dryer climate paired with a widespread exhumation of crystalline rocks and a reorganisation of the drainage network in the Central Alps (Schlunegger et al., 2001), (ii) tectonic extension along the Simplon detachment fault which could have lowered the surface topography in the Swiss Alps (Kuhlemann et al., 2001), and (iii) changes in the tectonic forcing where the uplift of the *Aar massif* resulted in a rerouting of the Alpine streams and a reduction in their erosive power (Kühni and Pfiffner, 2001). Irrespective of the proposed mechanisms, the reduction of the supply rates of sediment most likely contributed to the establishment of marine conditions in Switzerland. In this context, an increase in sediment fluxes after c. 17 Ma (Kuhlemann et al., 2002) could have resulted in the shift from marine to continental sedimentation giving way the OSM. Shifts towards larger $\delta^{18}\text{O}$ -values generally coincide with times when hiatuses are recorded in the Molasse basin (Fig. 8; see also Pippèr and Reichenbacher, 2017; Sant et al., 2017). We thus suggest that drops in global sea level of a few tens of meters initiated a phase of no deposition in the Swiss part of the Molasse basin, at least between OMM-I and OMM-II at c. 18 Ma, and between the OMM and the OSM.

15 7 Summary and Conclusion

In summary, we suggest that the Burdigalian transgression was ~~controlled through the related to~~ a combination of a deepening and widening of the basin and a reduction of ~~the sediment~~ supply rates ~~of sediments~~, which we ultimately relate to tectonic processes in the Alpine hinterland. In this context, ~~we consider that roll-back subduction was most likely responsible for the widening of the basin in the foreland and for the shift of the basin axis to distal positions. In addition,~~ roll-back subduction of the European mantle lithosphere, ~~and~~ delamination of crustal material ~~most likely resulted in the rapid exhumation of the Lepontine dome (Boston et al., 2017) and the associated rise of the Aar-massif (Herwegh et al., 2017) was most likely responsible for the widening of the basin in the foreland (Schlunegger and Kissling, 2015).2017).~~ In the Alpine hinterland, these processes occurred simultaneously with a slip along the Simplon detachment fault and thus with a change in the configuration ~~of exposed lithologies~~ ~~the drainage network~~ (Schlunegger et al., 2001; Kühni and Pfiffner, 2001), with the consequence that the sediment ~~fluxes~~ ~~flux~~ to the basin decreased. ~~This reduction in sediment flux, together with the tectonic widening of the basin, was thus likely to have controlled the transgression of the peripheral sea in Switzerland (Fig. 8). In addition, shifts in surface loads, caused by thrusting the rise of the Aar-massif, resulted in flexural adjustments in the Molasse basin, which. This could explain the establishment/development of distinct depositional environments and the formation of subtidal-shoals where a lateral bulge is expected. Because of the formation of shallow marine conditions, subtle changes in the eustatic sea level contributed to the occurrence of several hiatus/hiauses (Sant et al., 2017). While/Whereas these mechanisms are capable of explaining the establishment of the Burdigalian seaway and the formation of distinct sedimentological niches in Switzerland, the drainage reversal during OMM -times possibly requires a change in the tectonic processes at the slab scale. This study thus shows that tectonic and a scale that includes the subduction history of the entire mountain range, at least between the Eastern and Central Alps. Current explanations are still speculative and await the results on ongoing research in the~~

5 framework of the AlpArray initiative. At this stage, we conclude that the geodynamic processes in the Alps including: subduction mechanisms, delamination of crustal material and uplift of the Aar-massif, reorganization of the drainage network and lower sediment flux are reflected in the Swiss Molasse basin through the establishment of shallow marine conditions and a shift of the topographic axis towards more distal sites at 19 Ma. Accordingly, the Burdigalian transgression in Switzerland most likely had a tectonic driving force, but with amplifications through responses occurring on the surface signals can be extracted from the stratigraphic record provided that a detailed sedimentological and chronological database is available of the Alps.

References

- [Allen, J.R.L. : Sedimentary Structures. Their Characteristics and Physical Basis. Vol. I. Developments in Sedimentology 30A. Elsevier, Amsterdam, 593 p., 1982.](#)
- 5 [Allen, J.R.L. : Sedimentary Structures. Their Characteristics and Physical Basis. Vol. I. Developments in Sedimentology 30B. Elsevier, Amsterdam, 679 p., 1984.](#)
- Allen, P.A. : Reconstruction of ancient sea conditions with an example from the Swiss Molasse. *Marine Geology* 60, 455 – 473, 1984.
- Allen, P.A. : [Earth Surface Processes, 404 p. ISBN 0-632-03507-2, 1997.](#)
- 10 [Allen, P. A., and Homewood, P. : Evolution and mechanics of a Miocene tidal sandwave. *Sedimentology*, 31 \(1\), 63 – 81, 1984.](#)
- [Allen, P.A., Mange-Rajetky, A. and Matter, A. : Dynamic palaeogeography of the open Burdigalian seaway, Swiss Molasse basin. *Eclogae Geologicae Helvetiae*, 78, 351 – 381, 1985.](#)
- ~~[Allen, P.A. and Allen, J.R. : Basin Analysis: Principles and Applications. Malden, MA. Blackwell Pub., ix, 549 p., ISBN: 0632052074, 2005.](#)~~
- 15 Allen. P. A. and Bass. J. P. : Sedimentology of the Upper Marine Molasse of the Rhône-Alp region. Eastern France: Implications for basin evolution. *Eclogae geologicae Helvetiae* [Geologicae Helvetiae](#), 86(1), 121 – 171, 1993.
- Allen, P. A., Crampton, S. L. and Sinclair, H. D. : The inception and early evolution of the North Alpine foreland basin, Switzerland. *Basin Research*, 3(3), 143 – 163, 1991.
- 20 [Allen, P.A. and Allen, J.R. : Basin Analysis: Principles and Applications. Malden, MA. Blackwell Pub., ix, 549 p., ISBN: 0632052074, 2005.](#)
- [Baas, J. H. : Ripple, ripple mark, ripple structure. In: *Sedimentology. Encyclopedia of Earth Science, Springer, Berlin, Heidelberg*, 921 – 925, 1978.](#)
- Bates, C. C. : Rational theory of delta formation. *AAPG Bulletin*, 37(9), 2119 – 2162, 1953.
- Beaumont, C. : Foreland basins. *Geophysical Journal International*, 65, (2), 291 – 329, 1981.
- 25 Berger, J.-P. : Cartes paléogéographiques-palinspastiques du bassin molassique suisse (Oligocène inférieur – Miocène moyen). *N. Jb. Geol. Paläont. Abh.* 2002 (1), 1 – 44, 1996.
- Bieg, U., Süss, M. P., and Kuhlemann, J. : Simulation of tidal flow and circulation patterns in the Early Miocene (Upper Marine Molasse) of the Alpine foreland basin. *Analogue and Numerical Modelling of Sedimentary Systems: From Understanding to Prediction*, 40, 145 – 169, 2008.

- Boston, K.R., Rubatto, J., Hermann, J., Engi, M. and Amelin, Y. : Geochronology of accessory allanite and monazite in the Barrovian metamorphic sequence of the Central Alps, Switzerland. *Lithos*, 286 – 287, 502 – 518, 2017.
- [Bridge, J.S. and Tye, R.S. : Interpreting the dimensions of ancient fluvial channel bars, channels and channel belts from wireline-logs and cores. *AAPG Bulletin*, 84 \(8\), 1205 – 1228, 2000.](#)
- 5 Burbank, D. W., Engesser, B., Matter, A. and Weidmann, M. : Magnetostratigraphic chronology, mammalian faunas, and stratigraphic evolution of the Lower Freshwater Molasse, Haute-Savoie, France. *Eclogae Geologicae Helvetiae*, 85(2), 399 – 431, 1992.
- Cande, S.C. and Kent, D.V. : A new geomagnetic polarity time scale for the Late Cretaceous and Cenozoic. *Journal of geophysical research*, 97, 913 – 951, 1992.
- 10 Cande, S.C. and Kent, D.V. : Revised calibration of the geomagnetic polarity timescale for the Late Cretaceous and Cenozoic. *Journal of geophysical research*, 100, 6093 – 6095, 1995.
- Cederbom, C.E., Sinclair, H.D., Schlunegger, F. and Rahn, M. : Climate-induced rebound and exhumation of the European Alps. *Geology*, 32, 709 – 712, 2004.
- Cederbom, C.E., van der Beek, P., Schlunegger, F., Sinclair, H.D. and Oncken, O. : Rapid extensive erosion of the North Alpine foreland basin at 5–4 Ma – 4 Ma. *Basin Research*, 23(5), 528 – 550, 2011.
- 15 [Clifton, H.E. and Dingler, J.R. : Wave-Formed Structures and Paleoenvironmental Reconstruction. *Marine Geology*, 60, 165 – 198, 1984.](#)
- [Daidu, F., Yuan, W. and Min, L. : Classifications, sedimentary features and facies associations of tidal flats. *Journal of Palaeogeography*, 2 \(1\), 66 – 80, 2013.](#)
- 20 [Dam, G., and Andreasen, F. : High-energy ephemeral stream deltas; an example from the Upper Silurian Holmestrand Formation of the Oslo Region, Norway. *Sedimentary Geology*, 66 \(3-4\), 197 – 225, 1990.](#)
- Davies, J. and von Blanckenburg, F. : Slab breakoff: A model of lithosphere detachment and its test in the magmatism and deformation of collisional orogens. *Earth and Planetary Science Letters*, 129, 85 – 102, 1995.
- DeCelles, P. G. : Late Jurassic to Eocene evolution of the Cordilleran thrust belt and foreland basin system, western USA. *American Journal of Science*, 304 (2), 105 – 168, 2004.
- 25 DeCelles, P.G. and Giles, K.A. : Foreland basin systems: *Basin Research* 8, 105 – 123, 1996.
- Diem, B. : [Analytical method for estimating paleowave climate and water depth from wave ripple marks. *Sedimentology*, 32, 705 – 720, 1985.](#)
- 30 [Diem, B. : Die Untere Meeresmolasse zwischen der Saane \(Westschweiz\) und der Ammer \(Oberbayern\). *Eclogae Geologicae Helvetiae*, 79 \(2\), p. 493 – 559, 1986.](#)

- [Doppler, G. : Zur Stratigraphie der nördlichen Vorlandmolasse in Bayerisch-Schwaben. *Geologica Bavarica*, 94, 83 – 133, 1989.](#)
- Engesser, B. : Die Eomyidae (Rodentia, Mammalia) der Molasse der Schweiz und Savoyens. Systematik und Biostratigraphie. - Schweiz. Paläont. Abh. 112, 1 – 144, 1990.
- 5 Fertig, J., Graf, R., Lohr, H., Mau, J., Müller, M. : Seismic sequence and facies analysis of the Puchkirchen Formation, Molasse basin, south-east Bavaria, Germany. *Eur. Assoc. Pet. Geosci. Spec. Publ.* 1, 277 – 287, 1991.
- Flemings, P. B. and Jordan, T. E. : Stratigraphic modeling of foreland basins: Interpreting thrust deformation and lithosphere rheology. *Geology*, 18 (5), 430 – 434, 1990.
- Flemming, B.W. : *Geology, Morphology, and Sedimentology of Estuaries and Coasts. Treatise on Estuaries and Coasts*, 3 (2), 7 – 38, 2011.
- 10 [Frieling, D., Mazumder, R., and Reichenbacher, B. : Tidal sediments in the Upper Marine Molasse \(OMM\) of the Allgäu area \(Lower Miocene, Southwest-Germany\). *Neues Jahrbuch für Geologie und Paläontologie-Abhandlungen*, 254 \(1-2\), 151 – 163, 2009.](#)
- 15 [Froitzheim, N., Schmid, S.M. and Frey, M. : Mesozoic paleogeography and the timing of eclogite-facies metamorphism in the Alps: A working hypothesis. *Eclogae Geologicae Helvetiae*, 89, 81 – 110, 1996.](#)
- Fry, B., Deschamps, F., Kissling, E., Stehly, L. and Giardini, D. : Layered azimuthal anisotropy of Rayleigh wave phase velocities in the European Alpine lithosphere inferred from ambient noise. *Earth and Planetary Science Letters*, 297, 95 – 102, 2010.
- Füchtbauer, H. : Sedimentpetrographische Untersuchungen in der älteren Molasse nördlich der Alpen. *Eclogae Geologicae Helvetiae*, 61, 157 – 298, 1964.
- 20 Garefalakis, P. and Schlunegger, F. : Link between concentrations of sediment flux and deep crustal processes beneath the European Alps. *Scientific Reports*, 8(1), 183, 2018.
- Haldemann, E. G., Haus, H. A., Holliger, A., Liechti, W., Rutsch, R. F., and Della Valle, G. : *Geologischer Atlas der Schweiz, Blatt 1188 Eggiwil (Nr. 75): Schweizerische Geologische Kommission, scale 1:25 000, 1 sheet, 1980.*
- 25 [Hammer, B. : *Sedimentologie der Oberen Meeresmolasse im Raum St. Gallen. Unpublished Diploma thesis. Univ. Bern, Bern, Switzerland, 96 pp., 1984.*](#)
- Handy, M.R., Schmid, S.M., Bousquet, R., Kissling, E. and Bernoulli, D. : Reconciling plate-tectonic reconstructions of Alpine Tethys with the geological – geophysical record of spreading and subduction in the Alps. *Earth Science Reviews*, 102 (3–4), 121 – 158, 2010.
- 30 Handy, M.R., Ustaszewski, K. and Kissling, E. : Reconstructing the Alps-Carpathians-Dinarides as key to understanding switches in subduction polarity, slab gaps and surface motion. *International Journal of Earth Sciences*, 104 (1), 1 – 26, 2015.

- Herwegh, M., Berger, A., Baumberger, R., Wehrens, P. and Kissling, E. : Large-scale crustal-block-extrusion during Late Alpine collision. *Scientific Reports* 7, 413, 2017.
- Hilgen, F. J., Lourens, L. J., Van Dam, J. A., Beu, A. G., Boyes, A. F., Cooper, R. A., Krijgsman, W., Ogg, J.G., Piller, W.E. and Wilson, D. S. : The Neogene period. In: *The geologic time scale*, 923 – 978, 2012.
- 5 Homewood, P. and Allen, P.A. : Wave-, Tide-, and Current-Controlled Sandbodies in Miocene Molasse, Western Switzerland. *The American Association of Petroleum Geologists Bulletin* 65, 2534 – 2545, 1981.
- Homewood, P., Allen, P.A. and ~~Williams~~Williams, G.D. : Dynamics of the Molasse Basin of western Switzerland. *Spec. Publ. int. Ass. Sediment.*, 8, 199 – 217, 1986.
- Hurford, A. J. : Cooling and uplift patterns in the Lepontine Alps, south central Switzerland and an age of vertical movement on the Insubric fault line: *Contributions to Mineralogy and Petrology*, v. 93, 413 – 427, 1986.
- 10 Isler, A. and Murer, R. : *Geologische Karte der Schweiz, Kartenblatt 1149 Wollhusen 1:25'000*, Bundesamt für Landestopographie swisstopo, in press, 2019.
- [Jin, J., Aigner, T., Luterbacher, H.P., Bachmann, G.H., Müller, M. : Sequence stratigraphy and depositional history in the south-eastern German Molasse Basin. *Mar. Pet. Geol.* 12, 929 – 940, 1995.](#)
- 15 Jordan, T. E. : Thrust loads and foreland basin evolution, Cretaceous, western United States. *AAPG bulletin*, 65 (12), 2506 – 2520, 1981.
- Jordan, T. E. and Flemings, P. B. : Large-scale stratigraphic architecture, eustatic variation, and unsteady tectonism: A theoretical evaluation. *Journal of Geophysical Research: Solid Earth*, 96 (B4), 6681 – 6699, 1991.
- Jost, J., Kempf, O. and Kälin, D. : Stratigraphy and palaeoecology of the Upper Marine Molasse (OMM) of the central Swiss Plateau. *Swiss Journal of Geosciences*, 109(2), 149 – 69, 2016.
- 20 Kälin, D. and Kempf, O. : High-resolution stratigraphy from the continental record of the Middle Miocene Northern Alpine Foreland Basin of Switzerland. *N. Jb. Geol. Paläont. Abh.*, 254, 177 – 235, 2009.
- Keller, B. : *Fazies und Stratigraphie der Oberen Meeresmolasse (Unteres Miozän) zwischen Napf und Bodensee*. Ph.D., Bern, 302 p., 1989.
- 25 Keller, B. : [Wirkung von Wellen und Gezeiten bei der Ablagerung der Oberen Meeresmolasse–Löwendenkmal und Gletschergarten–zwei anschauliche geologische Studienobjekte. *Mitteilungen der Naturforschenden Gesellschaft Luzern*, 31, 245 – 271, 1990.](#)
- [Keller, B.](#) : Facies of Molasse based on a section across the central part of the Swiss Plateau. *Swiss Bull. Angew. Geol.*, 17/2, 3 – 19, 2012.

- Keller, B., Bläsi, H.-R., Platt, N.H., Mozley, P.S. and Matter, A. : Sedimentäre Architektur der distalen Unteren Süßwassermolasse und ihre Beziehung zur Diagenese und den petrophysikal. Eigenschaften am Beispiel der Bohrungen Langenthal. - Nagra Technischer Bericht NTB 90-41, Nagra, Wettingen, 1990.
- 5 Kempf, O. Bolliger, T., Kälin, D., Engesser, B and Matter, A. : New magnetostratigraphic calibration of Early to Middle Miocene mammal biozones of the North Alpine foreland basin. *Mém. Trav. EPHE Inst. Montpellier* 21, 547 – 561, 1997.
- Kempf, O. : Magnetostratigraphy and facies evolution of the Lower Freshwater Molasse (USM) of eastern Switzerland. Ph.D., Bern, 138 p., 1998.
- 10 Kempf, O. and Matter, A. : Magnetostratigraphy and depositional history of the Upper Freshwater Molasse (OSM) of eastern Switzerland. *Eclogae Geologicae Helvetiae*, 92, 97–103, 1999.
- Kempf, O., Matter, A., Burbank, D.W. and Mange, M. : Depositional and structural evolution of a foreland basin margin in a magnetostratigraphic framework: the eastern Swiss Molasse basin. *International Journal of Earth Sciences*, 88, 253 – 275, 1999.
- 15 Kissling, E. : Deep structure of the Alps—what do we really know? *Physics of the Earth and Planetary Interiors*, 79 (1-2), 87 – 112, 1993.
- Kissling, E., and Schlunegger, F. : Rollback orogeny model for the evolution of the Swiss Alps. *Tectonics*, 37(4), 1097 – 1115, 2018.
- Kuhlemann, J. : [Post-collisional sediment budget of circum-Alpine basins \(Central Europe\). *Mem. Sci. Geol. Padova* 52, 1–91, 2000.](#)
- 20 [Kuhlemann, J., Frisch, W., Dunkl, I., Székely, B., Spiegel, C. : Miocene shifts of the drainage divide in the Alps and their foreland basin. *Z. Geomorphol., N.F.* 45, 239 – 265, 2001a.](#)
- [Kuhlemann, J., Frisch, W., Dunkl, I., and Székely, B. : Quantifying tectonic versus erosive denudation by the sediment budget: The Miocene core complexes of the Alps. *Tectonophysics*, 330\(1-2\), 1 – 23, ~~2001~~2001b.](#)
- 25 Kuhlemann, J., Frisch, W., Székely, B., Dunkl, I., and Kázmér, M. : Post-collisional sediment budget history of the Alps: tectonic versus climatic control. *International Journal of Earth Sciences*, 91(5), 818 – 837, 2002.
- Kuhlemann, J. and Kempf, O. : Post-Eocene evolution of the North Alpine Foreland Basin and its response to Alpine tectonics. *Sedimentary Geology* 152, 45 – 78, 2002.
- Kühni, A. and Pfiffner, O. A. : The relief of the Swiss Alps and adjacent areas and its relation to lithology and structure: topographic analysis from a 250-m DEM. *Geomorphology*, 41(4), 285 – 307, 2001.
- 30 [Leclair, S.F. and Bridge, J.S. : Quantitative interpretation of sedimentary structures formed by river dunes. *Journal of Sedimentary Research*, 71, 713 – 716, 2001.](#)

- [Lemcke, K., Engelhardt, W. V., and Füchtbauer, H. : Geologische und sedimentpetrographische Untersuchungen im-Westteil der ungefalteten Molasse des süddeutschen-Alpenvorlandes. Beihefte zum Geologischen Jahrbuch, 11, 1 – 182, 1953.](#)
- [Lihou, J.C, and Allen, P.A. : Importance of inherited rift margin structures in the early North Alpine Foreland Basin, Switzerland. Basin Research, 8, 425 – 442, 1996.](#)
- 5 Lippitsch, R., Kissling, E. and Ansorge, J. : Upper mantle structure beneath the Alpine orogen from high-resolution teleseismic tomography. *Journal of Geophysical Research*, 108(B8), 2376, 2003.
- Lourens, L. J., F.J. Hilgen, J. Laskar, Shackleton, N. J., and Wilson, D. : *The Neogene Period. A Geologic Time Scale 2004*, Cambridge University Press, 409 – 440, 2004.
- 10 Lu, G., Winkler, W., Rahn, M., von Quadt, A. and Willett, S.D. : Evaluating igneous sources of the Tavayannaz formation in the Central Alps by detrital zircon U–Pb age dating and geochemistry. *Swiss Journal of Geosciences*, 111(3), 399 – 416, 2018.
- Malzer, O., Rögl, F., Seifert, P., Wagner, L., Wessely, G., Brix, F. : *Die Molassezone und deren Untergrund. Erdöl und Erdgas in Österreich*, 281 – 322, 1993.
- 15 Mancktelow, N. : The Simplon Line: a major displacement zone in the western Lepontine Alps. *Eclogae Geologicae Helvetiae*, 78(1), 73 – 96, 1985.
- Mancktelow, N. S., and Grasemann, B. : Time-dependent effects of heat advection and topography on cooling histories during erosion. *Tectonophysics*, 270 (3-4), 167 – 195, 1997.
- Matter, A. : *Sedimentologische Untersuchungen im östlichen Napfgebiet (Entlebuch – Tal der Grossen Fontanne, Kt. Luzern).* [EelogareEclogae](#) *Geologicae Helvetiae*, 57, 315 – 429, 1964.
- 20 Matter, A., Homewood, P., Caron, C., Rigassi, D., van Stuijvenberg, J., Weidmann, M. and Winkler, W. : *Flysch and Molasse of western and central Switzerland. Exc. Guidebook No. 126A 26th Int. Geol. Congr. Schweiz. Geol. Komm. Wepf and Co. Publ., Basel, 1980.*
- Mazurek M, Hurford A, Leu W. : Unravelling the multi-stage burial history of the Swiss Molasse basin: Integration of Apatite fission track, vitrinite reflectance and biomarker isomerisation analysis. *Basin Research*, 18, 27 – 50, 2006.
- 25 Mein, P. : Résultats du groupe de travail des vertébrés: Biozonation du Néogène méditerranéen à partir des Mammifères. In: Sénès, J. (ed.), *Report Report on Activity of the RCMNS Working groups (1971-1975)*, 78 – 81, Bratislava, 1975.
- Mein, P. : Rapport d'activité du Groupe de Travail Vertébrés Mise à jour de la biostratigraphie du Néogène basée sur les Mammifères. *Ann. géol. Pays Héilen., Tome hors série, 3, 1367-72. (VII International Congress on Mediterranean Neogene, Athens, 1979), 1979.*
- 30 Mein, P. : Updating of MN zones. In: Lindsay, E., Fahlbusch, V. and Mein, P. (eds.), *European Neogene mammal chronology. NATO ASI, Life Sci. 180, 73 – 90. Plenum Press, New York, 1989.*

- [Mey, J., Scherler, D., Wicker, A., Egholm, D., Tesauro, M., Schildgen, T.F., and Strecker, M. : Glacial isostatic uplift of the European Alps. *Nature Communications*, 7, 13382, 2016.](#)
- [Miall, A.D. : Lithofacies types and vertical profile models in braided river deposits, a summary. In: MIALL, A.D. \(Ed.\): *Fluvial sedimentology*. p. 597-604. -*Can. Soc. Petr. Geol. Mem.* 5, 1978.](#)
- 5 [Miall, A.D. : Architectural-Element Analysis : A New Method of Facies Analysis Applied to Fluvial Deposits. *Earth-Sci. Rev.* 22, 261 – 308, 1985.](#)
- [Miall, A. D. : *The Geology of Fluvial Deposits. Sedimentary Facies, Basin Analysis, and Petroleum Geology.* Springer. 582 p., 1996.](#)
- 10 [Miller, M.C. and Komar, P.D. : Oscillation Sand Ripples Generated by Laboratory Apparatus. *Journal of Sedimentary Research*, 50\(1\), 173 – 182, 1980a.](#)
- [Miller, M.C. and Komar, P.D. : A field investigation of the relationship between oscillation ripple spacing and the near-bottom water orbital motions. *Journal of Sedimentary Research*, 50 \(1\), pp.183 – 191, 1980b.](#)
- ~~[Miller, K.G., Mountain, G.S., Browning, J.V., Kominz, M., Sugarman, P.J., Christie-Blick, N., Katz, M.E. and Wright, J.D. : Cenozoic global sea level, sequences, and the New Jersey transect: results from coastal plain and continental slope drilling. *Rev. Geophys.*, 36, 569 – 601, 1998.](#)~~
- 15 [Miller, K.G., Mountain, G.S., the Leg 150 Shipboard Party, and Members of the New Jersey Coastal Plain Drilling Project : Drilling and dating New Jersey Oligocene–Miocene sequences: Ice volume, global sea level, and Exxon records. *Science* 271\(1\), 92 – 94, 1996.](#)
- 20 [Miller, K.G., Mountain, G.S., Browning, J.V., Kominz, M., Sugarman, P.J., Christie-Blick, N., Katz, M.E. and Wright, J.D. : Cenozoic global sea level, sequences, and the New Jersey transect: results from coastal plain and continental slope drilling. *Rev. Geophys.*, 36, 569 – 601, 1998.](#)
- [Nichols, P.G. : *Sedimentology & Stratigraphy.* Blackwell Sci., 355 p., 1999.](#)
- 25 [Ortner, H., Fügenschuh, B., Zerlauth, M., Hinsch, R., Friedrich, A., Hofmann, F., and Neumeier, G. : Geometry, sequence and amount of thrusting in the sub-Alpine Molasse of Austria and Bavaria. *Fragile Earth: Geological processes from global to local scales and associated hazards: Boulder, Geological Society of America A*, 39, 2011.](#)
- [Pippèr, M. and Reichenbacher, B. : Late Early Miocene palaeoenvironmental changes in the North Alpine Foreland Basin. *Palaeogeography, Palaeoclimatology, Palaeoecology* 468, 485 – 502, 2017.](#)
- [Pfiffner, O.A. : Evolution of the north Alpine foreland basin in the Central Alps. Special Publication, International Association of Sedimentologists 8, 219 – 228, 1986.](#)
- 30 [Pfiffner, O. A., Schlunegger, F. and Buitter, S. J. H. : The Swiss Alps and their peripheral foreland basin: Stratigraphic response to deep crustal processes. *Tectonics*, 21\(2\), 2002.](#)

- Platt, N. H. and Keller, B. : Distal alluvial deposits in a foreland basin setting—the Lower Freshwater Miocene), Switzerland: sedimentology, architecture and palaeosols. *Sedimentology*, 39 (4), 545 – 565, 1992.
- [Python, C. : Geologische Karte der Schweiz, Kartenblatt 1185 Fribourg 1:25'000, Bundesamt für Landestopographie swisstopo, 1996.](#)
- 5 Reichenbacher, B., Krijgsman, W., Lataster, Y., Pipperr, M., Van Baak, C. G., Chang, L., Kälin, D., Jost, J., Doppler, G., Jung, D., Priet, J., Abdul Aziz, H., Böhme, M., Garnish, J., Kirscher, U. and Bachtadse, V. : A new magnetostratigraphic framework for the Lower Miocene (Burdigalian/Ottnangian, Karpatian) in the North Alpine Foreland Basin. *Swiss Journal of Geosciences*, 106(2), 309 – 334, 2013.
- 10 [Reichenwallner, S. : Die vulkanische Aktivität in den Westalpen hergeleitet aus detritischem Amphibol und Klinopyroxen im Taveyannaz-Sandstein. Unpublished Ms-thesis, University of Bern, Bern, 57 pp. 2019.](#)
- [Reineck, H.E. and Singh, I. B. : Depositional sedimentary environments. Springer, 549 p., 1980.](#)
- [Rust, B.R. and Gibling, M.R. : Braidplain evolution in the Pennsylvanian South Bar Formation, Sydney basin, Nova Scotia, Canada. *Journal of Sedimentary Petrology*, 60 \(1\), 59 – 72, 1990.](#)
- 15 [Salvermoser, S. Zur Sedimentologie gezeiten-beeinflusster Sande in der Oberen Meeresmolasse und Süssbrackwassermolasse \(Ottnangium\) von Niederbayern und Oberösterreich. *Münchner Geologische Hefte, A*, 26: 1 – 179, 1999.](#)
- Sant, K., V. Palcu, D., Mandic, O., and Krijgsman, W. : Changing seas in the Early–Middle Miocene of Central Europe: a Mediterranean approach to Paratethyan stratigraphy. *Terra Nova*, 29(5), 273 – 281, 2017.
- Schaad, W., Keller, B. and Matter, A. : Die Obere Meeresmolasse (OMM) am Pfänder: Beispiel eines Gilbert-Deltakomplexes. *Eclogae Geologicae Helvetiae, Geol. Helv.*, 85, 145 – 168, 1992.
- 20 [Shanmugam, G. : Deep-marine tidal bottom currents and their reworked sands in modern and ancient submarine canyons. *Marine and Petroleum Geology*, 20 \(5\), 471 – 491, 2003.](#)
- Schlunegger, F., Burbank, D.W., Matter, A., Engesser, B. and Mödden, C. : Magnetostratigraphic calibration of the Oligocene to Middle Miocene (30–15 Ma) mammal biozones and depositional sequences of the Swiss Molasse Basin. *Eclogae Geologicae Helvetiae, Geol. Helv.*, 89, 753 – 788, 1996.
- 25 Schlunegger, F., Leu, W. and Matter, A. : Sedimentary Sequences, Seismic Facies, Subsidence Analysis, and Evolution of the Burdigalian Upper Marine Molasse Group, Central Switzerland. *The American Association of Petroleum Geologists* 81, 1185 – 1207, [1997/1997a](#).
- [Schlunegger, F., Jordan, T.E., and Klaper, E.M. : Controls of erosional denudation on foreland basin evolution: The Oligocene central Swiss Molasse Basin as an example. *Tectonics*, 16, 823 – 840, 1997b.](#)
- 30 [Schlunegger, F., Slingerland, R. and Matter, A. : Crustal thickening and crustal extension as controls on the evolution of the drainage network of the central Swiss Alps between 30 Ma and the present: constraints from the stratigraphy of the North Alpine Foreland Basin and the structural evolution of the Alps. *Basin Research*, 86, 717 – 750, 1998.](#)

- Schlunegger, F. and Willett, S. : Spatial and temporal variations in exhumation of the central Swiss Alps and implications for exhumation mechanisms. Geological Society, London, Special Publications, 154(1), 157 – 179, 1999.
- Schlunegger, F. and Hinderer, M. : Crustal uplift in the Alps: why the drainage pattern matters. Terra Nova, 13(6), 425 – 432, 2001.
- 5 Schlunegger, F., and Kissling, E. : Slab rollback orogeny in the Alps and evolution of the Swiss Molasse basin. Nature Communications, 6, 8605, 2015.
- Schlunegger, F., Anspach, O., Bieri, B., Böning, P., Kaufmann, Y., Lahl, K., Lonschinski, M., Mollet, H., Sachse, D., Schubert, C., Stöckli, G. and Zander, I. : Geologische Karte der Schweiz, Kartenblatt 1169 Schüpflheim 1:25'000, Bundesamt für Landestopographie swisstopo, 2016.
- 10 [Schlunegger, F. and Castellort, S. : Immediate and delayed signal of slab breakoff in Oligo / Miocene Molasse deposits from the European Alps. Scientific Reports, 6, 31010, 2016.](#)
- [Schmid, S. M., Pfiffner, O. A., Froitzheim, N., Schönborn, G., and Kissling, E. : Geophysical-geological transect and tectonic evolution of the Swiss-Italian Alps. Tectonics, 15\(5\), 1036 – 1064, 1996.](#)
- 15 [Schmid, S. M., Fügenschuh, B., Kissling, E. and Schuster, R. : Tectonic map and overall architecture of the Alpine orogen. Eclogae Geologicae Helvetiae, 97\(1\), 93 – 117, 2004.](#)
- Short, A. D. : Coastal Processes and Beaches. Nature Education Knowledge 3(10): 15, 2012.
- Sinclair, H.D., Coakley, B.J., Allen, P.A. and Watts, A.B. : Simulation of foreland basin stratigraphy using a diffusion model of mountain belt uplift and erosion: An example from the Central Alps, Switzerland. Tectonics 10, 599 – 620, 1991.
- Sinclair, H.D. and Allen, P.A. : Vertical versus horizontal motions in the Alpine orogenic wedge: stratigraphic response in the foreland basin. Basin Research 4, 215 – 232, 1992.
- 20 [Spicher, A. : Geologische Karte der Schweiz, 1, 500,000. Schweiz](#)
[Sinclair, H. D. : Plan-view curvature of foreland basins and its implications for the palaeostrength of the lithosphere underlying the western Alps. Basin Research 8.2, 173-182, 1996.](#)
- ~~Geol. Komm., Basel, 1980.~~
- 25 Strunck, P. and Matter, A. : Depositional evolution of the western Swiss Molasse. Eclogae Geologicae Helvetiae, 95, 197 – 222, 2002.
- [Tesauro, M., Kaban, M.K. and Cloething, S.A.P.L. : Global model for the lithospheric strength and effective elastic thickness: Tectonophysics 602, 78 – 86, 2013.](#)
- [Tesauro, M., Kaban, M.K. and Cloething, S.A.P.L. : How rigid is Europe's lithosphere? Geophys. Res. Lett. 36, 1 – 6, 2009.](#)

Ustaszewski, K., Schmid, S.M, Fügenschuh, B., Tischler, M., Kissling, E. and Spakman, W. : A map-view restoration of the Alpine-Carpathian-Dinaridic system for the Early Miocene. *Swiss Journal of Geosciences*, 101 (SUPPL. 1), 273 – 294, 2008.

5 [Waschbusch, P.J., and Royden, L.H. : Spatial and temporal evolution of foredeep basins: lateral strength variations and inelastic yielding in continental lithosphere. *Basin Research*, 4, 179 – 196, 1992.](#)

Wanner, J., Gislér, C., Jost, J., Christener, F. Ninck, T. : Geologische Karte der Schweiz, Kartenblatt 1148 Sumiswald 1:25'000, Bundesamt für Landestopographie swisstopo, in press, 2019.

Wehrens, P. : Structural evolution in the Aar Massif (Haslital transect): Implications for midcrustal deformation. Ph.D., Bern, 2015.

10 Wehrens, P., Baumberger, R., Berger, A. and Herwegh, M. : How is strain localized in a meta-granitoid, mid-crustal basement section? Spatial distribution of deformation in the central Aar massif (Switzerland), *Journal of Structural Geology*, 94, 47 – 67, 2017.

Willett, S. D. : Late Neogene erosion of the Alps: A climate driver?. *Annual Review of Earth and Planetary Sciences*, 38, 411-437, 2010.

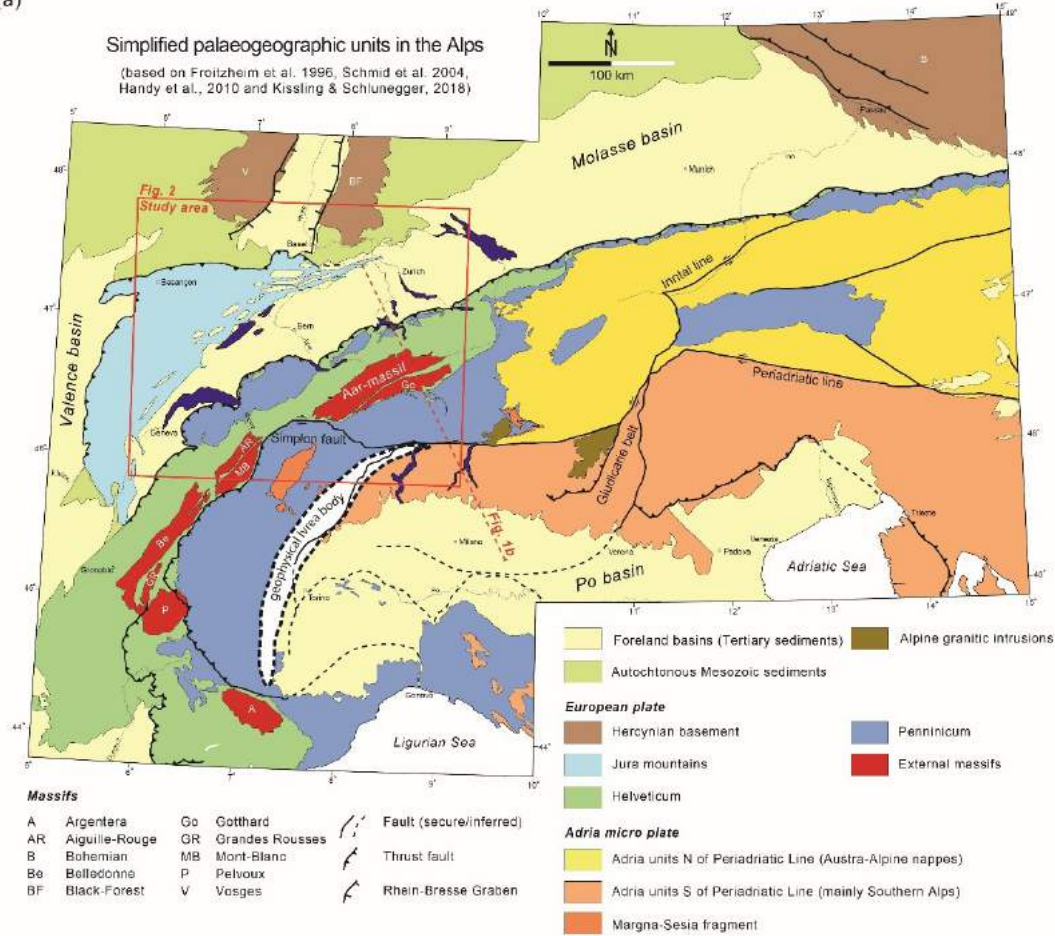
15 [Yalin, M.S. : Geometrical properties of sand waves. *Journal of the Hydraulics Division, ASCE*, 90, 105 – 119, 1964.](#)

Zachos, J., Pagani, M., Sloan, L. Thomas, E. and Billups, K. : Trends, rhythms and aberrations in global climate 65 Ma to present, *Science*, 292, 686 – 693, 2001.

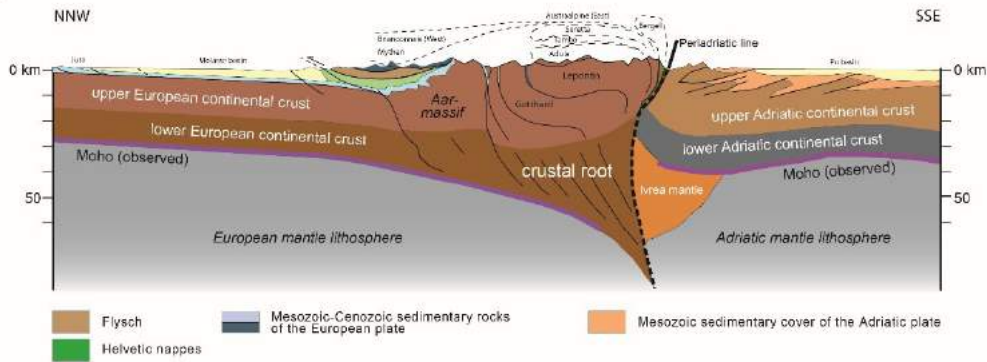
(a)

Simplified palaeogeographic units in the Alps

(based on Froitzheim et al. 1996, Schmid et al. 2004, Handy et al., 2010 and Kissling & Schlunegger, 2018)



(b)



Author contribution

F.S. designed the study. P.G. carried out the experiments, collected and interpreted the data with support by F.S.. The figures and photos were done/taken by P.G. with support by F.S. F.S. and P.G. wrote the text."

5

Competing interest

10 The authors declare that they have no conflict of interest.

Tables and Figures

Table 1: Lithofacies encountered in the Entlen section

| <u>Facies assemblages</u> | <u>Structures and Bedforms</u> | <u>Depositional setting & references</u> |
|--|--|---|
| <u>Mcl, Mm, Mp, Mfl, Mle</u> | <u>Climbing ripples (Mcl), mudstone drapes (Md) and flaser- (Mfl) and lenticular-bedding (Mle) within parallel-laminated (Mp) and massive-bedded mudstones (Mm)</u> | <u>Wave-dominated environment: Backshore setting, where sediments were deposited within a swampy area. Root-casts, reddish mottling and caliche nodules represent palaeo-sol formation.</u> <u>Keller, 1989; Miall, 1996 ; Daidu et al., 2013</u> |
| <u>Md, Mfl, Mle,</u> | <u>Mudstone drapes (Md), flaser- (Mfl) and lenticular-bedding (Mle)</u> | <u>Wave-dominated environment with strong tidal influence: Backshore to nearshore setting, where Mle mostly form in the supratidal (mudflat) and Mfl form in the intertidal (sandflat) or alternatively in the subtidal, if ripple crests are fully preserved.</u> <u>Keller, 1989 ; Shanmugam, 2003; Daidu et al., 2013</u> |
| <u>Sct_r, Sct_a, Scr</u> | <u>Trough- and tabular-cross-beds (Sct_r, Sct_a) superimposed by current-ripple marks (Scr) which record an opposite flow direction.</u> | <u>Wave-dominated environment with strong tidal influence: Nearshore setting, deposits of (subtidal) sanddunes and sandwaves.</u> <u>Baas, 1978; Allen and Homewood, 1984; Jost et al., 2016</u> |
| <u>Sg, Shf, Sm, Sp, Sv</u> | <u>Pebbly-lags (Sg), Shell-fragments (Shf) within massive- to parallel-laminated sandstones (Sm, Sp), occasionally with sand-volcanoes (Sv)</u> | <u>Wave-dominated environment: Foreshore to nearshore setting within the beach area, deposited at the surf-and-swash zone.</u> <u>Allen et al., 1985; Dam and Andreassen, 1990; Keller, 1990; Miall, 1996; Jost et al., 2016</u> |
| <u>Sbr, Scr, Sos, Sc, Sm, Sp</u> | <u>Ripple marks (Sbr, Scr, Sos) and cross-beds (Sc) within massive-bedded and parallel-laminated sandstones (Sm, Sp)</u> | <u>Wave-dominated environment: Nearshore to foreshore setting, where ripple marks form at the wave area, while Sp form at the surf-and-swash zone (beach area)</u> <u>Baas, 1978; Reineck and Singh, 1980; Clifton and Dingler, 1984; Allen, J. 1984; Keller, 1989; 1990</u> |
| <u>Spw, Sc, Sos, Sm</u> | <u>Sandstone beds with a planar base and a wavy top (Spw) internally cross-bedded (Sc), superimposed by oscillation-ripple marks (Sos) within massive-bedded sandstones (Sm)</u> | <u>Wave-dominated environment: Nearshore to offshore setting, high-energetic storm deposits (tempestites)</u> <u>Allen, J., 1982; 1984; Clifton and Dingler, 1984; Miller and Komar, 1980a; 1980b; Diem, 1986; Rust and Gibling, 1990</u> |

Table 2: Lithofacies encountered in the Napf units

| <u>Facies assemblages</u> | <u>Structures and Bedforms</u> | <u>Depositional setting & references</u> |
|---------------------------|--|--|
| <u>Gc, Gm</u> | <u>Cross- (Gc) and massive-bedded (Gm) conglomerates</u> | <u>Fluvial-dominated environment: megafan deposits within a braided river system. Gm, Gc form in active channels.</u> <u>Platt and Keller, 1992; Schlunegger et al., 1997</u> |
| <u>Sc, Sm, Mp</u> | <u>Cross- (Sc) and massive-bedded (Sm) sandstones with parallel-laminated mudstones (Mp)</u> | <u>Fluvial-dominated environment: megafan deposits within a braided river system. Sc, Sm from crevasse-splay deposits. Mp (often yellowish-reddish mottled with caliche nodules and root casts) are evident for palaeo-sol genesis on a floodplain.</u> <u>Allen, J., 1982; 1984; Rust and Gibling, 1990; Dam and Andreasen, 1990; Keller, 1990</u> |

Table 3: Lithofacies encountered in the Sense section

| <u>Facies assemblages</u> | <u>Structures and Bedforms</u> | <u>Depositional setting & references</u> |
|--|--|--|
| <u>Gm, Gc</u> | <u>Massive- to cross-bedded conglomerates (Gm, Gc)</u> | <u>Fluvial-dominated environment: Terrestrial setting, where coarse-grained rivers deposited material. Platt and Keller, 1992; Schlunegger et al., 1997</u> |
| <u>Sc, Sg, Sct_r, Sm</u> | <u>Cross-bedded sandstones (Sc) with top-, fore- and bottom-sets with pebbly lags (Sg) and within trough-cross- (Sct_r) and massive-bedded sandstones (Sm)</u> | <u>Fluvial-dominated environment with tidal influence: Foreshore setting, where deltas, or alternatively estuaries, enter the sea: Sc and Sg mark Gilbert-Delta-type deposits, while Sct_r and Sm mark mouth bar deposits (or alternatively: sanddunes). Allen, J., 1982; 1984; Allen and Homewood, 1984; Rust and Gibling, 1990; Dam and Andreassen, 1990</u> |
| <u>Gm, Gc, Mm, Sm, Sg</u> | <u>Massive- to cross-bedded conglomerates (Gm, Gc) within massive-bedded sand- and mudstones (Sm, Mm). Occasionally, pebbles only occur as isolated layers (Sg)</u> | <u>Tidal-dominated environment with fluvial influence (river inflow): Nearshore setting. Terrestrial derived material washed into subtidal by high energetic floods. Dam and Andreassen, 1990; Platt and Keller, 1992; Miall, 1996; Schlunegger et al., 1997</u> |
| <u>Mm, Mp, Mf</u> | <u>Massive-bedded (Mm) and parallel-laminated (Mp) mudstones with bioturbation (Mf)</u> | <u>Tidal-dominated environment: Backshore setting, deposits of the supratidal (mudflat). Dan and Andreassen, 1990; Keller, 1990; Miall, 1996</u> |
| <u>Sm, Mm, Mf, Sf</u> | <u>Strongly bioturbated (Mf, Sf) massive-mud- and sandstones (Mm, Sm)</u> | <u>Tidal-dominated environment: Backshore to foreshore setting, deposits of mud- (supratidal) and sandflats (intertidal) Dan and Andreassen, 1990; Keller, 1990; Miall, 1996; Nichols, 1999</u> |
| <u>Scr, Md, Sct_a, Sf</u> | <u>Current-ripples (Scr) and tabular cross-beds (Sct_a) with mudstone drapes (Md), occasionally with heavily bioturbated sandstones (Sf)</u> | <u>Tidal-dominated environment: Foreshore setting, deposits of the intertidal (sandflat), where bioturbation occurs (Sf). Mudstone drapes record slack-water phases. Baas, 1978; Reineck and Singh, 1980; Allen and Homewood, 1984; Shanmugam, 2003; Nichols, 1999</u> |
| <u>Sc, Sce</u> | <u>Cross-bedded (Sc) sandstones, occasionally forming epsilon cross-beds (Sce)</u> | <u>Tidal-dominated environment: Foreshore to nearshore setting, deposits of a (meandering) tidal channel. Allen, J., 1982; 1984; Frieling et al., 2009</u> |
| <u>Sos, Sbr, Sp</u> | <u>Oscillation- and branching-ripple marks that grade into parallel-laminated sandstones</u> | <u>Tidal-dominated environment with strong wave influence: Foreshore to nearshore setting, deposits of the beach area (surf-and-swash zone) and the wave-transformation area. Reineck and Singh, 1980; Clifton and Dingler, 1984; Allen, J. 1984; Keller, 1990</u> |
| <u>Sct_a, Scr, Md, Sct_r, Sm</u> | <u>Tabular- (Sct_a) and trough-cross-bedded (Sct_r) sandstones, superimposed with current-ripples (Scr) and mudstone drapes (Md) within massive-bedded sandstones (Sm)</u> | <u>Tidal-dominated environment with fluvial influence (river inflow): Foreshore to nearshore environment. Estuaries (Sct_a, Scr, Md) entering the sea, building up mouth-bar deposits or alternatively subtidal sanddunes (Sct_r, Sm).</u> |

Yalin, 1964; Baas, 1978; Allen and Homewood, 1984; Dam and Andreassen, 1990; Jost et al., 2016

| | | |
|---------------------------------|--|--|
| <u>Sct_r, Scr, Md</u> | <u>Trough-cross-beds (Sct_r) superimposed by current-ripple marks (Scr) and mudstone drapes (Md)</u> | <u>Tidal-dominated environment: Nearshore setting, deposits of (subtidal) sanddunes and sandwaves. <i>Baas, 1978; Allen and Homewood, 1984; Shanmugam, 2003; Jost et al., 2016.</i></u> |
| <u>Spw, Sos, Sg</u> | <u>Sandstone beds with a planar base and a wavy top (Spw), superimposed by oscillation-ripple marks (Sos) and embedded with pebbles (Sg)</u> | <u>Tidal-dominated environment with wave influence: Nearshore to offshore setting, high-energetic storm deposits (tempestites) <i>Reineck and Singh, 1980; Miller and Komar, 1980a; 1980b; Clifton and Dingler, 1984; Diem 1986; Miall, 1996</i></u> |

5 **Table 4: Lithofacies encountered at the St. Magdalena site & Gurten drill core**

| <u><i>Facies assemblages</i></u> | <u><i>Structures and Bedforms</i></u> | <u><i>Depositional setting & references</i></u> |
|--|--|---|
| <u>Sct_r, Scr, Sc, Sm Md</u> | <u>Trough-cross-beds (Sct_r) and cross-bedded sandstones (Sc) superimposed by current-ripple marks (Scr) and mudstone drapes (Md), often within massive-bedded sandstones (Sm)</u> | <u>Tidal-dominated environment: Nearshore setting, deposits of (subtidal) sanddunes (or mouth-bar deposits) and megaripples. We infer these deposits as sediments of subtidal shoals. <i>Baas, 1978; Allen, J., 1982; 1984; Allen and Homewood, 1984; Rust and Gibling, 1990; Dam and Andreassen, 1990; Shanmugam, 2003</i></u> |

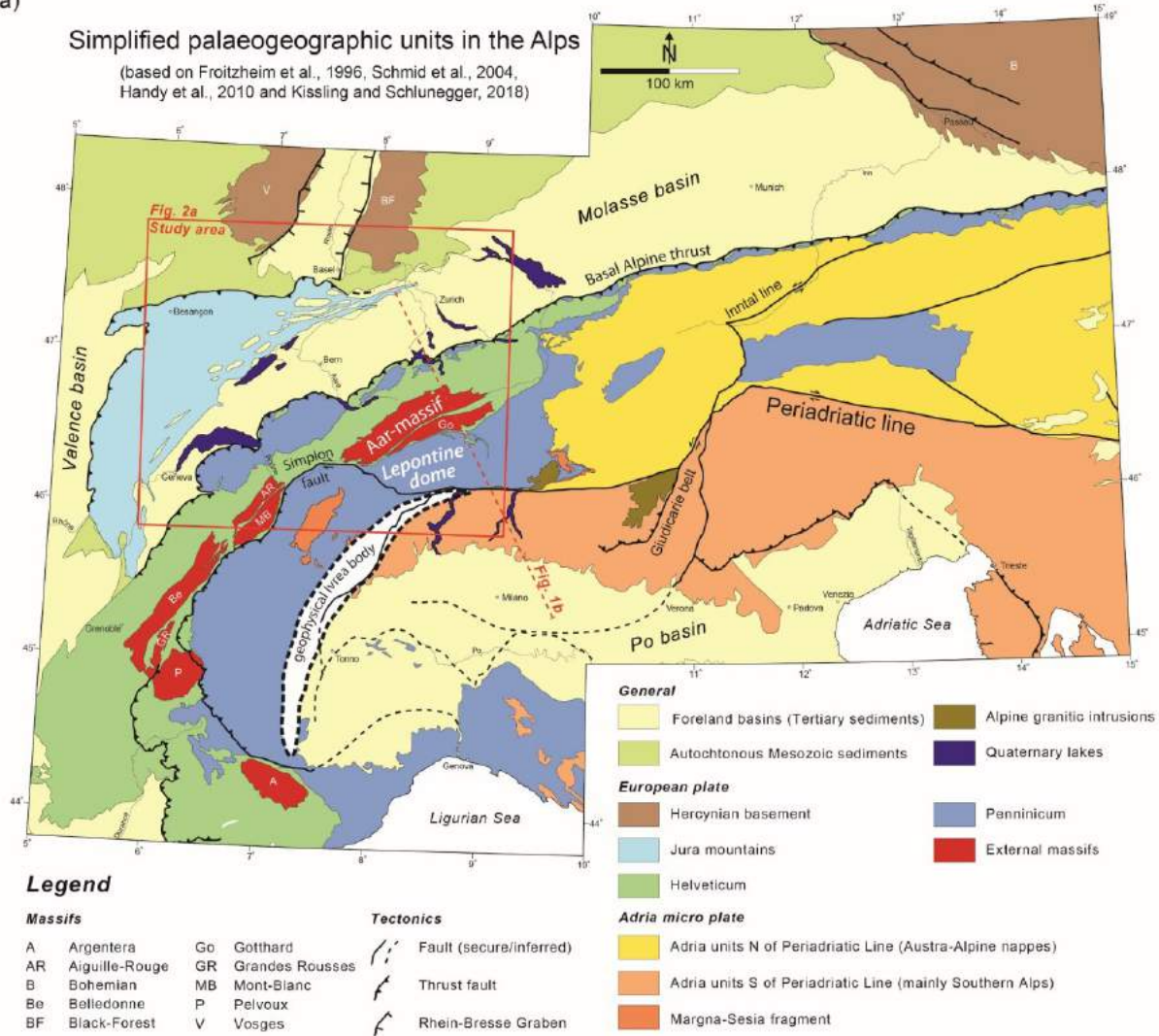
Table 5: Lithofacies encountered in the Lake Neuchâtel and Wohlen areas

| <u><i>Facies assemblages</i></u> | <u><i>Structures and Bedforms</i></u> | <u><i>Depositional setting & references</i></u> |
|--|--|--|
| <u>Sec, Sc, Scr, Shf, Sg</u> | <u>Calcareous, shelly-sandstones (Sec; “Muschelsandstein”) are made up of cross-bedded sandstones (Sc), contain coquinas and shell-fragments (Shf) and pebbles (Sg) in places.</u> | <u>Tidal-dominated environment: Offshore setting, mega-sandwaves deposited under strong tidal-currents. Pebbly lags (Sg) are interpreted as pebbles flushed into the sea by flood-events. <i>Baas, 1978 ; Allen et al., 1985; Rust and Gibling, 1990 ; Miall, 1996 ; Jost et al., 2016</i></u> |
| <u>Sct_a, Sct_r, Slc</u> | <u>Coarse-grained sandstones (Slc, “Grobsandstein”) with trough (Sct_r) and tabular (Sct_a) cross-bedded geometries.</u> | <u>Tidal-dominated environment: Nearshore to offshore setting, sandwaves, or alternatively sanddunes, similar to the subtidal-shoal deposits (see St. Magdalena site), however larger in diameters, but similar thicknesses. <i>Allen and Homewood, 1984; Jost et al., 2016</i></u> |

(a)

Simplified palaeogeographic units in the Alps

(based on Frotzheim et al., 1996, Schmid et al., 2004, Handy et al., 2010 and Kissling and Schlunegger, 2018)



(b)

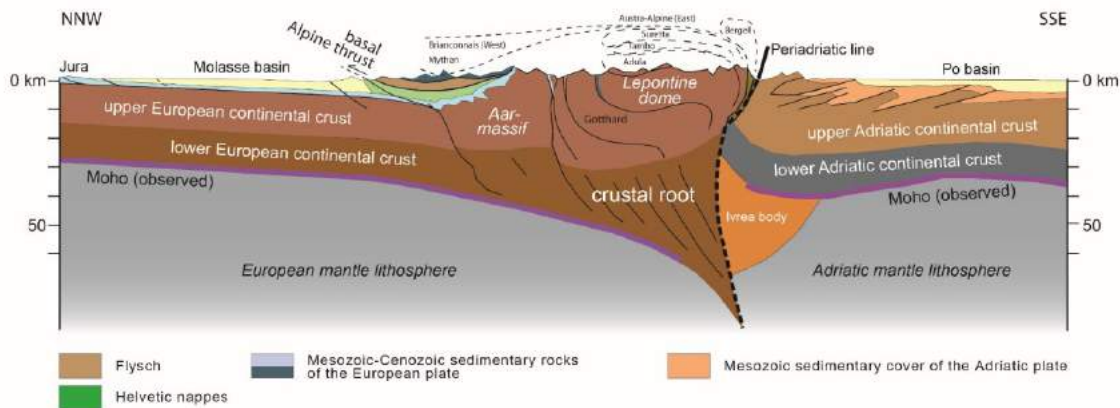


Figure 1: a) Simplified geological map of the European Alps. It is based on the compilation by Kissling and Schlunegger (2018) and was updated by using additional information published in Handy et al. (2015) and in Pippèr and Reichenbacher (2017).

b) Simplified geological-geophysical section through the central European Alps, taken and modified adapted from Kissling and Schlunegger (2018). Note location of Fig. 2a.

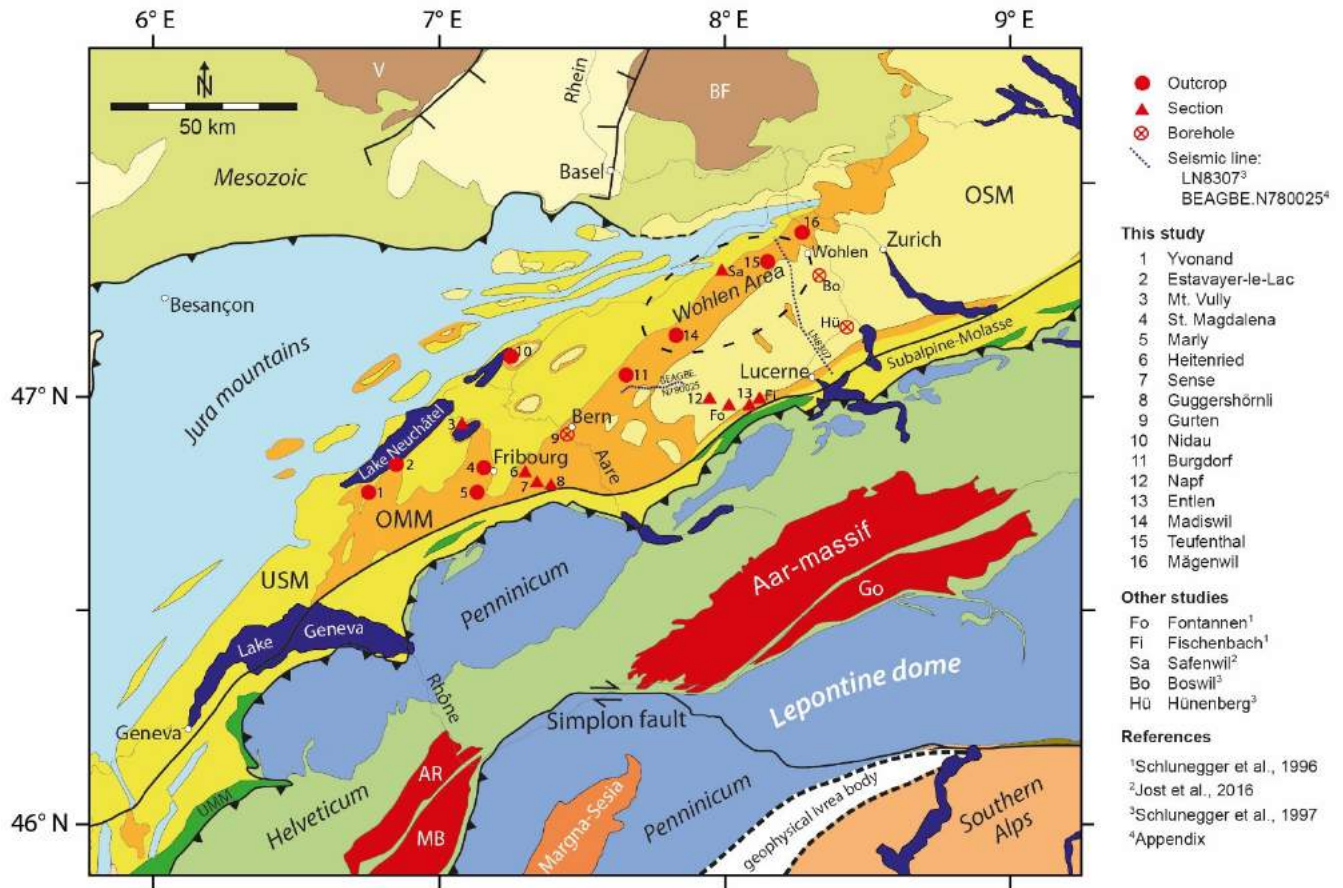
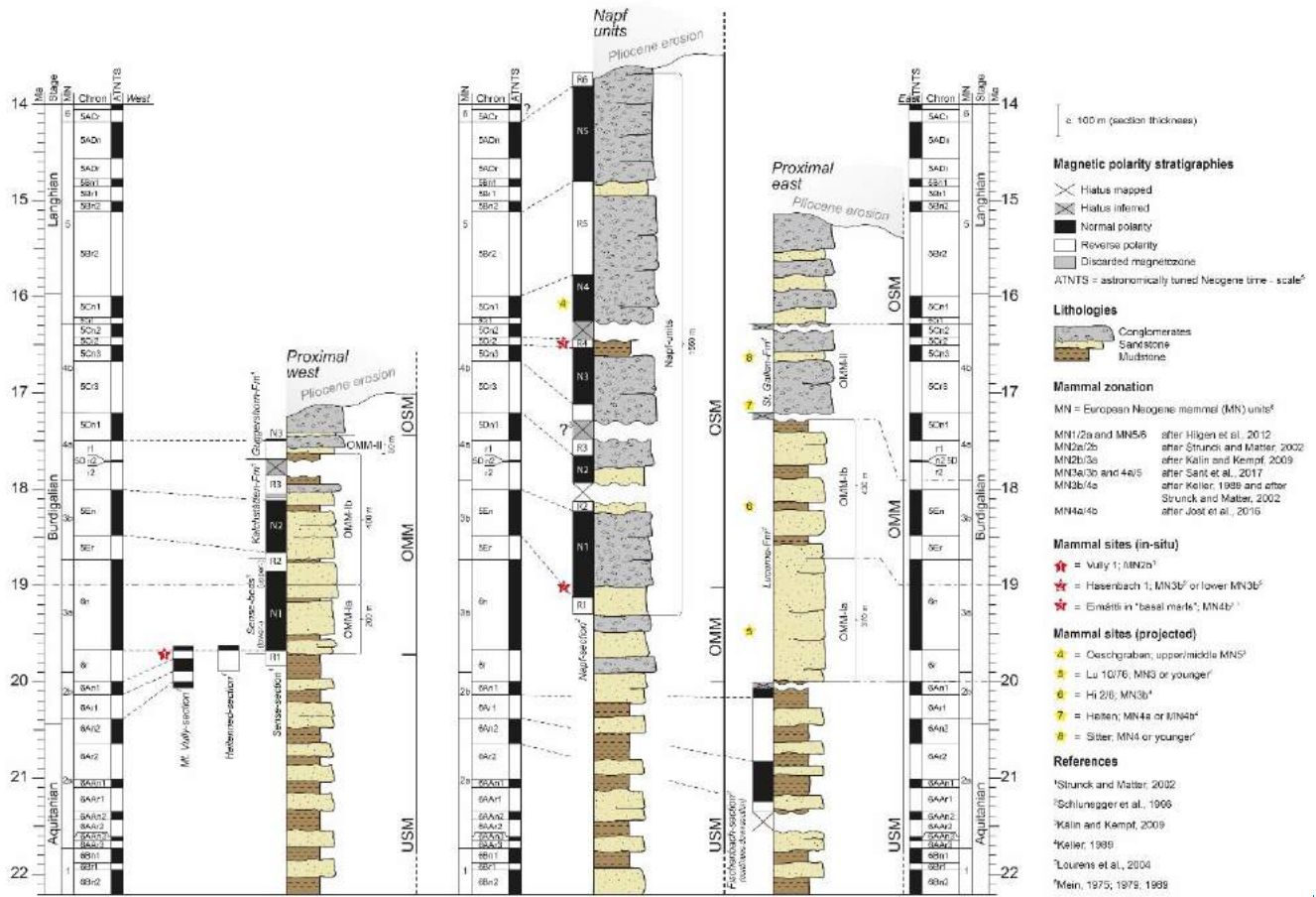
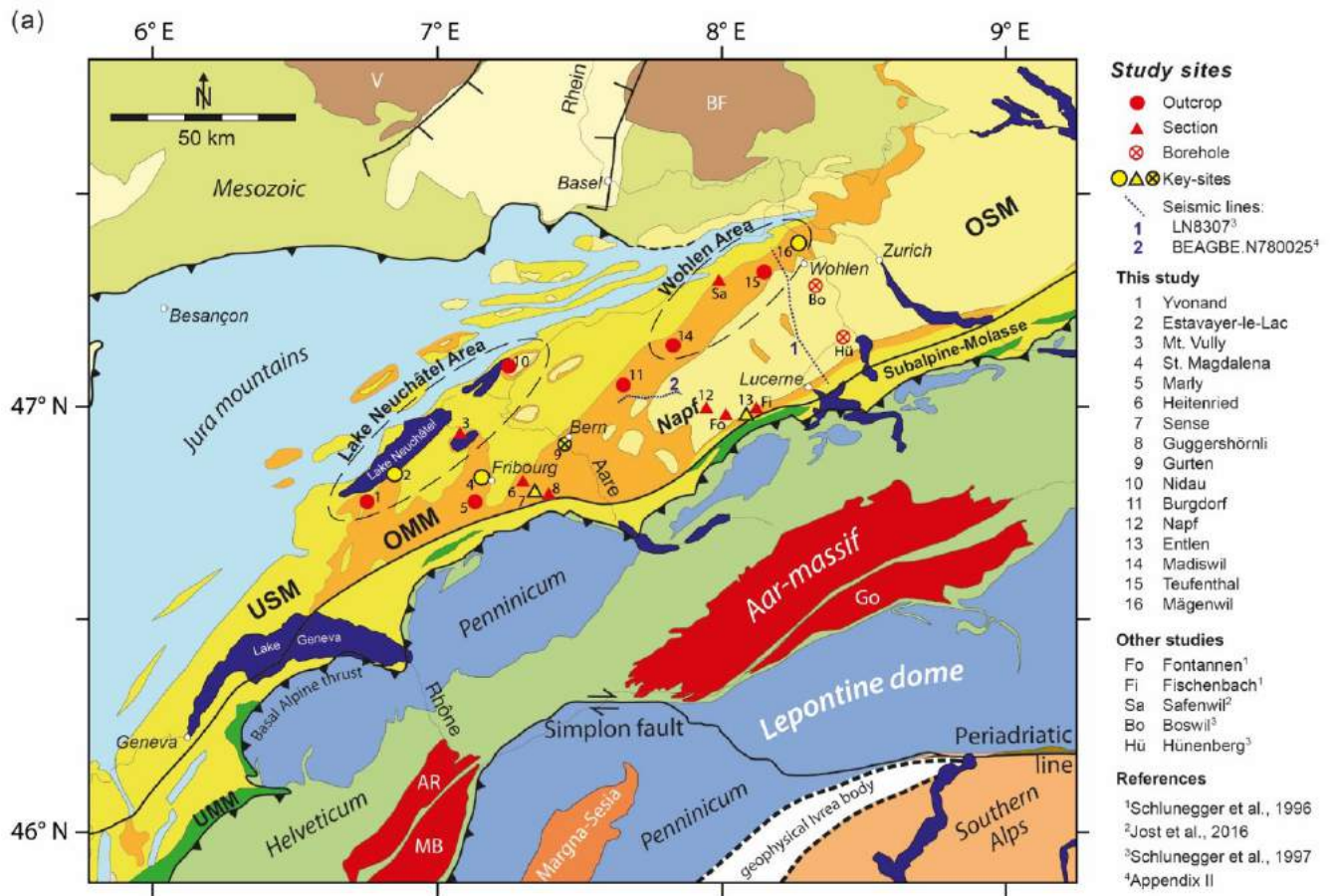


Figure 2: Simplified geological-geophysical section through the central European Alps, taken and modified from Kissling and Schlunegger (2018).





Massifs

- AR Aiguille-Rouge
- BF Black-Forest
- Go Gotthard
- MB Mont-Blanc
- V Vosges

Tectonics

- Fault (secure/inferred)
- Thrust fault
- Rhein-Bresse Graben

Other

- Quaternary (recent) lakes

Lithology & Palaeogeography

General

- Tertiary sediments
- Autochthonous Mesozoic sediments
- Alpine granitic intrusions

Molasse

- Upper Freshwater Molasse (OSM)
- Upper Marine Molasse (OMM)
- Lower Freshwater Molasse / Subalpine M. (USM)
- Lower Marine Molasse (UMM)

European plate

- Hercynian basement
- Jura mountains
- Helveticum
- Penninicum
- External massifs

Adria micro plate

- Adria units (Southern Alps)
- Magna-Sesia fragment

Map mod. after Frotzheim et al., 1996; Schmid et al., 2004; Handy et al., 2010 and Kissling and Schlunegger, 2018

(b)

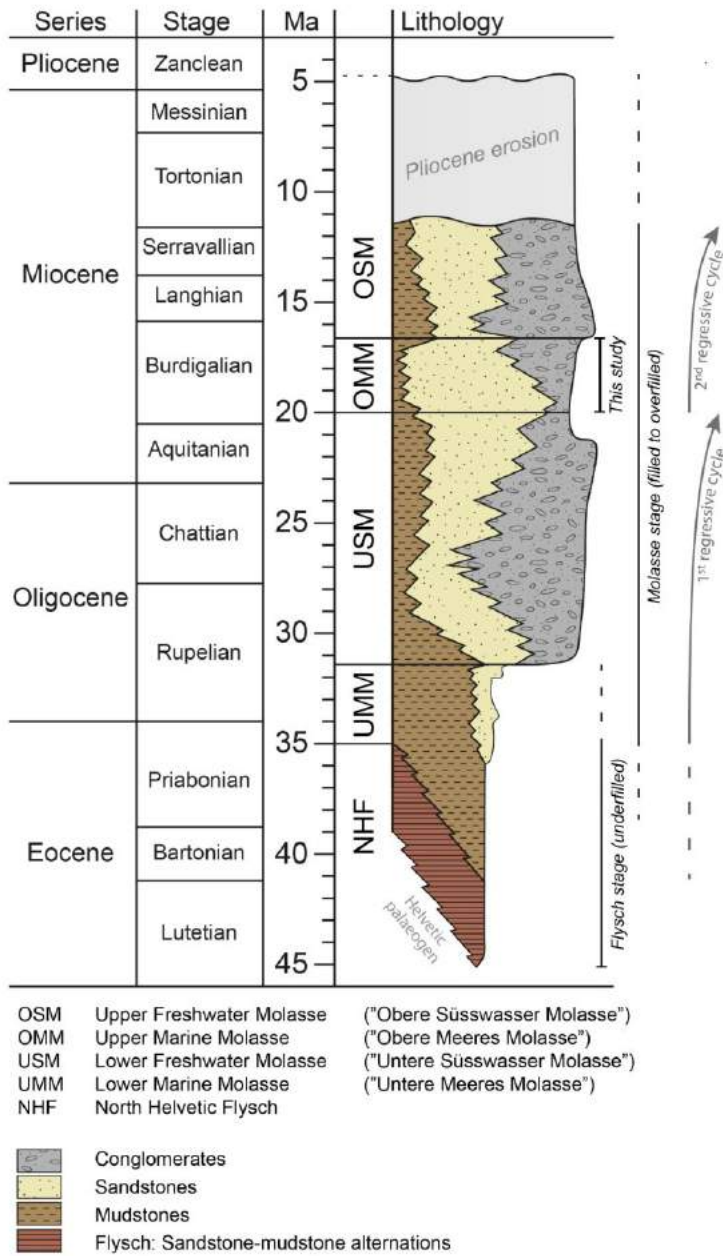
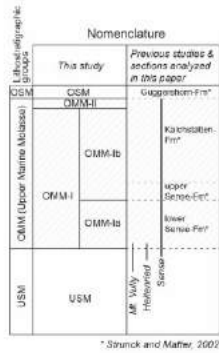


Figure 2: a) Detailed geological map of the area between Geneva and Zurich adapted from Kissling and Schlunegger (2018) showing the locations of data points referred to in this paper. The OMM deposits at sites 1 to 16 have been mapped at the scale of 1:25'000, which was used to reproduce Fig. 6. In addition, the observations of the sections outcrops and the drill core at sites 2, 4, 7, 9, 12, 13 and 16 are explicitly described in chapters 4 and 5 of this paper. Please refer to Fig. 1 for the complete legend. **b)** Lithostratigraphic scheme of the Molasse deposits in Switzerland. Modified after Keller (1989).

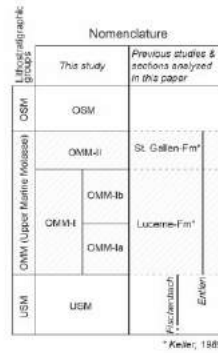
(a) Lithostratigraphic scheme to the west of the Napf



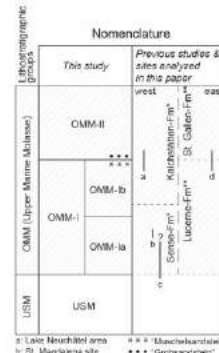
Lithostratigraphic scheme at the Napf



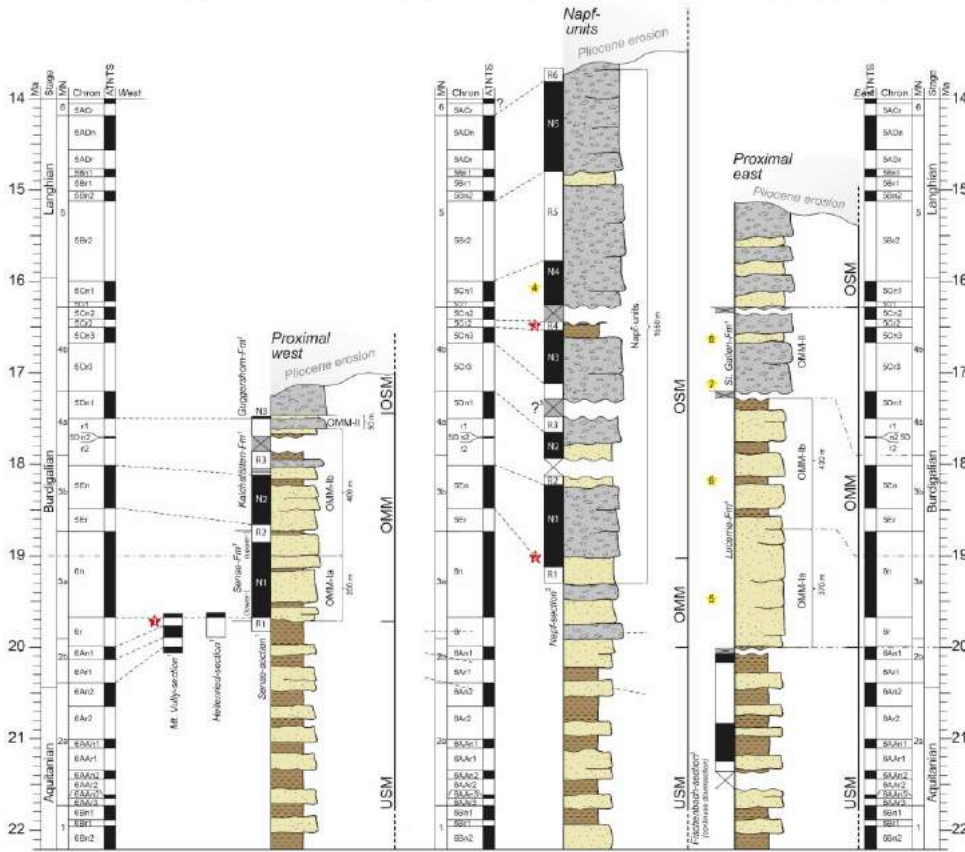
Lithostratigraphic scheme to the east of the Napf



Lithostratigraphic scheme of sections in the distal basin



(b)



Legend

Section thickness

c. 100 m

Magnetic polarity stratigraphies

- ⊗ Hiatus mapped
- ⊗ Hiatus inferred
- Normal polarity
- Reverse polarity
- ▨ Discarded magnetozones
- ATNTS = astronomically tuned Neogene time - scale¹

Lithologies

- ☐ Conglomerates
- ☐ Sandstones
- ☐ Mudstones

Mammal zonation

- MN = European Neogene mammal (MN) units¹
- MN1/2a and MN5/6 after Hagen et al., 2012
- MN2-2b after Strunk and Mather, 2002
- MN3a/3b after Kain and Kempf, 2009
- MN3a/3b and 4a/5 after Sani et al., 2017
- MN3b/4a after Keller, 1989 and after Strunk and Mather, 2002
- MN4a/4b after Jost et al., 2016

Mammalian sites (in-situ)

- ★ = Waly 1, MN2b¹
- ★ = Hasenbach 1: MN3b¹ or lower MN3b¹
- ★ = Emättli in 'basal marls'; MN4¹⁻¹

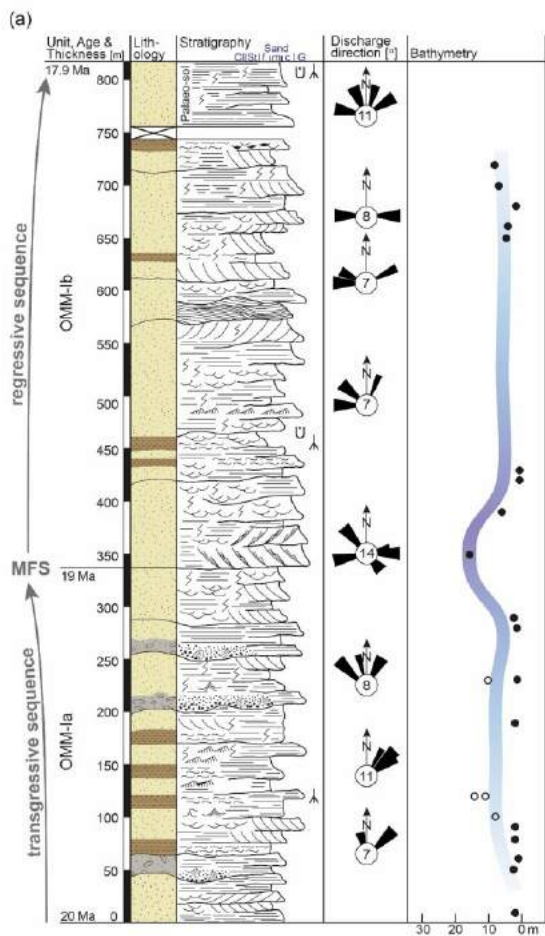
Mammalian sites (projected)

- 4 = Deachgraben; upper/middle MN5²
- 5 = Lu 1076; MN3 or younger²
- 6 = H 20; MN3b³
- 7 = Halten; MN4 or MN4b⁴
- 8 = Stier; MN4 or younger⁴

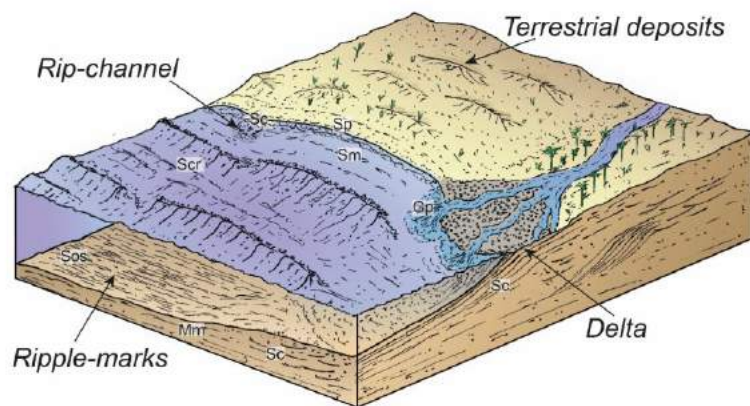
References

- ¹Strunk and Mather, 2002
- ²Schlunegger et al., 1996
- ³Kain and Kempf, 2009
- ⁴Keller, 1989
- ⁵Lourens et al., 2004
- ⁶Main, 1975; 1979; 1989

|



- | | | | |
|--|---|--|---|
| | Exposure gap | | Thickness of set-thickness* |
| | Gravels | | Oscillation ripple-marks* *see supplement |
| | Sandstones | | Mean water depth inferred from facies assemblages |
| | Mudstones | | |
| | [Gp] Pebbly-lags | | [Mm] Mudstone, massive-bedded |
| | [Spw] Sandstone, planar base and wavy top | | [Mp] Mudstone, parallel-laminated |
| | [Sc] Sandstone, cross-beds | | [Md] Mudstone, mudstone drapes |
| | [Scr] Sandstone, current-ripple marks | | Fossil traces / Bioturbation |
| | [Sv] Sandstone, sand-volcanoes | | Root casts |
| | [Shf] Sandstone, shell-fragments | | |
| | [Sm] Sandstone, massive-bedded | | |
| | [Sos] Sandstone, oscillation-ripple marks | | |
| | [Sp] Sandstone, parallel-laminated | | |



(b)

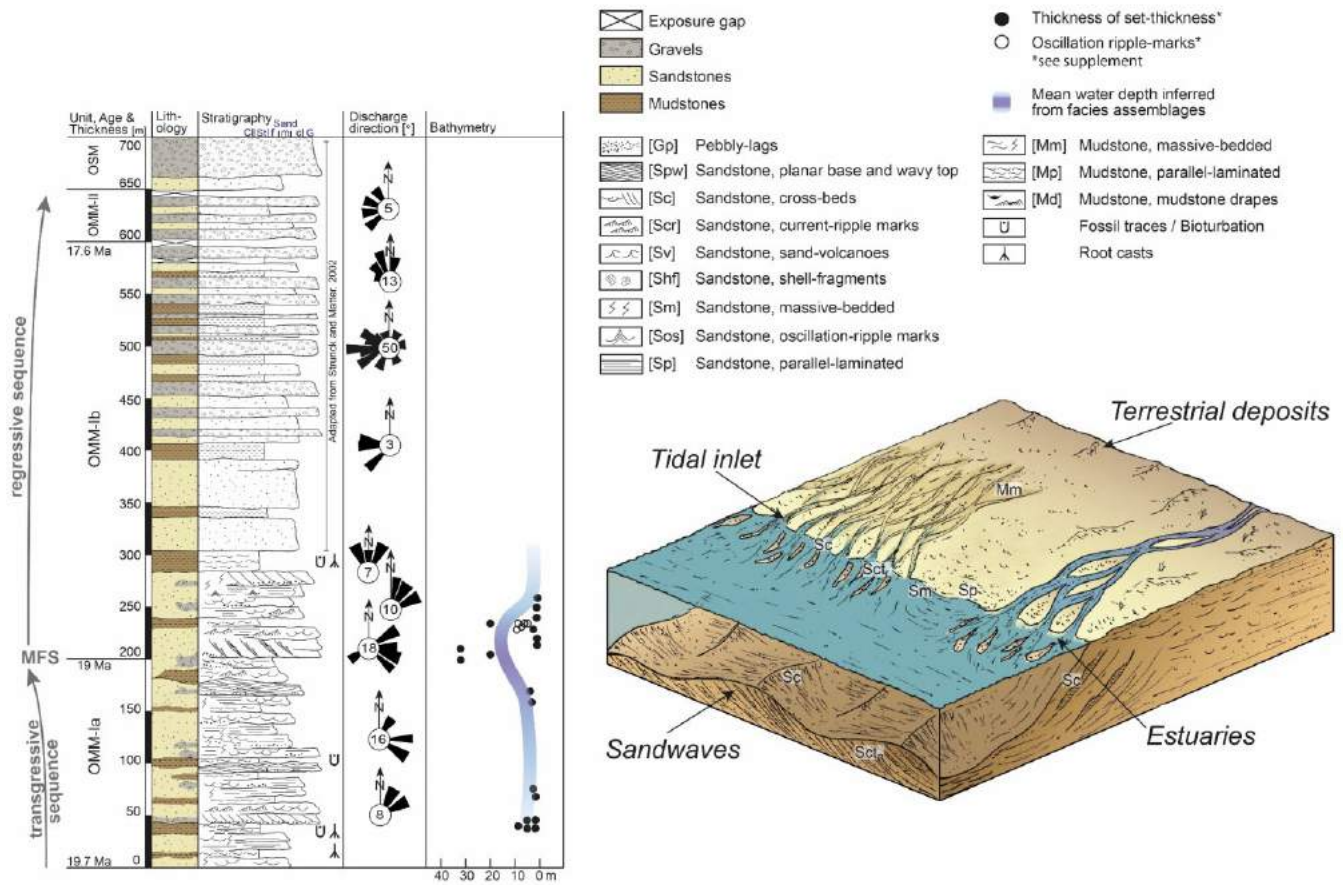
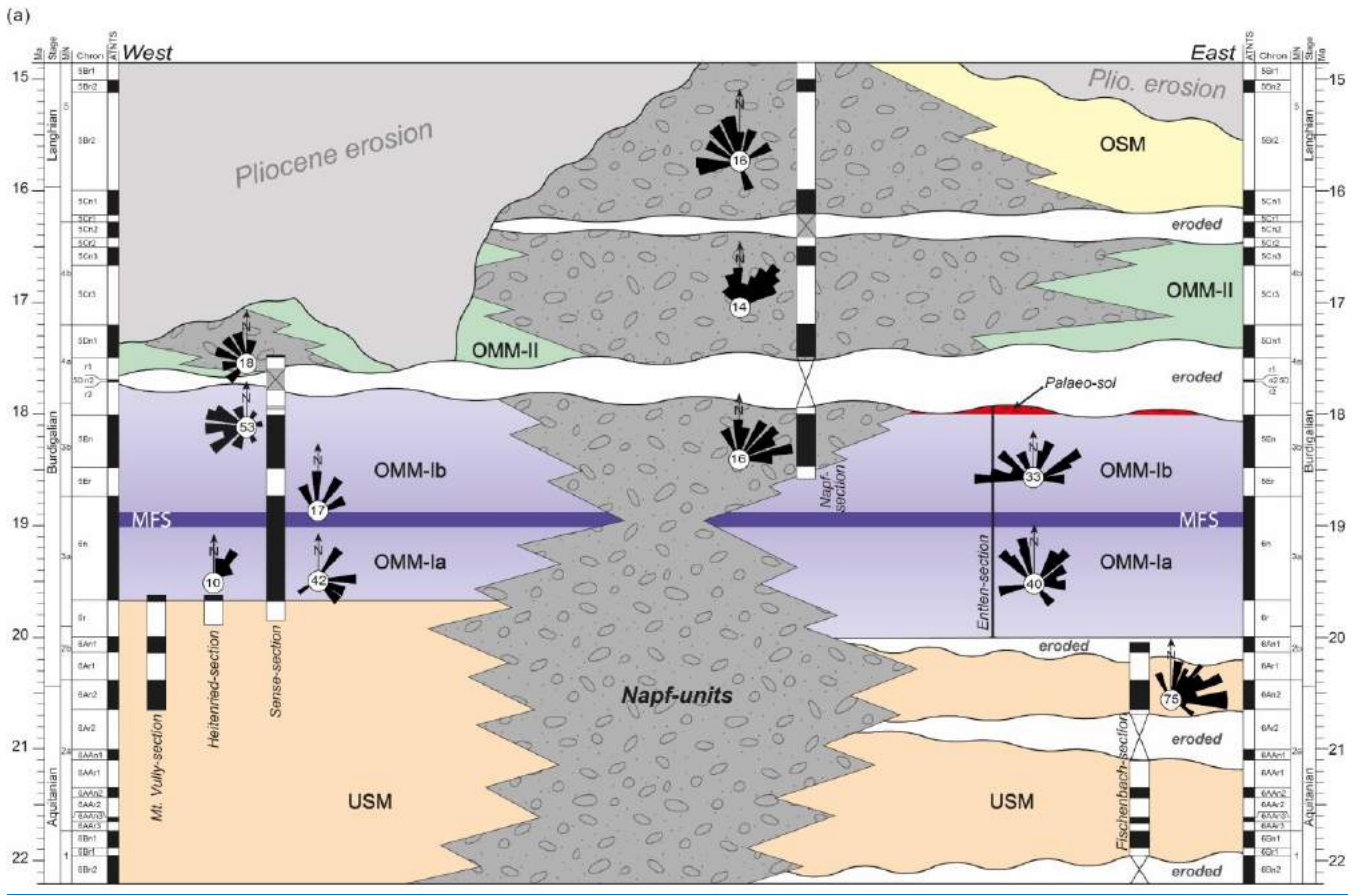


Figure 4: Sedimentological logs of a) the Entlen and b) the Sense section. See Fig. 2a for locations of sections, Fig. 5 for chronological framework of the deposits and the tables for further sedimentological details and abbreviations of the lithofacies, and for references to sedimentological work. The block-diagrams illustrate the palaeo-geographical conditions from a conceptual point of view. Note that the palaeo-bathymetric values are minimum estimates and that the mean water depths have been inferred from the assignment of lithofacies to depositional environment. This might explain why the numerical values for water-depths based on cross-bed thicknesses and our inferred mean water-depth estimates deviate between c. 200 m and 250 m for the Sense-section.



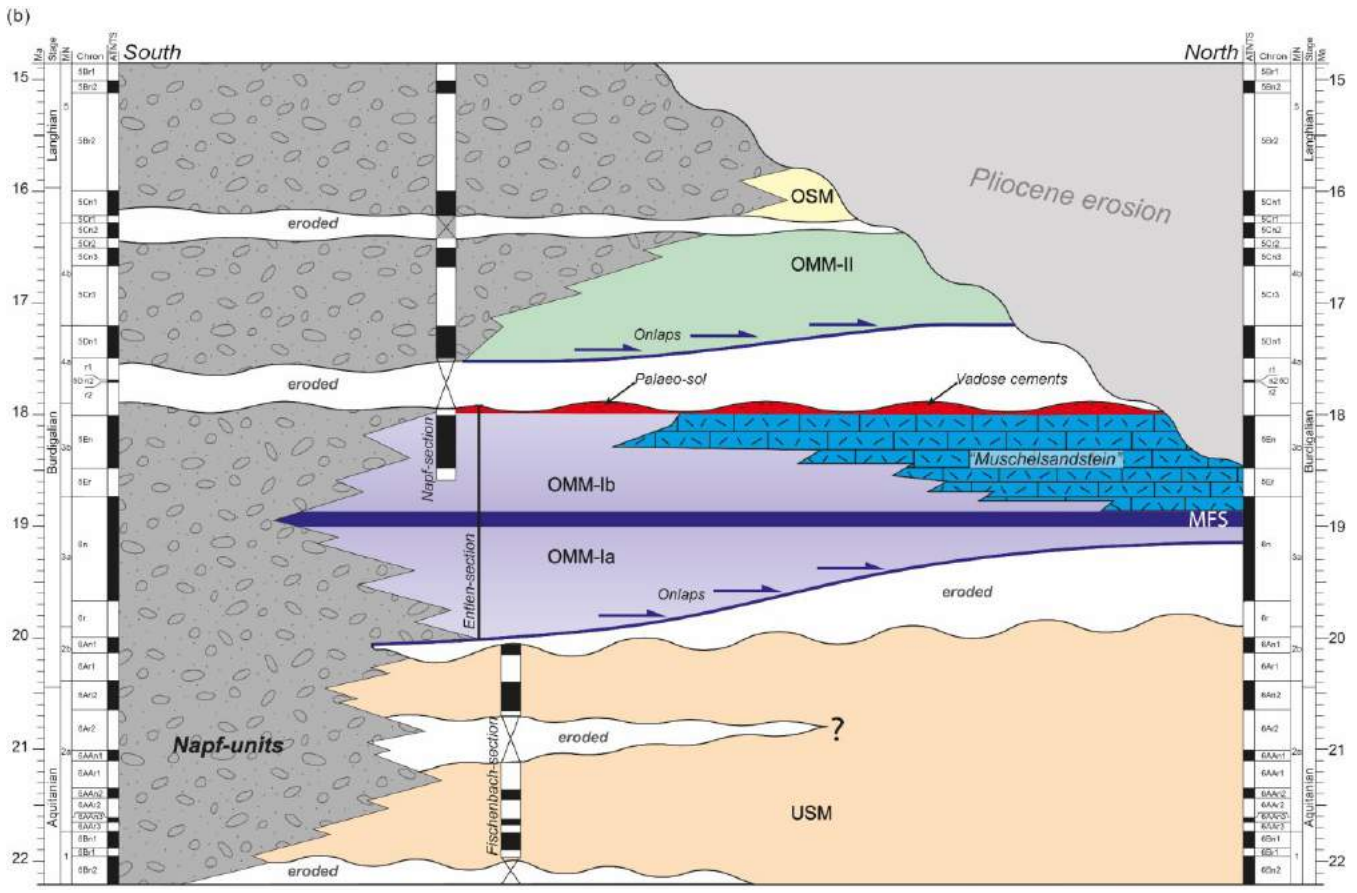
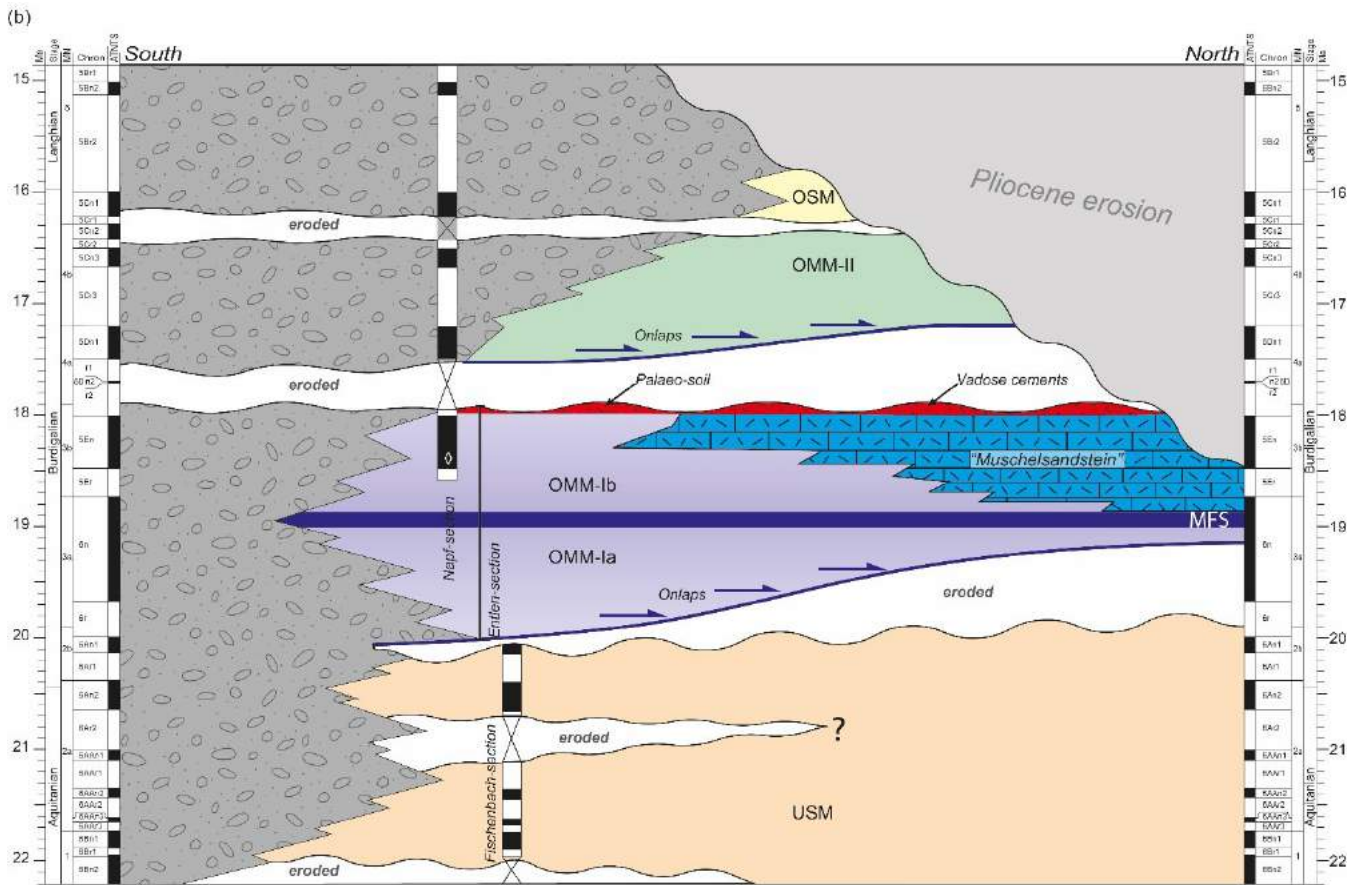
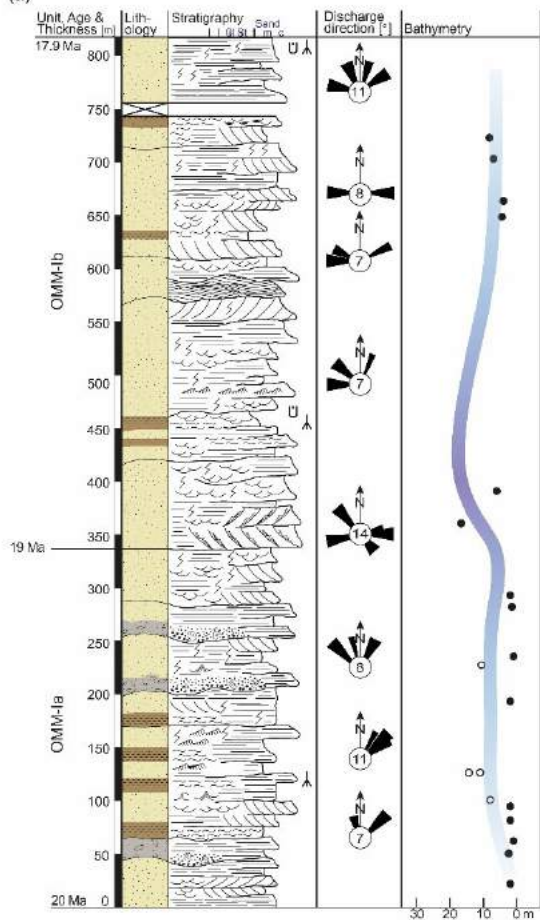


Figure 5 **Chronological:** **a)** West-East chronological (Wheeler) diagram of the Molasse deposit sequence at the proximal basin border between Fribourg and Lucerne (Fig. 22a). The following magnetostratigraphic data have been used: Mt. Vully, Heitenried and Sense (Strunck and Matter, 2002), and Napf and Fischenbach (Schlunegger et al., 1996). Palaeo-discharge transport directions from Heitenried and the upper part of the Sense-section are taken from Strunck and Matter (2002). Note, that the Entlen-section is not calibrated with magnetostratigraphic data but has been adjusted using regional information (see text for further details and Fig. 33b for synthetic sections of the region). MFS = Maximum-flooding surface. Note that the Pliocene phase of erosion removed most of the OMM-II records in western Switzerland. We infer marine conditions in the western Swiss Molasse basin during OMM-II times because: (i) marine conditions were present east of the Napf-units, and (ii) material transport occurred towards the west, which implies that marine conditions were also present west of the Napf megafan at that time, as confirmed by mapping (e.g., Wanner et al., 2019). **b)** North-South chronological (Wheeler) diagram of the Molasse sequence between Entlen (site 13) and Madiswil (site 14, both on Fig. 2a). See text for further details. The onlaps (blue arrows) are based on interpretations from seismic-stratigraphic data (Schlunegger et al., 1997). MFS = Maximum-flooding surface.



b) Chronological (Wheeler) diagram of the Molasse sequence across the basin within a section between Entlen (site 13) and Madiswil (site 14, both on Fig. 2). See text for further details. The onlaps (blue arrows) are based on interpretations from seismostratigraphic data (Schlunegger et al., 1997). MFS = Maximum flooding stage.

(a)

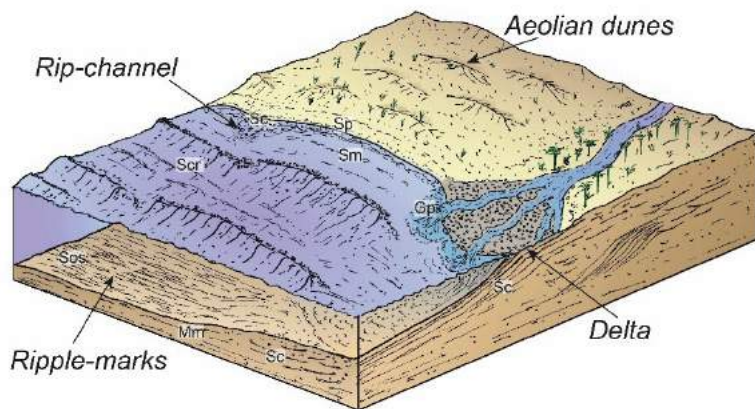


- Exposure gap
- Gravels
- Sandstone
- Mudstone

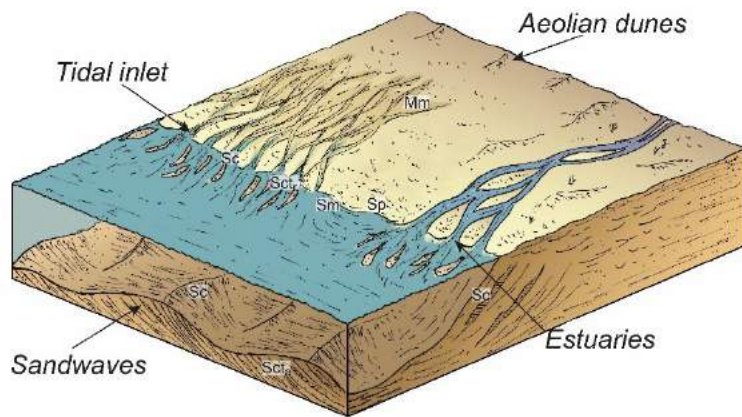
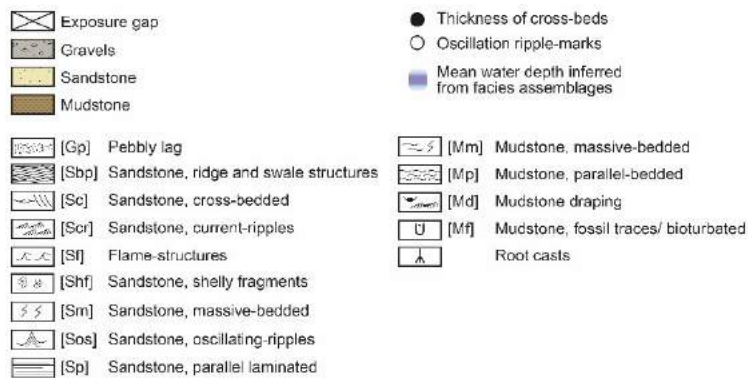
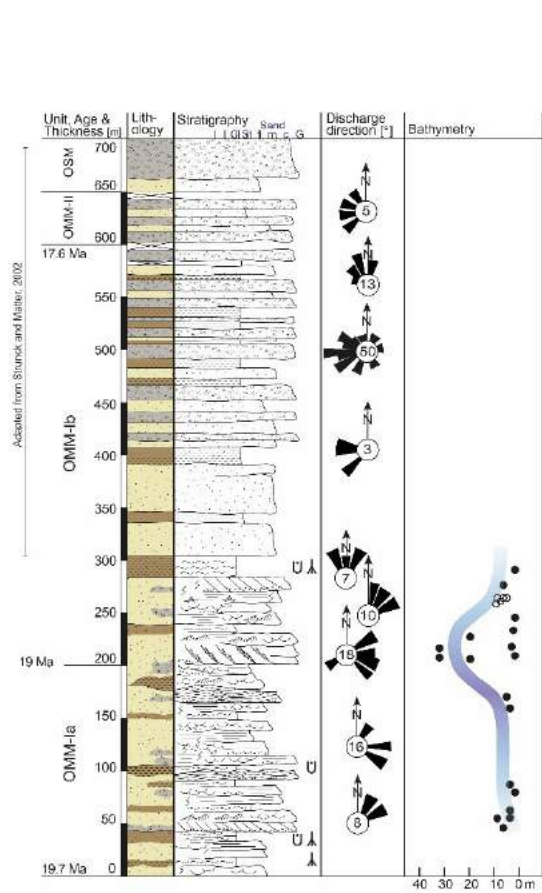
- [Gp] Pebbly lag
- [Sbp] Sandstone, ridge and swale structures
- [Sc] Sandstone, cross-bedded
- [Scr] Sandstone, current-ripples
- [Sf] Flame-structures
- [Shf] Sandstone, shelly fragments
- [Sm] Sandstone, massive-bedded
- [Sos] Sandstone, oscillating-ripples
- [Sp] Sandstone, parallel laminated

- Thickness of cross-beds
- Oscillation ripple-marks
- Mean water depth inferred from facies assemblages

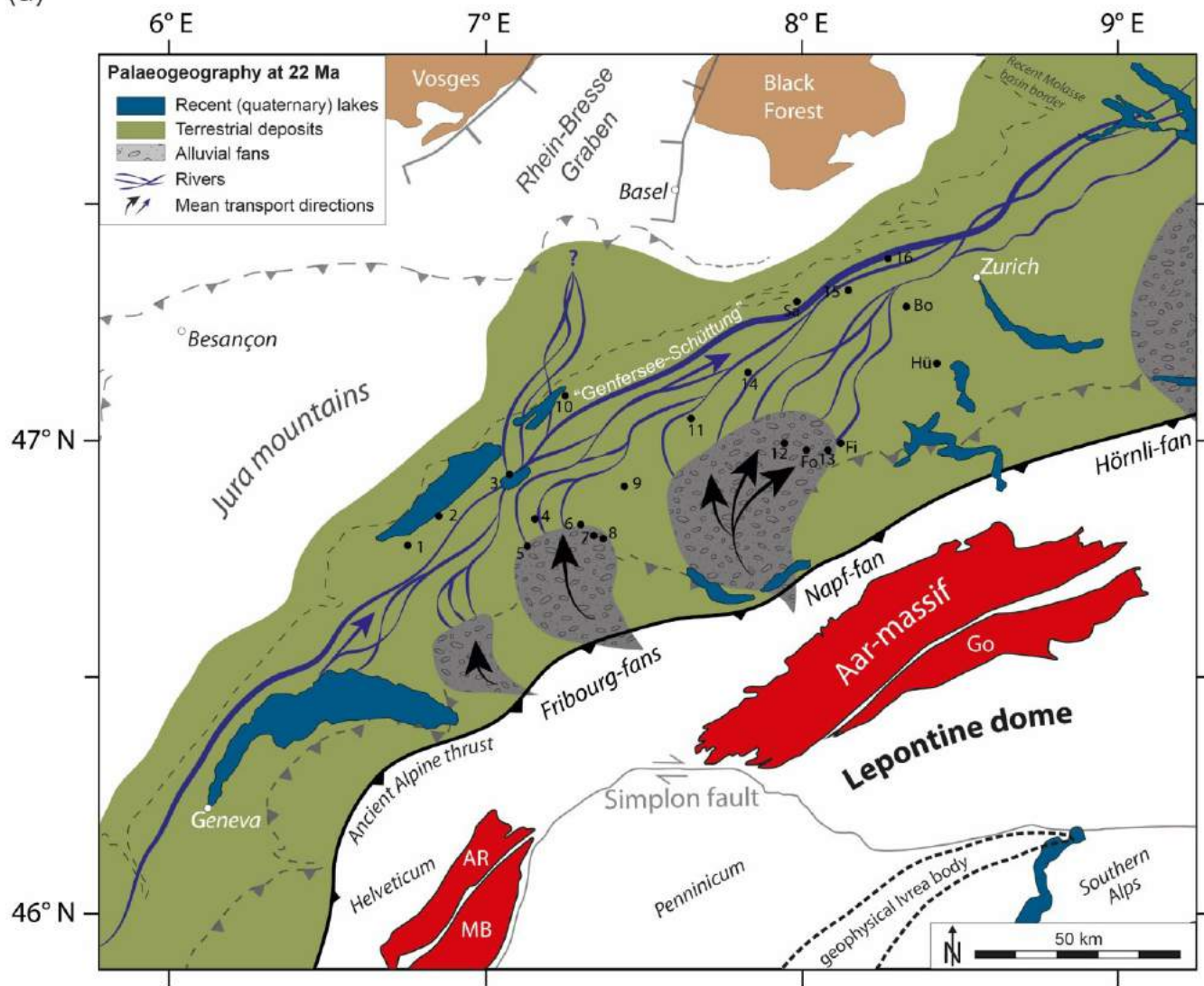
- [Mm] Mudstone, massive-bedded
- [Mp] Mudstone, parallel-bedded
- [Md] Mudstone draping
- [Mf] Mudstone, fossil traces/ bioturbated
- Root casts



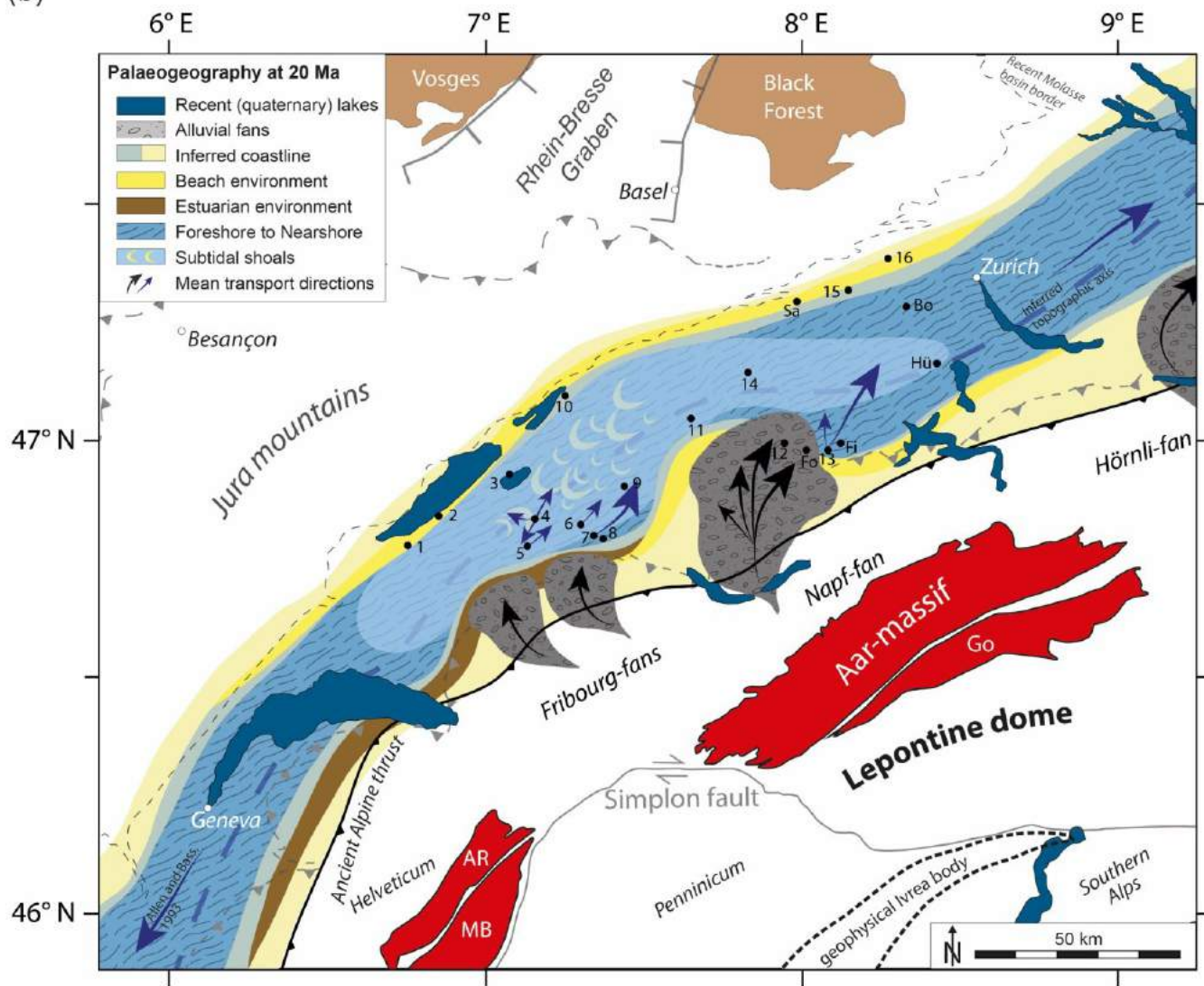
(b)



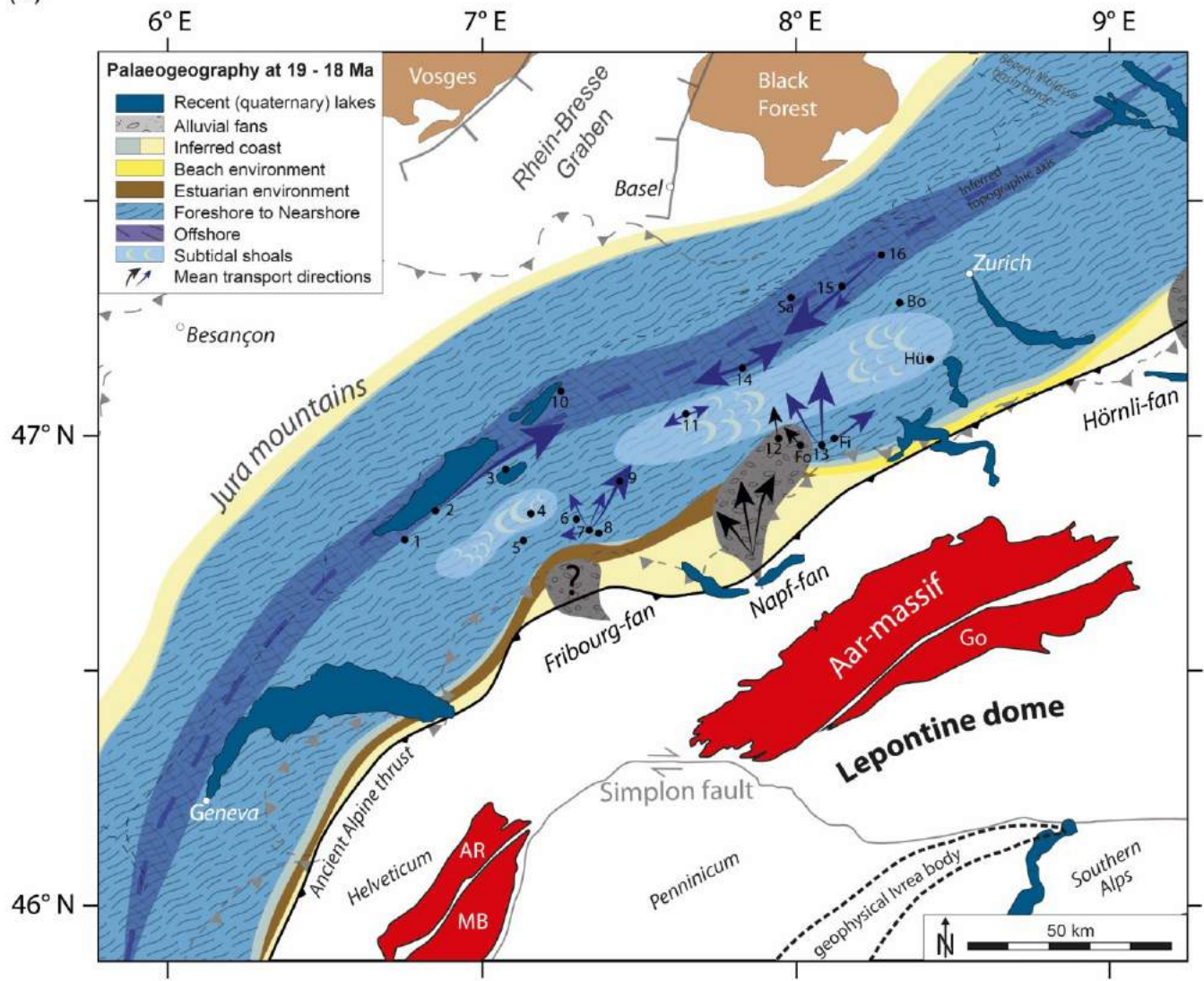
(a)



(b)



(c)



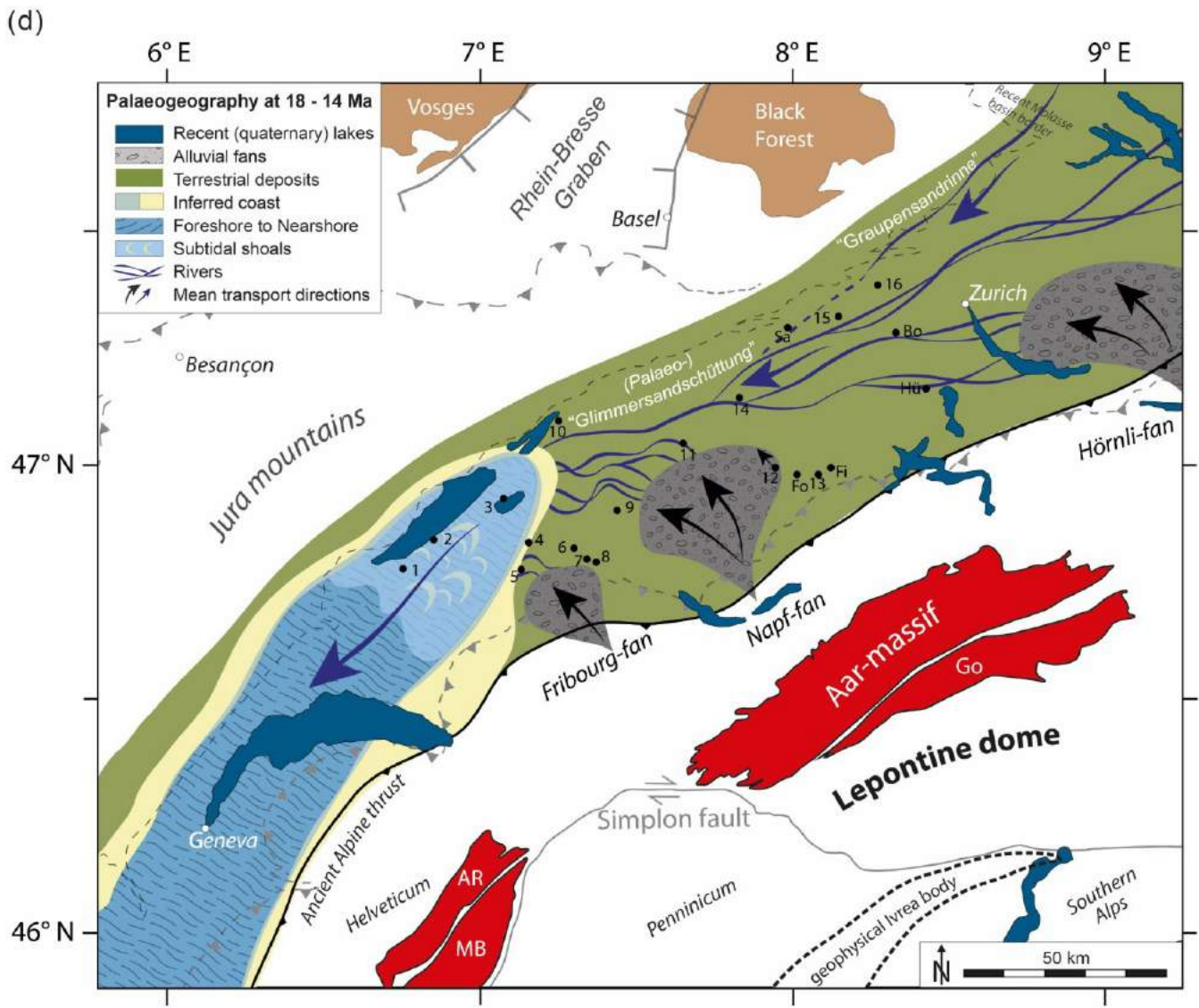
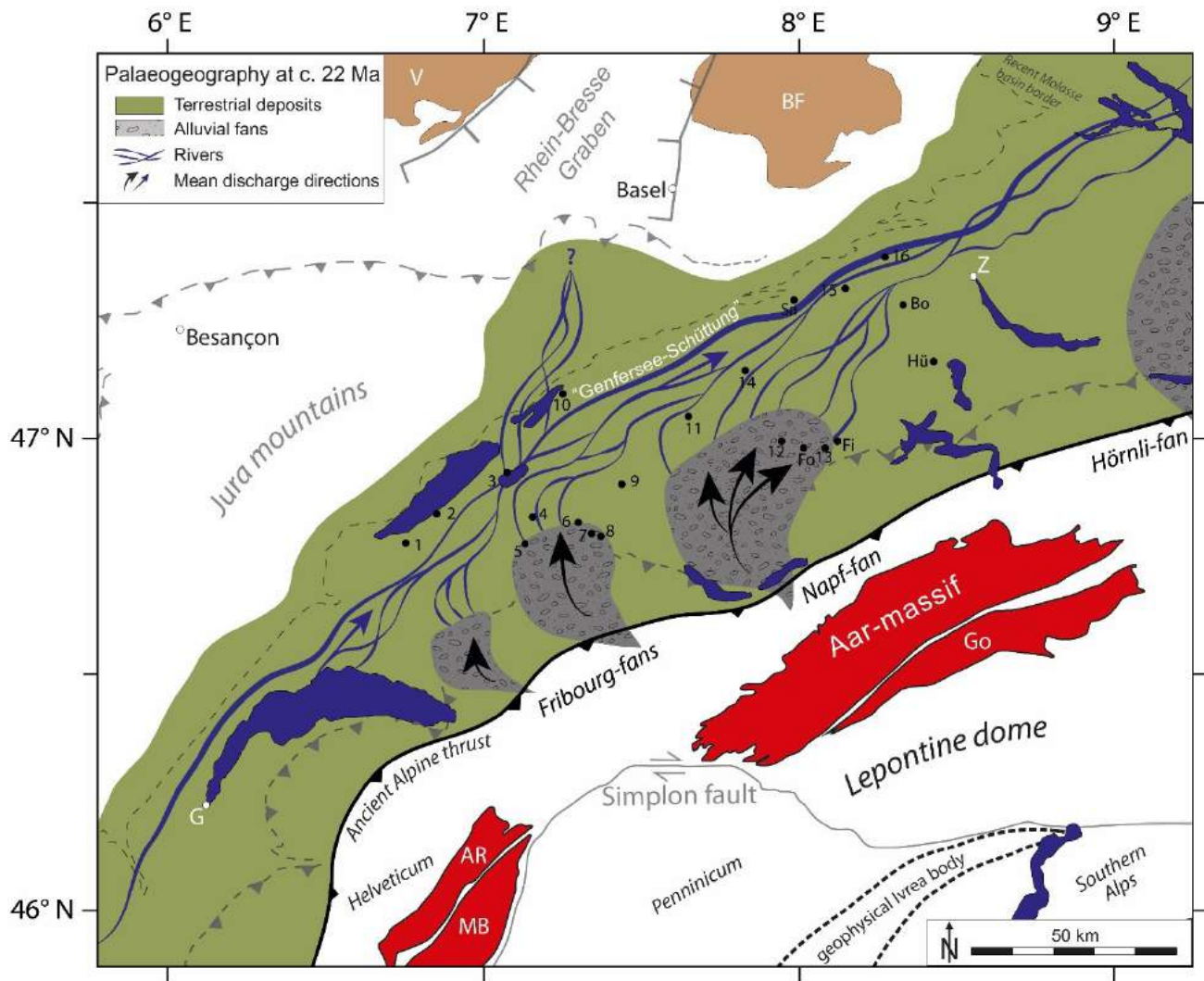


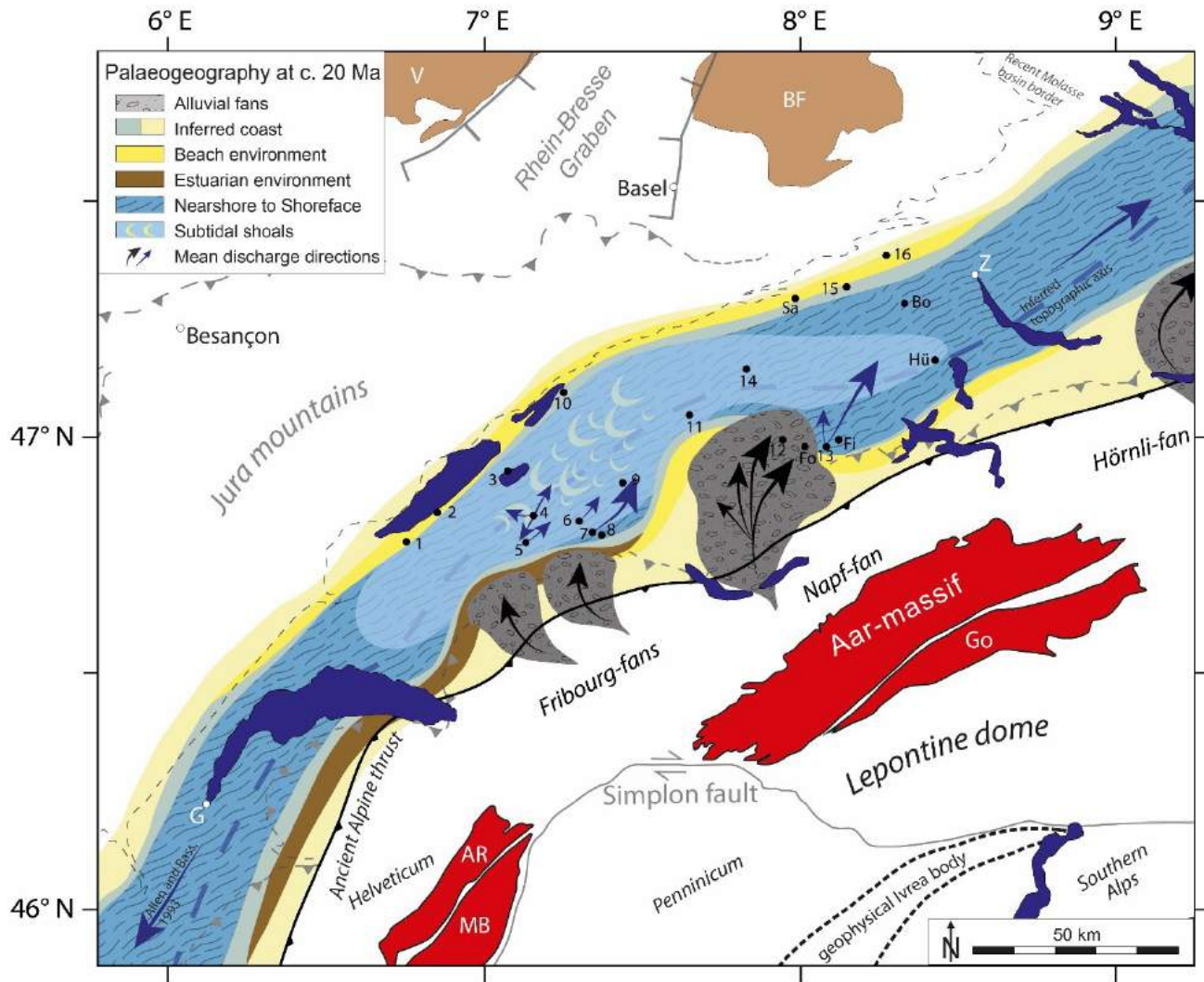
Figure 5 (a and b): Sedimentological log of the a) Entlen and b) Sense section. See Fig. 2 for location of sections, Fig. 4 for chronological framework of the deposits and Table S1 (supplement) for further sedimentological details and abbreviations of the lithofacies. The block diagrams illustrate the palaeogeographical conditions from a conceptual point of view. Please note that the palaeo-bathymetry values are minimum estimates, and that the mean water depths have been inferred from the assignments of the lithofacies to the depositional environment. This might explain why the numerical values for water depths based on cross bed thicknesses and our inferred mean water depth estimates deviate, in particular between c. 200 m and 250 m of the Sense section.

10

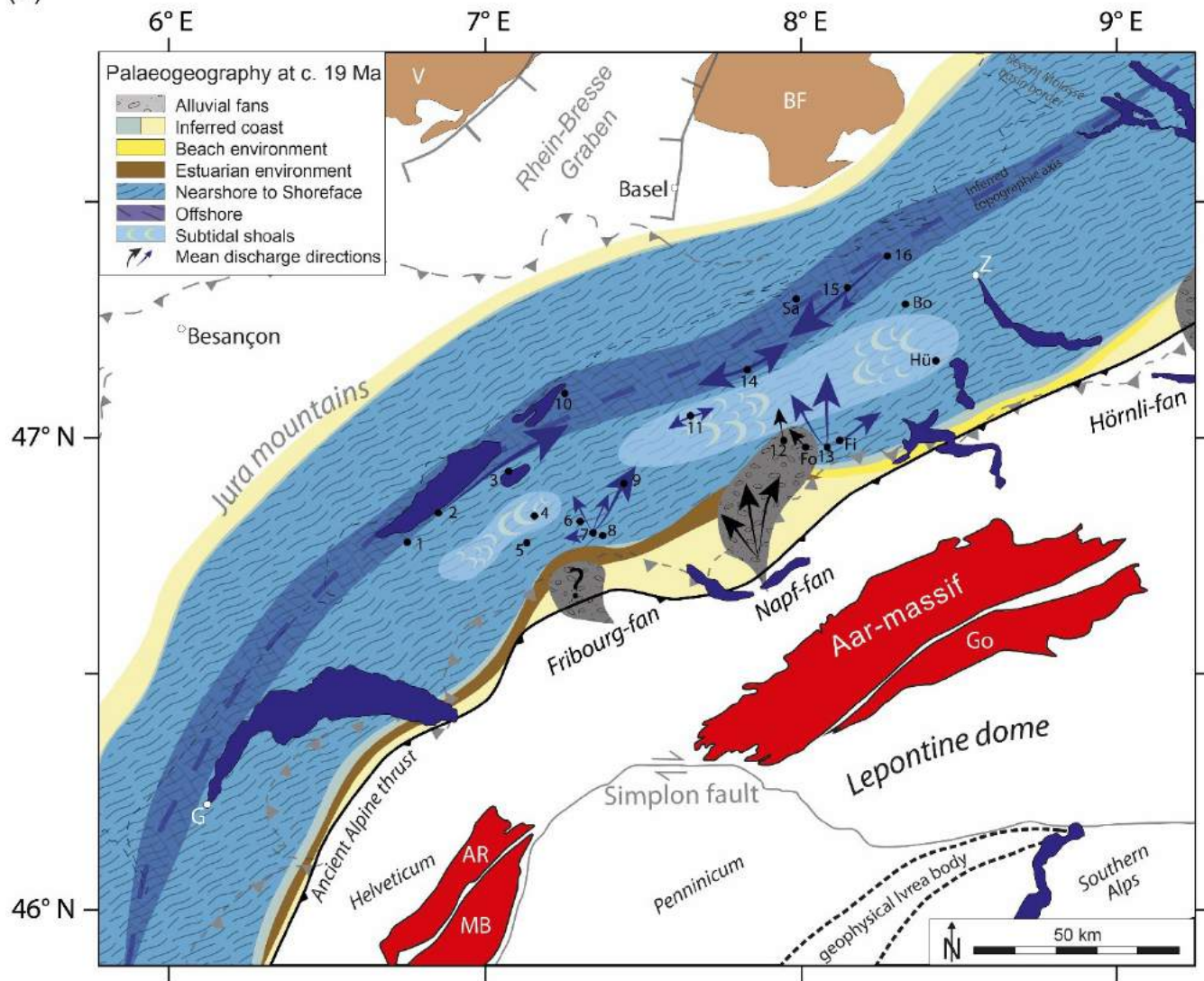
(a)



(b)



(c)



(d)

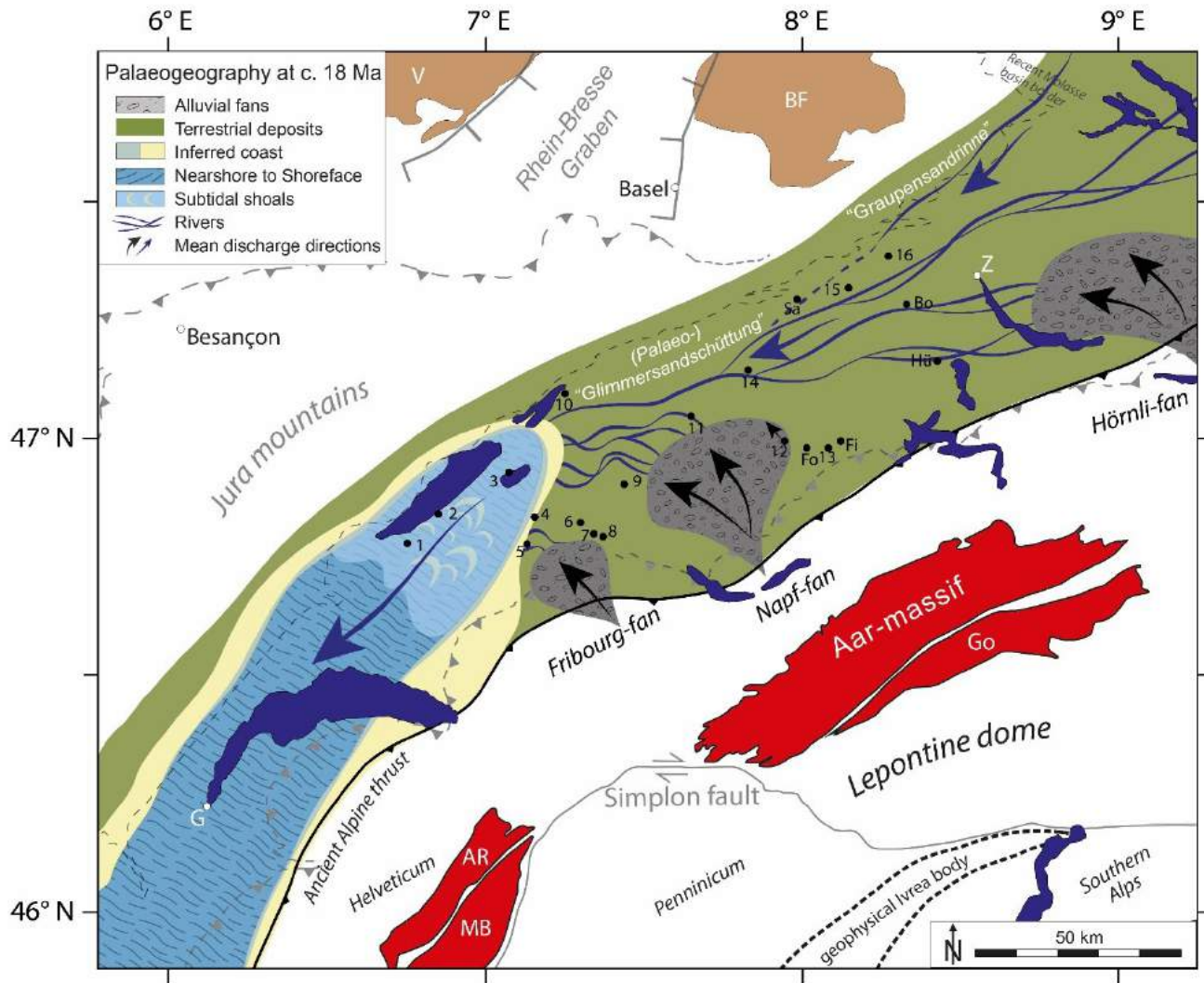
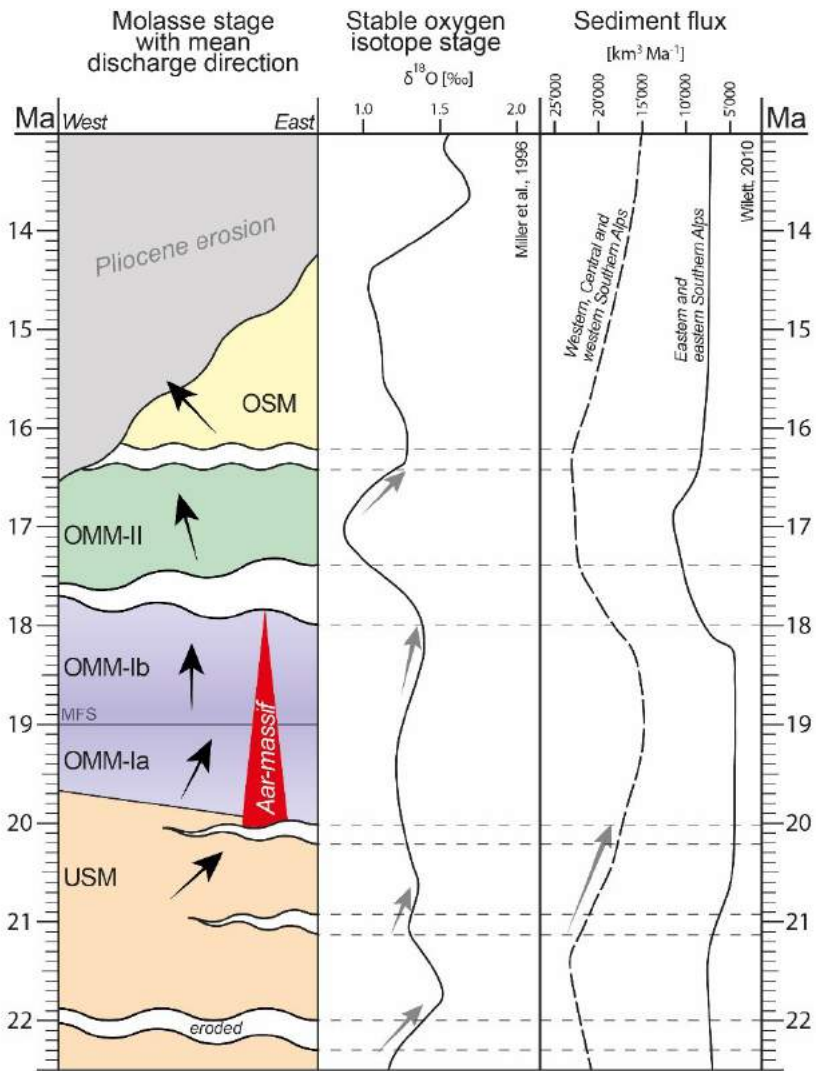


Figure 6 (a to d): Palaeogeographical situation: Palaeogeographical reconstructions of the Molasse basin at **different stages: a) USM (c. 22 Ma), b) OMM-Ia (c. 20 Ma), c) OMM-Ib (c. e. 19 Ma and d) e. 18 Ma) and d) OMM-II to OSM (c. 18- 14 Ma)** modified after Kuhlemann and Kempf (2002). **Please note** based on own observations **Note** that all maps **also** show **the** present-day lithotectonic units within the Alps and the Jura mountains for orientation purposes (dashed lines and grey-coloured lines). We acknowledge, that the **positionpositions** of these and the surface patterns (such as lakes) were **certainly** different during deposition of the Molasse deposits. The location of the palaeo-thrust fronts (thick line) **have been are** adapted from Kuhlemann and Kempf (2002). Black dots mark study sites for orientation purposes. Please refer to Fig. 1 for the complete legend.

10



Situation of the Alps at c. 20 - 18 Ma

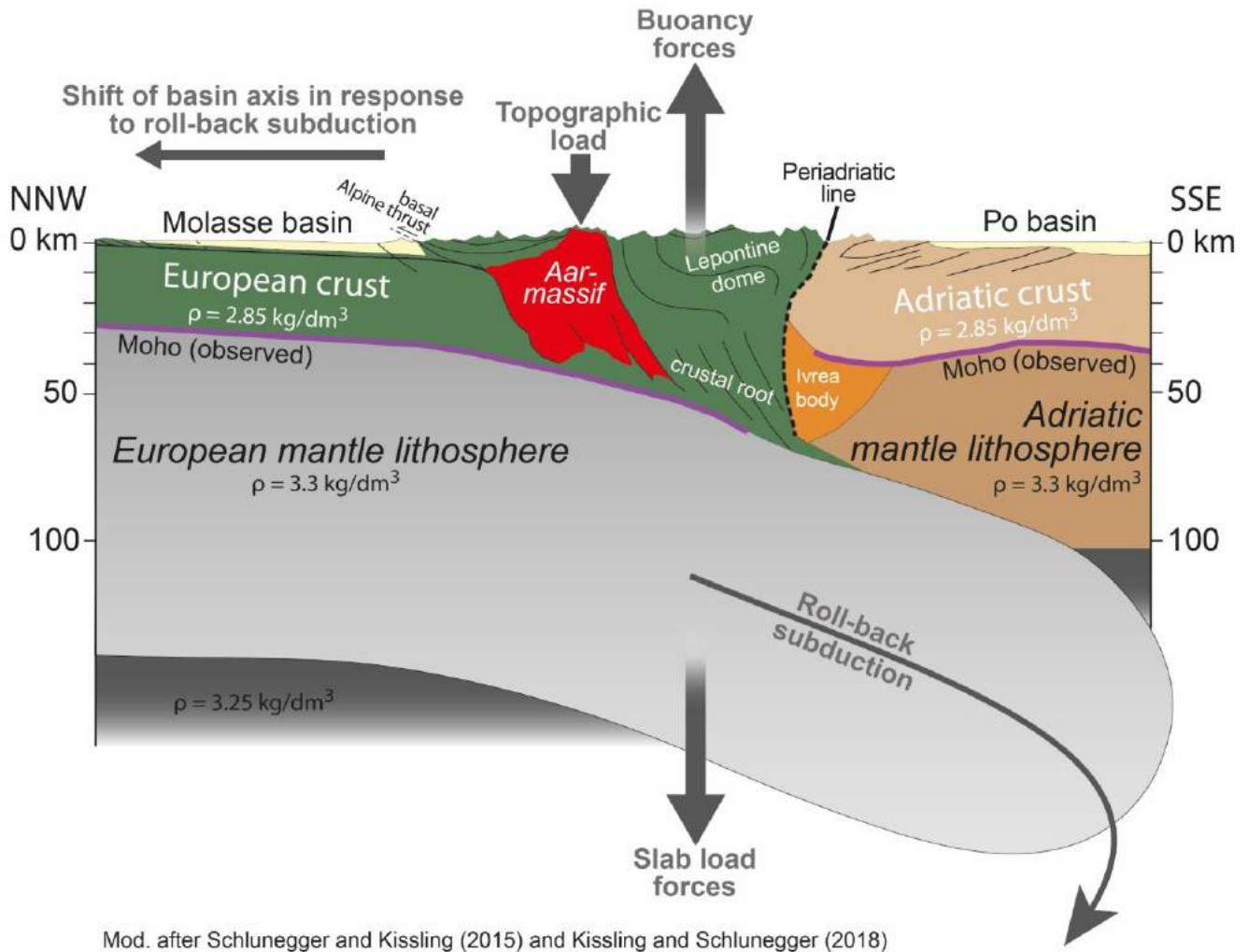


Figure 7: [Simplified geological-geophysical model of the Alpine orogen for the time between 20-18 Ma, showing the most important geodynamic forces that might have shaped the Molasse basin. Modified after Schlunegger and Kissling \(2015\) and Kissling and Schlunegger \(2018\).](#)

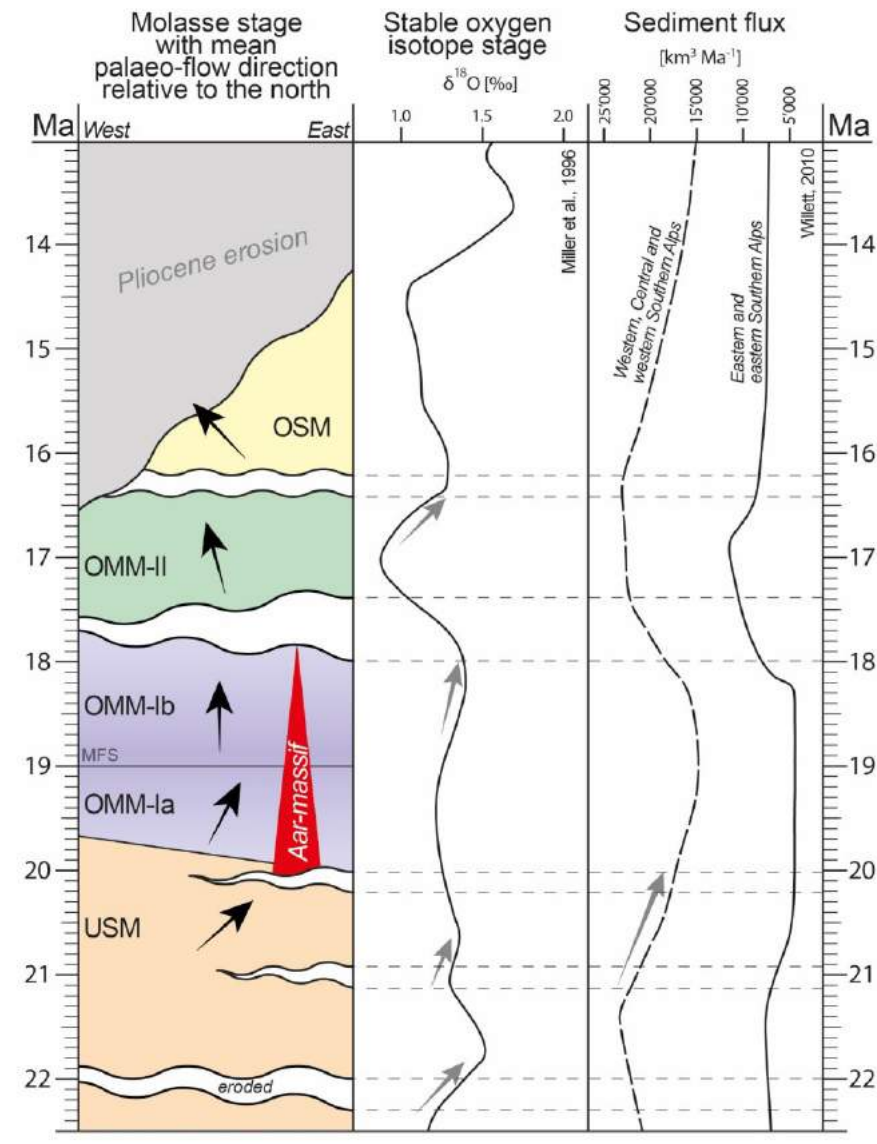


Figure 8: Molasse stages (USM, OMM and OSM) with mean dischargepalaeo-transport directions with hiatus (black arrows), hiatuses plotted against stable oxygen isotope stages (Miller et al., 1996) and sediment flux (Kulemann, 2000; Willett, 2010). The red triangle marks demarcates the onset of delamination and fast rapid exhumation of the Aar-massif (Herwegh et al., 2017). Grey arrows mark drops demarcate falls in sea level and decreases in sediment flux possibly contributing to the related hiatus hiatuses. MFS = Maximum-flooding stages surface.